INFORMATION TO USERS

This manuscript has been reproduced from the microfilm master. UMI films the text directly from the original or copy submitted. Thus, some thesis and dissertation copies are in typewriter face, while others may be from any type of computer printer.

The quality of this reproduction is dependent upon the quality of the copy submitted. Broken or indistinct print, colored or poor quality illustrations and photographs, print bleedthrough, substandard margins, and improper alignment can adversely affect reproduction.

In the unlikely event that the author did not send UMI a complete manuscript and there are missing pages, these will be noted. Also, if unauthorized copyright material had to be removed, a note will indicate the deletion.

Oversize materials (e.g., maps, drawings, charts) are reproduced by sectioning the original, beginning at the upper left-hand corner and continuing from left to right in equal sections with small overlaps.

Photographs included in the original manuscript have been reproduced xerographically in this copy. Higher quality 6" x 9" black and white photographic prints are available for any photographs or illustrations appearing in this copy for an additional charge. Contact UMI directly to order.

Bell & Howell Information and Learning
300 North Zeeb Road, Ann Arbor, MI 48106-1346 USA
800-521-0600

PARTICLE SYSTEMS WITH QUASIHOMOGENEOUS INTERACTION

by

CRISTINA STOICA
Diploma, University of Bucharest, 1991
Doctor in Sciences, Astronomical Institute of Romanian Academy, 1997

A Dissertation Submitted in Partial Fulfillment
of the Requirements for the Degree of

DOCTOR OF PHILOSOPHY

in the Department of Mathematics and Statistics.
We accept this dissertation as conforming
to the required standard.

Dr. Florin Diacu, Supervisor, Department of Mathematics & Statistics, University of Victoria

---

Dr. Reinhard Illner, Department of Mathematics & Statistics, University of Victoria

---

Dr. Rod Edwards, Department of Mathematics & Statistics, University of Victoria

---

Dr. Arif Babul, Outside Member, Department of Physics & Astronomy, University of Victoria

---

Dr. Ernesto Perez, External, Universidad Autonoma Metro-Iztapalapa, Mexico City, Mexico

Supervisor: Dr. Florin Diacu

Abstract

In this dissertation we analyse from a qualitative standpoint motion in a quasihomogeneous potential field: we offer a complete description of the flow associated with the two-body problem in quasihomogeneous field, obtain necessary and sufficient conditions for the block regularization of the flow and we propose an alternative model for the helium atom within the framework of a Manev-type interaction. We call a potential *quasihomogeneous* if it is of the form $A/r^{\alpha} + B/r^{\beta}$, where r is the distance between the two mass points, $0 < \alpha < \beta$ are real parameters and $A > 0$ and $B > 0$ inertia factors.

To obtain the full description of the flow associated with the two-body problem in quasihomogeneous fields, we use diffeomorphic transformations that lead to an equivalent analytic system and at least differentiable integral energy relation. For each level of energy, we introduce the fictional invariant collision manifold and the infinity manifolds. We offer and analyse the global flow picture and we point out the Lebesgue measure of the set of initial conditions that lead to collision for each different case with respect to α and β,

The next chapter focuses on the smoothness of the flow in the neighborhood of the collision manifold. In question is the possibility of extending solutions beyond singularities maintaining good properties with respect to initial data. In this case the singularity set for the system is said to be *block regularizable*. It is proved that the singularity set block regularizable if and only if $\beta = 2 - \frac{2}{n}$, where n is a positive integer, $n \geq 2$. Also, the physical interpretation of this result is pointed out, namely that block regularization is in fact the mathematical expression of constrain imposed over the classical scattering angle.

The last chapter presents a model for the Helium atom within the framework of classical mechanics. The set up consists of a planar isosceles 3-body problem formed by one neutron and two electrons, whose law of motion is given by a Manev-type potential with charges. We first describe the qualitative features of the local flow near triple collision, find several properties of the global flow and finally we prove the existence of a large open, connected, positive-measure manifold of bounded and collisionless solutions.

Examiners:

Dr. Florin Diacu Supervisor, Department of Mathematics & Statistics, University of Victoria

Dr. Reinhard Illner, Department of Mathematics & Statistics, University of Victoria

Dr. Rod Edwards, Department of Mathematics & Statistics, University of Victoria

Dr. Arif Babul, Outside Member, Department of Physics & Astronomy, Univ. of Victoria

Dr. Ernesto Perez, External, Univ. Autonoma Metro-Iztapalapa, Mexico City, Mexico

Contents

Abstract ii
Contents iv
Acknowledgements vi
Dedication vii

Chapter 1 Introduction 1

Chapter 2 The Global Flow 8

2.1 Equations of Motion 8

2.2 The Collision Manifold and Near Collision Orbits 12

2.2.1 The Collision Manifold 12
2.2.2 The Reduced System Near Collision (RSC) 15
2.2.3 The Global Flow for Negative Energy 20
2.2.4 Zero Energy Flow in RSC 27
2.2.5 Positive Energy Flow in RSC 30

2.3 The Flow at Infinity 33

2.3.1 The Infinity Manifolds 35
2.3.2 The Reduced System Near Infinity (RSI) 35
2.3.3 Positive Energy Flow in RSI 37
2.3.4 Zero Energy Flow in RSI 40

2.4 The Global Flow for Non-Negative Energy 41

2.4.1 The Global Flow for Positive Energy 42
2.4.2 The Global Flow for Zero Energy 43

Chapter 3 Regularization and the Scattering Problem **53**

3.1 Isolating Blocks about an Invariant Set 53

3.2 Block Regularization 59

3.3 Levi-Civita Regularization 61

3.4 Physical Interpretation: The Scattering Problem 62

Chapter 4 A Helium Atom Model **67**

4.1 Equations of Motion 67

4.2 Transformations 70

4.3 Relative Behaviour of U and V 72

4.4 The Flow on the Collision Manifold 74

4.5 The Poincaré Map 76

4.7 The Zero-Energy Case 85

4.8 The Positive-Energy Case 90

4.9 The Negative-Energy Case 92

Bibliography **102**

Acknowledgements

First of all, I wish to thank to Dr. Vasile Mioc, artisan of my postgraduate scholastic achievements, for the time and patience invested in me.

Many thanks to Dr. Florin Diacu, for offering me the opportunity of a challenge in mind and spirit in a new world.

Many thanks to Dr. Reinhard Illner, for his constant support during the last three years and for having always a good and warm advice for me.

Thanks to Dr. Sean Bohun, my teacher of the Canadian way of things, to Dr. Holger Teismann, wonderful friend and sounding board for my frustrations and to Dr. Sam Kaplan, amazing research partner.

Thanks to Teri Wood, for spending part of her vacation graphing the figures for my thesis. Also, thanks to all my friends and all the people that, one way or another, have been part of my life in the last three years and are not mentioned here.

Last but not least, I thank to my husband and my soulmate, Gheorghe Stoica, for loving me the way I am.

To Romania, land of my becoming

and

to Canada, land of my fulfillment

Chapter 1

Introduction

In early 90's Diacu (see[Dia]) noticed that several types of potentials used in the dynamics of particles are contained in a larger class of potentials called *quasihomogeneous* and which have the form $W = U + V$, for which $U(r) = Ar^{-\alpha}$ and $V(r) = Br^{-\beta}$ are homogeneous functions of degrees $-\alpha$ and $-\beta$, respectively. but whose sum W is not necessarily homogeneous (α, β, A, and B are constants with $0 \leq \alpha < \beta$ and r is the distance between particles).

The purpose of such an extension is to unify the mathematical framework for many of the potentials encountered in astronomy, physics, and chemistry: Newton ($U(r) = 0$, $V(r) = Gr^{-1}$, where G is the gravitational constant), Coulomb ($U(r) = 0$, $V(r) = -Ar^{-1}$, where $A > 0$ is a constant and charges are taken into account), Van der Waals ($U(r) = 0$, $V(r) = r^{-6}$), Manev ($U(r) = Gr^{-1}$, $V(r) = \frac{3G^2}{c^2}r^{-2}$, where G is the gravitational constant and c is the speed of light), Schwarzschild ($U(r) = Gr^{-1}$, $V(r) = \delta r^{-3}$, where $\delta > 0$ is a constant), Birkhoff ($U(r) = r^{-1}$, $V(r) = -Br^{-2}$, where $B > 0$ is a constant), Lennard-Jones ($U(r) = -r^{-6}$, $V(r) = 2r^{-12}$), Liboff ($U(r) = r^{-3}$, $V(r) = r^{-4}$), and others, some of them defined in anisotropic spaces. To this class of applications we can add the atomic potential presented in Chapter 3, which is of the type $W(r) = -r^{-1} - \gamma r^{-2}$, with $\gamma > 0$ small

and in which charges are also taken into account.

The present dissertation offers a qualitative study of the differential equations describing the quasihomogeneous relative two-body problem. Using a rigorous and complete analytical description of the global flow, we prove that within the class of quasihomogeneous potentials $Ar^{-\alpha} + Br^{-\beta}$, with $0 < \alpha < \beta$, $A > 0$, $B > 0$, the power $\beta = 2$ plays a border-case mathematical role between $\beta < 2$ and $\beta > 2$, which have radically different dynamical behavior. We offer a structural theorem concerning the block regularization problem for quasihomogeneous fields together with its physical interpretation. Also, we perform a global study of the dynamics of a three-body isosceles problem in a particular quasihomogeneous potential providing, in a classical framework, a model for the helium atom.

In Chapter 2, we set-up the equations of motion for a two particle system interacting by a quasihomogeneous law within the classical framework of a two-parameter family of systems with two degree of freedom. The underlying idea is that diffeomorphic transformations applied to systems of ordinary differential equations preserve the behaviour of the flow, modifying only the rate at which solutions move along the orbits.

We start by using McGehee-type diffeomorphic transformations in order to regularize the equations of motion, blow-up the collision singularity and replace it by the collision manifold pasted on the phase space. We provide the description of the fictitious flow on it and notice that in case $\beta = 2$ the flow is degenerate.

In the next subsection, we use the symmetry of the flow with respect to rotations and introduce the *The Reduced System Near Collision* (RSC), as a local chart over the flow in which the collision manifold is contained. We use the energy integral and conclude that the reduced flow lies on a two-dimensional surface. Discretizing our analysis in subcases with respect of the energy level and the parameters α and β, as a first result, we point out that for negative energy levels the flow lies on a compact

surface, implying that all orbits are bounded. Subsequently, we offer all the possible scenarios of motion, first in the case of bounded motion (i.e. for negative energy levels), then, completing the analysis in (RSC), for zero and positive levels of energy, each time pointing out the Lebesque measure of the set of initial data leading to collision. As a conclusion, we deduce that the latter is zero if and only of $\beta < 2$.

In the case of unbounded motion, using an inverse transformation, we bring the fictional infinity point into the origin and introduce *The Reduced System Near Infinity* (RSI). For each fixed zero or positive energy level, a so-called *infinity manifold* is revealed, describing the behaviour of the orbits at the blow-up infinity point. We complete the phase portraits in (RSI) and, finally, using a two-sided chart (RSC)-(RSI), we are able to picture the flow globally. We conclude by stating two theorems (one for zero energy case, one for positive energy case) which. together with the results for the negative total energy, offer the full description of the two-body problem in quasihomogeneous potentials.

Chapter 3 concerns regularization issues. In question here is the possibility of extending solutions beyond singularities maintaining good properties with respect to initial data, a procedure also called *block regularization*.

We start by presenting the mathematical theory behind the block regularization concept. We introduce the necessary definitions and state the main theorems following the set-up developed by Conley and Easton in [Con-E]) and McGehee in [McG1]. We notice that a required condition for block regularization is the isolation of the set of singularities and, as a consequence, the existence of an isolating block. Therefore, as first a step, we prove that the collision singularity for the quasihomogeneous problem is isolated if and only if $\beta < 2$.

We continue by constructing the so-called map across the block which is a one-to-one map between solutions ending in the singularity but not exiting it, and solutions exiting the singularity. The main idea is that if the map across the block

can be uniquely extended to a one-to-one correspondence between all solutions ending in the singularity and all solutions exiting the singularity, then solutions passing close to singularities will determine uniquely an extention for a solution ending in a singularity. Thus one can construct an extended flow with the property of differentiability with respect to initial data and the singularity is said to be block regularizable. Following the later guidelines and making use of different parametrizations for the differential system, we find that the quasihomogeneous problem is block regularizable if and only if $\beta = 2 - 2/n$, where n is a positive integer, $n \geq 2$.

We end the Chapter by pointing out an interesting connection between block regularization and the classical scattering problem. We show that block regularization can be regarded as a constraint over the scattering angle of a particle undergoing a fictional collision.

Let us assume that the trajectory of a particle is scattered by a gravitational source characterized by a quasihomogeneous potential. Computing the scattering angle in the classical framework and imposing on the particle to follow the same exit trajectory line as the impact parameter is approaching zero (by negative or positive values), we obtain that β must be of the form $2 - 2/n$, where n is a positive integer, $n \geq 2$. For these values of β, the test particle will follow at the limit the same trajectory line before and after deviation. Moreover, we notice that the orbit is a *reflection* i.e. the particle leaves in the opposite direction after "collision" if and only if $\beta = 2 - 2/n$, where n is an even number. Similarly, the orbit is a *transmission* i.e. the particle passes through without any change in direction and sense, if and only if $\beta = 2 - 2/n$, where n is an odd number.

In other words, the calculated condition for block regularization is in fact the mathematical expression of a constraint on the classical scattering angle. In the mathematical environment, we impose conditions on the flow to be extended over the singularity set blown-up into the collision manifold, a process performed main-

taining the good properties of the solutions with respect to initial data. In the classical mechanics framework, we ask orbits supporting a fictitious collision to obey the continuity with respect to initial data. The outcome is the same, i.e. for the quasihomogeneous problem, $\beta = 2 - 2/n$, where n is a positive integer, $n \geq 2$.

Chapter 4 is a study over an isosceles three-body problem with charges in a particular type of quasihomogeneous potential. The interaction is assumed to be generated by a sum of two homogeneous terms $W = U + V$, where U and V vary inversely with respect to the distance and to the square of the distance, respectively.

In Section 4.1 we state the problem and the equations of motion. We consider 3 particles moving in a plane. Two of them, called *electrons*, have mass μ, whereas the third, called *nucleus*, has mass 1. We attach to the electrons negative charges and to the nucleus a positive one. The interactive potential is given to be of the form $\mathcal{W} = \mathcal{U} + \mathcal{V}$, where:

$$\mathcal{U}(\mathbf{q}) = -\sum_{i<j} \frac{e_i e_j}{|\mathbf{q}_i - \mathbf{q}_j|}, \quad \mathcal{V}(\mathbf{q}) = -\gamma \sum_{i<j} \frac{e_i e_j}{|\mathbf{q}_i - \mathbf{q}_j|^2}.$$

$e_1 = e_2 = -\mu, e_3 = 1$, γ and μ are small positive constants, and $\mathbf{q} = (\mathbf{q}_1, \mathbf{q}_2, \mathbf{q}_3)$ is the *configuration* of the particle system.

First, we show that binary collisions between electrons never take place and express the equations in a new set of coordinates, which are more convenient for our purpose. In the next section, we apply McGehee-type transformations (see [McG2]) in order to blow up the triple-collision singularity and be able to study the dynamics near it. From the geometrical point of view this means pasting a so-called *collision manifold* to the phase space. A first goal is to describe the flow on the collision manifold. Though this flow has no correspondent in physical reality, using the continuity of solutions with respect to initial data, we can determine the flow's behaviour near this manifold and understand what happens in the neighbourhood of triple collisions. This will be achieved in Sections 4.4 - 4.6.

In Section 4.3 we discuss the relative behaviour of the transformed functions U and V for different values of the parameter μ. This allows us to understand in Section 4.4 the topology of the collision manifold as well as its flow. We see that the collision manifold is homeomorphic to a sphere and that the flow is similar to the parallel circles that describe the geographic latitude of the earth: it consists of two equilibria (the north and south poles N and S) and the periodic orbits (the geographical parallels) in-between them.

In Section 4.5 we prepare the mathematical background for understanding the motion of the particles near triple collision. For this we compute the linear part of the Poincaré map associated with every periodic orbit of the collision manifold. We find out that the orbits of the northern hemisphere have an eigenvalue of modulus larger than 1, those of the southern hemisphere have an eigenvalue of modulus smaller than one, whereas both eigenvalues corresponding to the equator have modulus 1.

Using the latter results, we provide a complete local description of the flow near the collision manifold, independently of the energy level. We show that the south pole S has a 1-dimensional local stable manifold, every periodic orbit of the southern hemisphere has a 2-dimensional local stable manifold, the equator has a 2-dimensional local stable manifold and a 2-dimensional local unstable manifold, every periodic orbit of the northern hemisphere has a 2-dimensional local unstable manifold, and the north pole N has a 1-dimensional local unstable manifold. These imply that the set of triple-collision solutions has positive measure.

In section 4.7 we analyze the zero-energy case. Through suitable transformations we first paste to the phase space an *infinity manifold* I, which also turns out to be a sphere. The flow on this manifold consists of two equilibrium solutions, an infinity north pole $\bar{N}$ and an infinity south pole $\bar{S}$, and of orbits that spiral around the sphere and connect these equilibria. Thus the phase space in the zero-energy case is given by the region between two concentric spheres: the collision manifold C

and the infinity manifold I. We then show that the flow is increasing with respect to the variable represented on the vertical axis. Only three classes of orbits exist in this case: capture-collision, ejection-escape, and capture-escape, none of them interesting from the point of view of the helium atom. In the next section, we show that the qualitative behaviour of the flow for positive energy is qualitatively similar to that of zero energy.

In Section 4.9 we analyse the flow for negative energy and prove the existence of a large open and connected manifold of orbits that remain bounded and do not encounter ejections or collisions. For this we show that the motion of the particles is described by the same type of second-order equation that models the forced harmonic oscillator. As we mentioned before, the orbits in this set are of interest for the helium atom.

Chapter 2

The Global Flow

2.1 Equations of Motion

The quasihomogeneous two-body problem is a two-parameter family of classical systems with two degrees of freedom describing the relative motion of two mass points interacting with respect to each other following a *quasihomogeneous* law of motion. A force field is said to be *quasihomogeneous* if it is generated by a potential $U = V + W$, where $V(\mathbf{x}) = A/x^{\alpha}$ and $W(\mathbf{x}) = B/x^{\beta}$, ($x$ being the distance between the particles) with $0 < \alpha < \beta$ and $A > 0$, $B > 0$.

$U(\mathbf{x})$ being a function depending only on distance, the force is central, and, consequently, the motion is planar and described by a Hamiltonian system of ordinary differential equations:

$$\begin{cases} \dot{\mathbf{x}} = \frac{\partial H}{\partial \mathbf{y}} \\ \dot{\mathbf{y}} = -\frac{\partial H}{\partial \mathbf{x}}, \end{cases} \tag{2.1}$$

where $\mathbf{x} = (x_1, x_2) \in \mathbf{R}^2 - \{(0,0)\}$, $\mathbf{y} \in \mathbf{R}^2$ and the Hamiltonian function is:

$$H(\mathbf{x}, \mathbf{y}) = \frac{1}{2}y^2 - \frac{A}{x^{\alpha}} - \frac{B}{x^{\beta}}, \tag{2.2}$$

where we denote $x := \sqrt{x_1^2, x_2^2}$ and $y := \sqrt{y_1^2, y_2^2}$. Since the system is conservative, the energy integral writes:

$$H(\mathbf{x}(t), \mathbf{y}(t)) = h \text{ (constant)}. \tag{2.3}$$

Also, since the force is central, the angular momentum is conserved and:

$$x_1 y_2 - x_2 y_1 = c \text{ (constant)}. \tag{2.4}$$

The function $U(\mathbf{x})$ is real analytic and, for any initial data $(\mathbf{x}(0), \mathbf{y}(0)) \in (\mathbf{R}^2 - \{(0,0)\}) \times \mathbf{R}^2$, standard results from ordinary differential theory guarantee the existence and uniqueness of an analytic solution defined on a maximal interval (t^*-, t^*+), where $t^* \leq \infty$. If either $t^*- > -\infty$ or $t^*+ < \infty$, the solution is said to experience a singularity. For this particular system of equations, by imitating a proof of McGehee (see [McG2]), one can show that the singularities in solutions correspond to the singularities in the vector field. meaning that the physical system undergoes a collision i.e. $\mathbf{x}(t) \to \mathbf{0}$ as $t \to t^*$.

In order to remove the singularities and to regularize system (2.1) we shall resort to McGehee type transformations of the second kind (see [McG2]). First we apply the analytic diffeomorphism $(\mathbf{x}, \mathbf{y}) \to (r, \theta, v, u) \in ([0, \infty), [0, 2\pi), \mathbf{R}, \mathbf{R})$

$$\begin{cases} \mathbf{x} = r^{\gamma} e^{i\theta} \\ \mathbf{y} = r^{\delta}(v + iu) e^{i\theta}. \end{cases} \tag{2.5}$$

where

$$\begin{cases} \gamma = \frac{1}{\beta - \alpha} \\ \delta = -\frac{\beta}{2(\beta - \alpha)}. \end{cases} \tag{2.6}$$

In this manner we change the cartesian coordinates $(\mathbf{x}, \mathbf{y})$ into the rescaled polar coordinates (r, θ, v, u). Then we reparametrize the orbits by:

$$d\tau = r^{-\frac{\beta+2}{2(\beta-\alpha)}} dt. \tag{2.7}$$

Using prime to mark the differentiation with respect to the new (fictitious) time variable τ, the equations of motion (2.1) become:

$$\begin{cases} r' = (\beta - \alpha) r v \\ \theta' = u \\ v' = u^2 + \frac{\beta}{2} v^2 - \alpha A r - \beta B \\ u' = \frac{1}{2}(\beta - 2) u v. \end{cases} \tag{2.8}$$

By (2.5) - (2.7), the first integrals of energy and angular momentum read respectively

$$v^2 + u^2 = 2B + 2Ar + 2hr^{\frac{\beta}{\beta-\alpha}}, \tag{2.9}$$

$$\begin{cases} r^{\frac{(2-\beta)}{2(\beta-\alpha)}} u = c & \text{if} \quad \beta < 2, \\ u = c & \text{if} \quad \beta = 2. \\ u = c r^{\frac{(\beta-2)}{2(\beta-\alpha)}} & \text{if} \quad \beta > 2. \end{cases} \tag{2.10}$$

Both the equation of motion (2.8) and the first integrals (2.9) and (2.10) are now well defined for the boundary $r = 0$. The energy relation (2.9) foliates the phase space into the integral manifolds

$$M_h = \{(r, \theta, v, u) | \, v^2 + u^2 = 2B + 2Ar + 2hr^{\frac{\beta}{\beta-\alpha}}, \, \theta \in [0, 2\pi)\}, \tag{2.11}$$

whose topology may change with h. If restricted to $r = 0$, the energy relation becomes $v^2 + u^2 = 2B$. Therefore we define the *collision manifold* as the set:

$$\Lambda = \{(r, \theta, v, u) | \, r = 0, \, \theta \in [0, 2\pi) \quad \text{and} \quad u^2 + v^2 = 2B\}. \tag{2.12}$$

The flow restricted to Λ is well defined and given by:

$$\begin{cases} \theta' = u \\ v' = u^2 + \beta/2 v^2 - \beta B \\ u' = \frac{1}{2}(\beta - 2) u v. \end{cases} \tag{2.13}$$

Lemma 2.1.1 Suppose that $(r, \theta, v, u)(t)$ satisfies (2.1) and that $r \longrightarrow 0$ as $t \longrightarrow t^* \pm$. Then $\tau(t) \longrightarrow \mp\infty$.

Proof We prove that $t \longrightarrow t^* -$ implies that $\tau(t) \longrightarrow +\infty$, the other case being similar. The time rescaling (2.7) can be written as

$$\tau(t) = \tau_0 + \int_{t_0}^{t} r^{-\frac{\beta+2}{2(\beta-\alpha)}}(s)ds \tag{2.14}$$

from where one can see that $\tau(t)$ is defined for all $t_0 < t < t^*$ and is increasing. Hence $\tau(t) \longrightarrow \tau^*$ as $t \longrightarrow t^*-$, where τ^* may be infinity. Then $r(\tau) \longrightarrow 0$ as $\tau \longrightarrow \tau^*$. Since equations (2.8) are defined and smooth on M_h, and since Λ is a compact invariant set, it is impossible for a solution to approach Λ in finite time. Therefore $\tau^* = \infty$, and the lemma is proved.

In other words, the phase space can be extended analytically to contain the manifold $\{(r, \theta, v, u) | \ r = 0\}$, which is invariant under the flow and approached asymptotically in the new time variable τ. The energy integral (2.9) is at least of C^1 class meaning that it also extends smoothly under this boundary. For any choice of $0 < \alpha < \beta$ the angular momentum relation (2.10) has guaranteed only the continuity but this will not effect our results. Moreover, even with this lack in smoothness, the angular momentum relation tells us that collisions can occur if and only if $c = 0$ for $\beta < 2$ and that they might occur for non-zero c's for $\beta \geq 2$. In other words, for $\beta < 2$ collisions are possible if and only if the motion is radial. For $\beta \geq 2$ collision orbits can have a non-zero angular velocity.

We emphasize that the orbits of system (2.8) are the same as the orbits of system (2.1), only the parametrization is different. Any results concerning the solutions of system (2.8) can be seen as results for the solutions of system (2.1) as long as one is aware of the fact that the rate at which solutions move along the orbits is different.

2.2 The Collision Manifold and Near Collision Orbits

2.2.1 The Collision Manifold

Recall that the energy relation (2.9) foliates the phase space into the integral manifolds M_h (see (2.11)) and that, setting $r = 0$, we defined the collision manifold Λ.

It follows that Λ is an invariant set of orbits (if r is zero at a certain time, it is zero at any time) and, from the topological point of view, is a 2-dimensional cylinder in the 3-dimensional space of the coordinates $(\theta, v, u) \in \mathcal{S}^1 \times \mathbf{R} \times \mathbf{R}$. But, since $\theta \in \mathcal{S}^1$, the Λ cylinder may be identified with a torus, both being actually imbeded in the 4-dimensional full phase space. Also, Λ is the same for every h, therefore every energy level shares this boundary.

In other words, by means of McGehee's technique, we have blown up the singularity and pasted the torus Λ instead of it in the phase space.

In this section we perform a qualitative study of the flow on the collision manifold, this information describing the behaviour of solutions in the neighbourhood of collisions.

Using (2.12) in 2.13, the flow on Λ becomes:

$$\begin{cases} \theta' = u \\ v' = \frac{1}{2}(\beta - 2)(v^2 - 2B) \\ u' = \frac{1}{2}(\beta - 2)uv. \end{cases} \tag{2.15}$$

The equilibria are located at $(\theta_0, \pm\sqrt{2B}, 0)$, where $\theta_0 \in [0, 2\pi)$, i.e. there are two circles of degenerate equilibria on the Λ torus, at $u = 0$. The corresponding eigenvalues are ${\lambda_1}^c = 0, {\lambda_2}^c = (\beta - 2)(\sqrt{2B}), {\lambda_3}^c = \frac{1}{2}(\beta - 2)(\sqrt{2B})$, for $(\theta_0, +\sqrt{2B}, 0)$ and ${\lambda_1}^c = 0, {\lambda_2}^c = -(\beta - 2)(\sqrt{2B}), {\lambda_3}^c = -\frac{1}{2}(\beta - 2)(\sqrt{2B})$ for $(\theta_0, -\sqrt{2B}, 0)$.

Now the flow on Λ can be easily described.

For $\beta < 2$, since $v' > 0$ for $u \neq 0$, all orbits are heteroclinic, moving from the

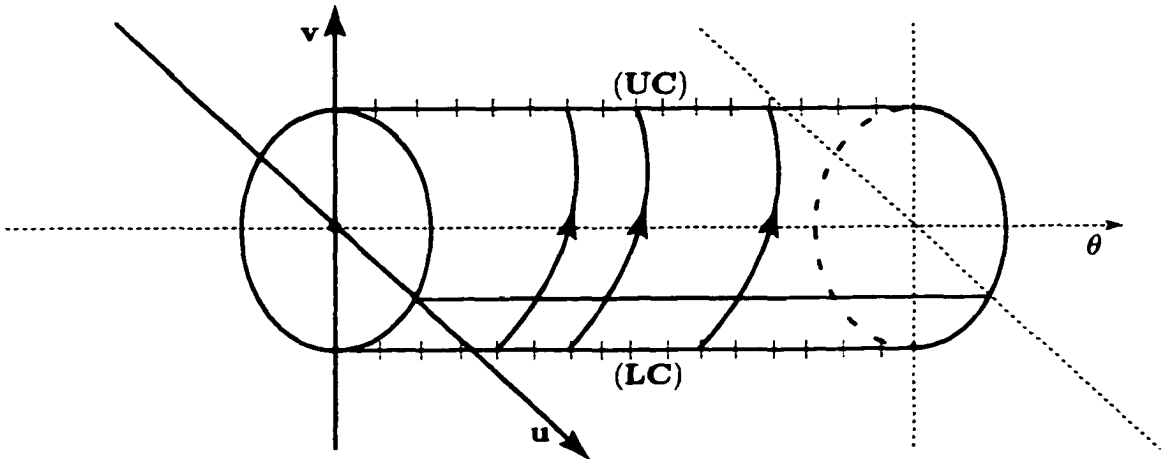

Figure 2.1: The flow on the collision manifold for $\beta < 2$.

lower circle (LC) of degenerate sources to the *upper circle* (UC) of degenerate sinks and filling in densely Λ (see Figure 2.1).

The case $\beta = 2$ is a bifurcation point in the class of potentials studied. Here the flow on the collision manifold is parallel to LC and to UP and becomes degenerate in any direction (see Figure 2.2).

For $\beta > 2$ all orbits are heteroclinic, moving from the UP to the LC and filling in densely Λ (see Figure 2.3).

Since on Λ we have $v^2+u^2 = 2B$, another manner to visualize the flow on the collision manifold is by introducing the angular variable χ such that $u + iv = \sqrt{2B}\, e^{i\chi}$, i.e.

$$\begin{cases} u = \sqrt{2B}\, cos\chi, \\ v = \sqrt{2B}\, sin\chi. \end{cases} \tag{2.16}$$

Then the flow on Λ is given by:

$$\begin{cases} \theta' = u, \\ \chi' = \left(1 - \frac{\beta}{2}\right)u. \end{cases} \tag{2.17}$$

and hence in the (θ, χ) plane the collision orbits are straight lines with slope $1 - \beta/2$

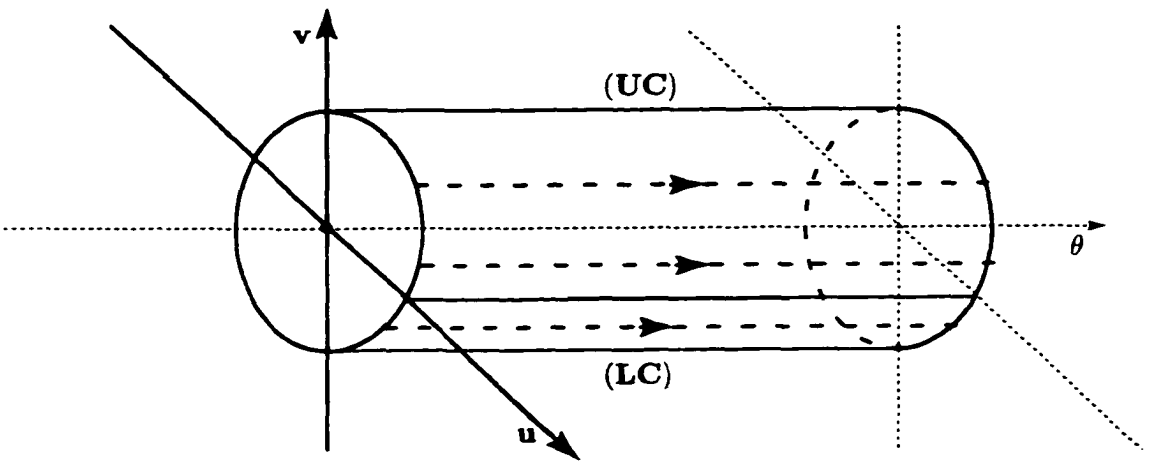

Figure 2.2: The flow on the collision manifold for $\beta = 2$.

(see Figure 2.4).

For the following lemma we use the notation:

$$S^{\pm} = \{(r, \theta, v, u) \in \Lambda \mid v = \pm\sqrt{2B}\} \tag{2.18}$$

By the definition of Λ,

$$S^{\pm} = \{(r, \theta, v, u) \in \mathbf{R}^4 \mid r = 0,\ v = \pm\sqrt{2B},\ u = 0\},$$

and hence S^+ and S^- are both circles. We denote by $\omega(p)$ the omega limit set of $p = (r, \theta, v, u)$ under the flow on M_h defined by the equations (2.8). Similarly, $\alpha(p)$ denotes the alpha limit set.

Lemma 2.2.1 Assume $\beta \neq 2$. Let $p(\tau) = (r, \theta, v, u)(\tau)$ be a solution of (2.8) and write $p_0 = p(\tau 0)$. Then (a) $r \longrightarrow 0$ as $\tau \longrightarrow +\infty$ if and only if $\omega(p_0) \subset S^-$, and (b)$r \longrightarrow 0$ as $\tau \longrightarrow -\infty$ in and only if $\alpha(p_0) \subset S^+$.

Proof We will prove only (a) since (b) is similar. Since Λ is exactly the set on M_h where $r = 0$, $r \longrightarrow 0$ as $\tau \longrightarrow +\infty$ if and only if $\omega(p_0) \subset \Lambda$. Since $S^- \subset \Lambda$, it therefore suffices to show that $\omega(p_0) \subset \Lambda$ implies $\omega(p_0) \subset S^-$. Using the energy relation (2.9) with $r = 0$, we can rewrite the equation for v in system (2.8) restricted to Λ as

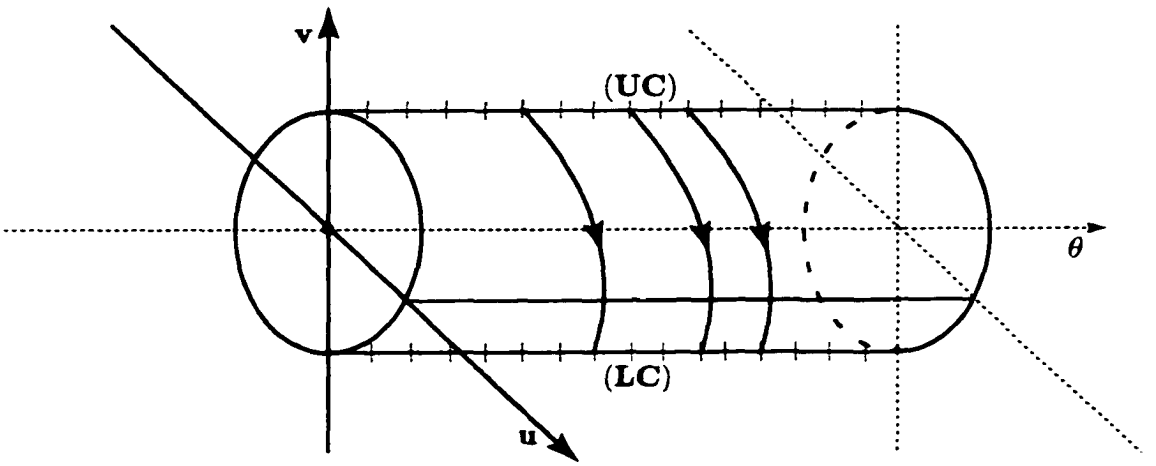

Figure 2.3: The flow on the collision manifold for $\beta > 2$.

$$v' = (1 - \frac{\beta}{2})u^2. \tag{2.19}$$

Therefore v defines a Liapunov function on Λ. Since a Liapunov function must be constant on an omega limit set ([Con]), we must have $v' = 0$ on $\omega(p_0)$. But $v' = 0$ on Λ exactly on on S^+ and S^-. We can rule out S^+ since v is positive in a neighborhood of S^+ and the first equation of (2.8) is increasing whenever v is positive. Therefore $\omega(p_0) \subset S^-$ and the proof is complete.

2.2.2 The Reduced System Near Collision (RSC)

By continuity with respect to initial data, the flow on the collision manifold provides a local image for the motion near the singularities. In order to describe the global flow we start by pointing out some general characteristics of the system (2.8).

For $\beta \neq 2$ the equilibria of system (2.8) are located at the collision points $(0, \theta_0, \pm\sqrt{2B}, 0)$, $\theta \in \mathcal{S}^1$ and their nature is determined by the corresponding eigenvalues:

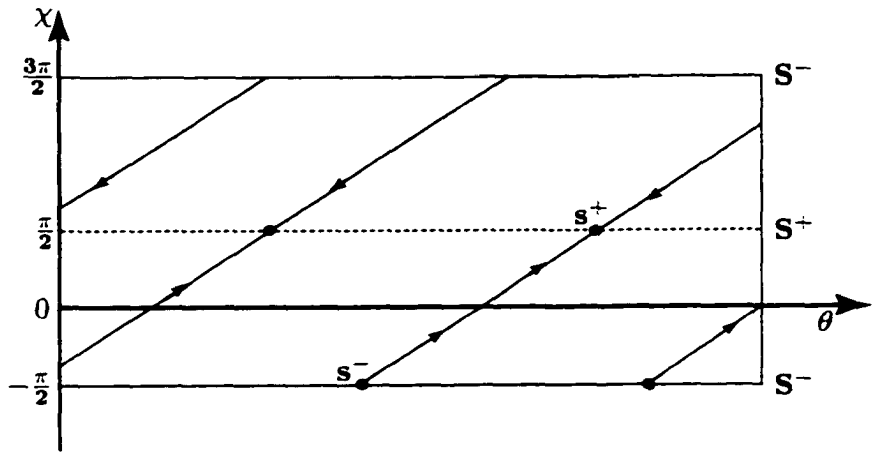

Figure 2.4: The flow on the collision manifold in (θ, χ) plane

$$\begin{cases} \lambda_1 = \pm\sqrt{2B} \\ \lambda_2 = 0 \\ \lambda_3 = \pm(\beta - 2)(\sqrt{2B}) \\ \lambda_4 = \pm\frac{1}{2}(\beta - 2)(\sqrt{2B}). \end{cases} \tag{2.20}$$

which depend explicitely on the value of parameter β.

Lemma 2.2.2 Assume $\beta \neq 2$. Let $(r, \theta, v, u)(t)$ be a solution of (2.1) such that $r \longrightarrow 0$ as $t \longrightarrow t^*\pm$. Then, as $t \longrightarrow t^*\pm$, $u(t) \longrightarrow \pm\sqrt{2B}$, and $\theta(t) \longrightarrow \theta^*$ for some constant θ^*. Furthermore, if $\beta < 2$, then $u(t) \equiv 0$ and $\theta(t) \equiv \theta^*$.

Proof We prove only the case $t \longrightarrow t^*-$, the other case being similar. By Lemma 2.1.1., it suffices to prove the same limits for system (2.8) as $\tau \longrightarrow \infty$. By Lemma 2.2.1. it suffices to prove these limits for all points in M_h on the stable manifolds of S^-.

On S^-, $u = 0$, therefore $\theta' = 0$, so S^- consists entirely of rest points. By (2.20), the eigenvalues at each of these rest points are 0, $\pm(\beta - 2)(\sqrt{2B})$ and $\pm\frac{1}{2}(\beta - 2)(\sqrt{2B})$, respectively. The zero eigenvalues corresponds to the tangential direction along S^-, while the two others correspond to normal directions. For $\beta \neq 2$, S^- has hyperbolic normal structure, and hence the stable manifold of S^- is the union

of the stable manifold of each of these points of S^- ([Fen]). Therefore the solution $(r, \theta, v, u,)(\tau)$ approaches some point on S^- i.e. $\theta \longrightarrow \theta^*$, $u \longrightarrow 0$, $v \longrightarrow \sqrt{2B}$.

If $\beta < 2$, by (2.20), the normal eigenvalues are both strictly positive. In this case the stable manifold is one dimensional (in the r direction) and consists only of points with $u = 0$ (see also Figures 2.5, 2.10 and 2.14). Since $\theta' = u = 0$, θ must be constant. Therefore $u \equiv 0$ and $\theta = \theta^*$ and the proof is complete.

Therefore, for $\beta < 2$, the angular momentum must be zero on a collision orbit. Furthermore, all motion takes place along a line.

For any β we have the converse, i.e. system (2.8) admits the surface $u = 0$ as invariant manifold. This means that if angular velocity is zero at a certain time, then it will be zero at any time (past or future).

In the particular case $\beta = 2$, system (2.8) takes the simpler form:

$$\begin{cases} r' = (\beta - \alpha) r v \\ \theta' = u \\ v' = u^2 + v^2 - \alpha A r - \beta B \\ u' = 0, \end{cases} \tag{2.21}$$

together with the integral relations

$$v^2 + u^2 = 2B + 2Ar + 2hr^{\frac{2}{2-\alpha}} \tag{2.22}$$

and

$$u = c. \tag{2.23}$$

One can notice that here the rescaled angular velocity u is in fact the angular momentum constant c and that each of the planes $u = c$ are invariant manifolds. The relative equilibria are located at $(r, \theta, v, u) = (0, \theta_0, \pm\sqrt{2B - u_0^2}, u_0)$, where $\theta \in \mathcal{S}^1$ and $|u_0| \in [0, \sqrt{2B}]$ and all of them are degenerate sources for $v > 0$, respectively, sinks for $v < 0$ on the r direction.

We return now to the particular form of system (2.8) and introduce the *Reduced System Near Collision* (RSC) defined by

$$\begin{cases} r' = (\beta - \alpha)rv \\ v' = u^2 + \frac{\beta}{2}v^2 - \alpha Ar - \beta B \\ u' = \frac{1}{2}(\beta - 2)uv. \end{cases} \tag{2.24}$$

The solutions of (2.8) are determined by the solutions of the reduced system in the sense that since the equations for (r, v, u) do not depend on θ, they can be solved independently. Once the RSC solved, θ follows consequently. In other words the 4-dimensional flow is invariant under rotations so we can factorize it by $\mathcal{S}^1$. Furthermore, the energy relation (2.9) does not depend on θ either. This allows us to reduce implicitely the reduced space RSC by another dimension since every fixed energy level h determines the 2-dimensional invariant surface

$$\tilde{M}_h := \{(r, \theta, v, u) | \, v^2 + u^2 = 2B + 2Ar + 2hr^{\frac{3}{3-\alpha}}\}, \tag{2.25}$$

on which the RSC orbits are confined.

As an observation, we chose to call the reduced system *near collision*, because in this parametrization we are able to see and describe the orbits in a neighborhood of collision. This is in contrast with the reduced system near infinity that will be introduced later and will allow us to describe in detail the orbits attaining infinity.

It is tempting to reduce the problem futher and apply the same reasoning for the invariant manifold determined by the angular momentum integral. Then, every orbit on $\tilde{M}_h$ would be uniquely determined by the angular momentum constant c and, as c varies, $\tilde{M}_h$ is filled in densely by orbits. In this manner, one would be able to see an orbit as the intersection of two 2-dimensional surfaces, one determined by h, the other by c. But the angular momentum relation is just continuous near the collision manifold, leading to uniqueness problems at the borderline $r = 0$. The good properties of the invariant manifolds on which the flow is confined are compromised near collisions, including the uniqueness and the continuity with respect to initial data. Consequently, each time we will use the angular momentum integral, we will

make sure that we are far enough from the collision subspace $\{r = 0\}$.

By (2.9), the energy manifold $\tilde{M}_h$ is a rotational surface with respect to the r axes in the reduced phase space (r, v, u). A simple sketch reveals that the orbits are all bounded (the rescaled radius vector r is bounded) for negative levels of energy h and possibly unbounded for $h \geq 0$. Also, exploiting the particular form of the vector field of (2.24), the phase curves are symmetric with respect to the planes $u = 0$ and $v = 0$ since $(r(\tau), -v(\tau), u(\tau)) = (r(-\tau), v(-\tau), u(-\tau))$ and $(r(\tau), -v(\tau), -u(\tau)) = (r(-\tau), v(-\tau), u(-\tau))$.

In the RSC the collision manifold torus is a circle and the circles of equilibria $(\theta, \pm\sqrt{2B}, 0)$, $\theta \in \mathcal{S}^1$ correspond to the equilibria points $C^{\pm} = (0, \pm\sqrt{2B}, 0)$. We will abuse the terminology by further calling *equilibria*, *periodic orbits*, etc. what appear to be such orbits in the RSC. In full phase space these must be regarded $\times\mathcal{S}^1$, i.e. manifolds of solutions. For instance, an equilibrium of the RSC is a relative equilibria in the full phase space and physically it represents a circular orbit with constant angular velocity; a periodic orbit in RSC is an invariant torus of solutions in the 4-dimensional phase space and physically it represents periodic (rosette-shaped closed trajectories if $u \neq 0$, radial libration if $u = 0$) or rather quasiperiodic (unclosed orbits filling densely an annulus; see [Arno] and [Del]) motion; an arc of phase curve in the upper $(v > 0)$/lower $(v < 0)$ half space of RSC corresponds in the physical space to spiral $(u \neq 0)$ or radial $(u = 0)$ motion performed outwards/inwards, etc.

In order to state our main results we will use the following:

Definition 2.2.2 A solution of system (2.8) is called a *capture* orbit if r tends to infinity in the past, an *escape* orbit if r tends to infinity in the future, an *ejection* orbit if r tends to 0 in the past, and a *collision* if r tends to 0 in the future. A *quasiperiodic* orbit is one for which r is bounded but does not become zero in the past or in the future; a *circular* orbit is a quasiperiodic orbit for which r is constant at any time, and an *oscillatory* orbit is one for which r becomes unbounded but

does not tend to infinity (ex. $\lim inf_{\tau\to\infty} r(\tau) < \infty$ and $\lim sup_{\tau\to\infty} r(\tau) = \infty$).

Let us denote by $f(r)$ the right hand side of (2.9), i.e.:

$$f(r) = 2B + 2Ar + 2hr^{\frac{\beta}{\beta-\alpha}}. \tag{2.26}$$

The equilibria of the RSC other that the collision ones at $C^{\pm} = (0, \pm\sqrt{2B}, 0)$ are obtained by setting $v = v' = 0$. This leads to solving the following equation in r:

$$f(r) = \alpha Ar + \beta B, \tag{2.27}$$

which admits different numbers of roots, depending on the level of h and the values of parameters the α and β.

In order to simplify further computations let us notice that to a solution of the above equation (2.27) $r = r_{cr}$ corresponds a pair of equilibria $R^{\pm} = (r_{cr}, 0, \pm\sqrt{f(r_{cr})})$ with eigenvalues given by $\lambda_1 = 0$ and the roots of

$$\lambda^2 = \alpha A(\alpha - 2)r_{cr} + \beta B(\beta - 2). \tag{2.28}$$

Again, the nature of these equilibria will depend on the values of parameters α and β.

2.2.3 Global Flow for Negative Energy

Case $0 < \alpha < \beta < 2$

If $h < 0$ is fixed one can depict the energy manifold $\tilde{M}_h$ as in Figure ?? and conclude immediately that all orbits are bounded. The equilibria points of collision/ejection are at $C^{\pm} = (0, \pm\sqrt{2B}, 0)$ and, by (2.20), both of them are saddles. Using calculus methods, one can check that (2.26) has one root $r = r_{cr}$ and consequently there are two equilibrium points at $R^{\pm} = \left(r_{cr}, 0, \pm\sqrt{f(r_{cr})}\right)$. Following formula (2.27) and taking into account that $h < 0$ and $0 < \alpha < \beta < 2$, we deduce that $R^{\pm}$ are degenerate centers which translates into stable circular motion in the physical space.

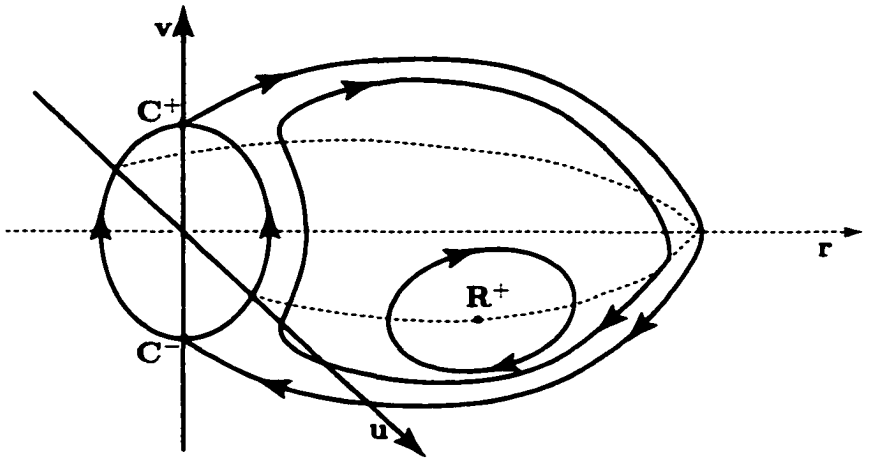

Figure 2.5: The global flow in RSC for $h < 0$ and $0 < \alpha < \beta < 2$

The collision/ejection orbits are confined to the invariant manifold $u = 0$ meaning that the motion is radial. The rest of the orbits in RSC are periodic, as it will be proved in the following lemma, meaning that in full unreduced phase space, they fill in densely the energy manifold $\tilde{M}_h$.

Lemma 2.2.3 For any set of initial conditions $p := (r_0, v_0, u_0)$ with $r_0 \neq 0$ and $u_0 \neq 0$, the orbit through p in RSC is periodic and of non-collisional type.

Proof: Let ϕ_p be the orbit with initial condition p. Since $\tilde{M}_h$ is compact, ϕ_p either begins and ends in one of the equilibria of $\tilde{M}_h$, namely $C^{\pm}$ or $R^{\pm}$, or is periodic. But if ϕ_p end (starts) in any of $C^{\pm}$, then it belongs all the time to the invariant manifold $u = 0$, which is a contradiction since we assumed $u_0 \neq 0$. It remaines that ϕ_p ends(starts) in one of $R^{\pm}$, but this is again a contradiction since both $R^{\pm}$ are centers. It follows that the $\alpha(\omega)$-limit set of p contains no fixed points and, by Poincaré theorem, the orbit through p is periodic.

Case $0 < \alpha < \beta = 2$

For $\beta = 2$ the reduced system (2.24) receives the simpler form

$$\begin{cases} r' = (\beta - \alpha) rv \\ v' = u^2 + v^2 - \alpha A r - \beta B \\ u' = 0, \end{cases} \tag{2.29}$$

Every point of the circle $v^2 + u^2 = 2B$ is an equilibrium, each of them being a degenerate source for $v > 0$, a degenerate sink for $v < 0$ and a degenerate saddle for $v = 0$. The invariant energy manifold N_h is sliced vertically by the invariant planes $u = c = constant$. In particular, for any $|c| < \sqrt{2B}$, the orbits are ending/ejecting in/from the collision manifold implying that the set of initial conditions in the (h, c) plane leading to collision/ejection has positive Leabesgue measure. Exploiting the particular form of the equation, one can actually compute the root of (2.27) obtaining

$$r_{cr} = \left[\frac{A(2-\alpha)}{2(-h)} \right]^{\frac{2-\alpha}{\alpha}} \tag{2.30}$$

and consequently the equilibria $R^{\pm} = (r_{cr}, 0, \pm\sqrt{f(r_{cr})})$. Their eigenvalues are given by $\lambda_1 = 0$, $\lambda_{2,3} = \pm i\sqrt{\alpha A(2-\alpha)}$, with the result that $R^{\pm}$ are degenerate centers. Moreover, since $(r_{cr}, f(r_{cr}))$ is the maximum point for $f(r)$ and the planes $u = c$ are invariant, one can deduce that for $\sqrt{2B} \leq |c| < f(r_{cr})$ the motion in RSC is periodic. For all values of $|u| = |c| < \sqrt{2B}$ the orbits are heteroclinic, connecting points on the collision/ejection circle symmetrically located with respect to the u axis. The phase portrait is skeched in Figure 2.6.

Case $0 < \alpha < 2 < \beta$

In this subcase, by (2.20), the collision equilibrium point $C^+ = (0, +\sqrt{2B}, 0)$ is a source and $C^- = (0, -\sqrt{2B}, 0)$ is a sink. Equation (2.27) requires a further analysis in order to determine its roots. Denoting

$$g(r) = f(r) - \alpha A r - \beta B, \tag{2.31}$$

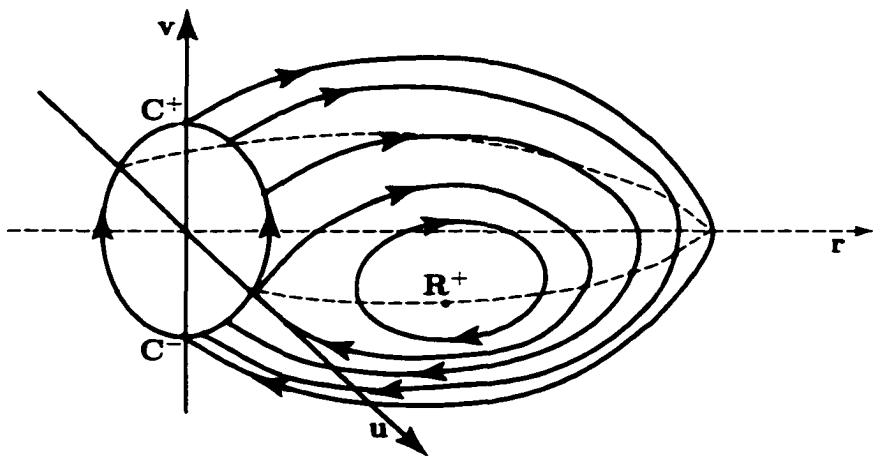

Figure 2.6: The global flow in RSC for $h < 0$ and $0 < \alpha < \beta = 2$

one can see that this function has a critical point at

$$r_0 = \left[\frac{A(2-\alpha)(\beta-\alpha)}{2(-h)\beta}\right]^{\frac{(\beta-\alpha)}{\alpha}}. \tag{2.32}$$

Using elementary calculus, we deduce that the equation (2.27) admits two, one or no roots as $g(r_0)$ is strictly positive, zero, or strictly negative, respectively.

If $g(r_0) > 0$, besides the collision rest points, the reduced system admits two pairs of equilibria at $R_1{}^{\pm} = \left(r_{cr(1)}, 0, \pm\sqrt{f(r_{cr(1)})}\right)$ and $R_2{}^{\pm} = \left(r_{cr(2)}, 0, \pm\sqrt{f(r_{cr(2)})}\right)$ with $r_{cr(1)} < r_0 < r_{cr(2)}$. As already mentioned, the eigenvalues attached to $R_i{}^{\pm}$ $(i = 1, 2)$ are given by $\lambda_1 = 0$ and $\lambda_{2,3}$ the roots of

$$\lambda^2 = \alpha A(\alpha-2)r_{cr(i)} + \beta B(\beta-2) \quad \text{where} \quad i = 1, 2. \tag{2.33}$$

In order to establish the nature of these equilibria, let us notice first that since $r_{cr(1)} < r_0$ is root of (2.27),

$$B(\beta-2) = r_{cr(1)}\left[A(2-\alpha) - 2(-h)(r_{cr(1)})^{\frac{\alpha}{(\beta-\alpha)}}\right] > r_{cr(1)}\left[A(2-\alpha) - 2(-h)(r_0)^{\frac{\alpha}{(\beta-\alpha)}}\right]. \tag{2.34}$$

Replacing r_0 in the previous relation with its exact value (2.32) it follows that

$$B(\beta-2) > \frac{\alpha A(2-\alpha)}{\beta} r_{cr(1)}, \tag{2.35}$$

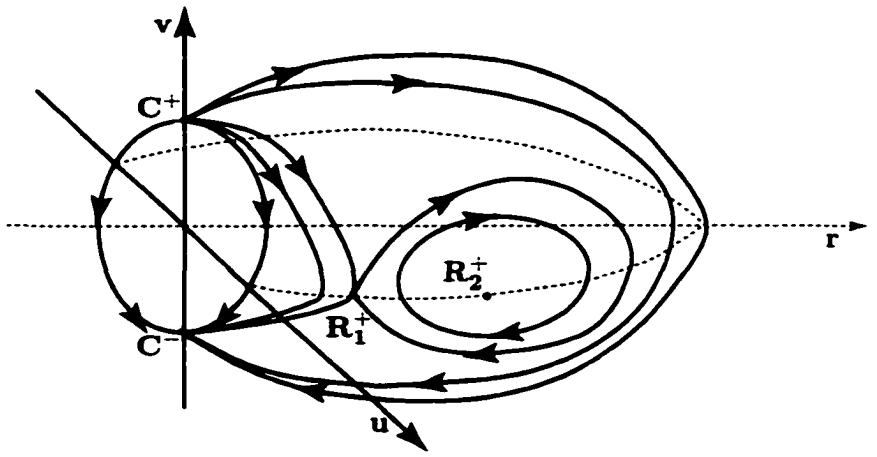

Figure 2.7: The global flow in RSC for $h < 0$ and $0 < \alpha < 2 < \beta$, case $g(r_0) > 0$

from where it results that for $i = 1$ the right hand side of (2.33) is positive. This implies that $R_1{}^{\pm}$ are degenerate saddles.

For $R_2{}^{\pm}$, $\lambda_1 = 0$ and, since $\alpha < \beta$,

$$\lambda^2 = \alpha A(\alpha - 2)r_{cr(2)} + \beta B(\beta - 2) < \alpha[A(\alpha - 2)r_{cr(2)} + B(\beta - 2)]. \qquad (2.36)$$

But $r_{cr(2)}$ is root of (2.27), i.e.

$$f(r_{cr(2)}) - \alpha A r_{cr(2)} - \beta B = A(2 - \alpha)r_{cr(2)} + B(2 - \beta) + 2h(r_{cr(2)})^{\beta/(\beta-\alpha)} = 0$$

from where

$$A(\alpha - 2)r_{cr(2)} + B(\beta - 2) = 2h(r_{cr(2)})^{\beta/(\beta-\alpha)}$$

. Replacing the last relation into (2.36) we obtain $\lambda^2 < 2\alpha h(r_{cr(2)})^{\beta/(\beta-\alpha)} < 0$, with the result that $R_2{}^{\pm}$ are degenerate centers.

The phase portrait is depicted in Figure 2.7. The orbits are all bounded and there is a set of initial conditions of positive Lebesgue measure that leads to ejection/collision trajectories. Also, there is a large set of initial conditions for which the orbits are periodic.

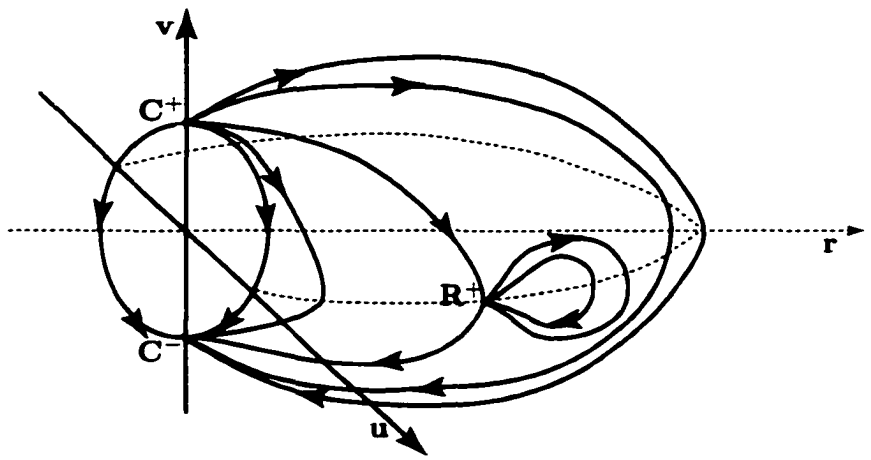

Figure 2.8: The global flow in RSC for $h < 0$ and $0 < \alpha < 2 < \beta$, case $g(r_0) = 0$

If $g(r_0) = 0$ there is a pair of equilibrium points at $R^{\pm} = (r_{cr}, 0, \pm\sqrt{f(r_{cr})})$ where $r_{cr} = r_0$ and the eigenvalues attached are given by $\lambda_1 = \lambda_2 = \lambda_3 = 0$. For the moment we cannot conclude anything about the nature of these rest points. A closer look at the vector field of system (2.24) reveals that r is increasing for $v > 0$ and decreasing for $v < 0$. Therefore, $R^{\pm}$ cannot be sinks or sources. If R^{+}, for instance, was a center, then it would be surrounded by closed periodic orbits. $\tilde{M}$ would be filled in by these orbits and the flow would be similar to that in Figure 2.5. But this is not possible since near the collision manifold Λ the continuity with respect to initial data would be contradicted (orbits on λ flow from C^{+} towards C^{-} and orbits near Λ would have opposite sense). We conclude that $R^{\pm}$ are degenerate saddles. The entire phase space is filled in by heteroclinic orbits that begin/end in collision (see Figure 2.8).

If $g(r_0) < 0$, besides the ejection-source/collision-sink equilibria there are no other rest points. The flow is depicted in Figure 2.9 and for any set of initial conditions the orbits are beginning/ending in collision.

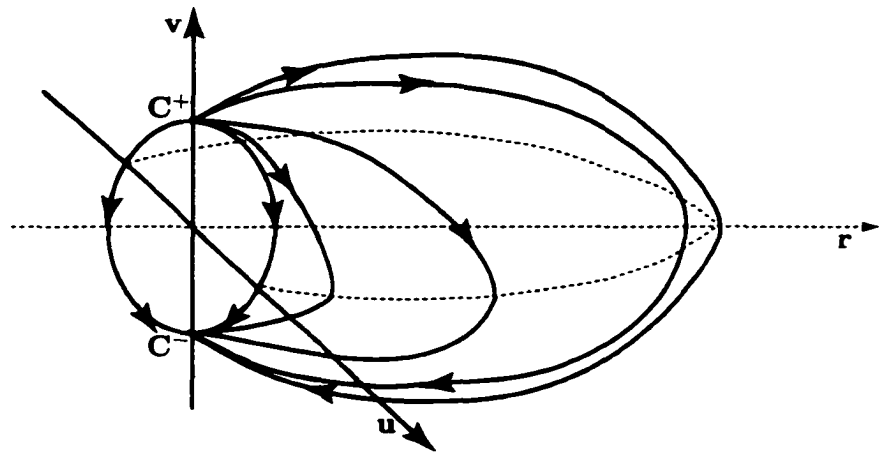

Figure 2.9: The global flow in RSC for $h < 0$ and $0 < \alpha < 2 < \beta$, case $g(r_0) < 0$, and for $2 \leq \alpha < \beta$

Case $2 \leq \alpha < \beta$

The phase portrait is fully analogous to that given in Figure 2.9. The invariant manifold M_h is filled in densely by heteroclinic orbits joining the source C^+ with the sink C^-.

We end this subsection by summarizing the above conclusions in the following statement:

Theorem 2.2.4 (*The global flow for negative energy*)

Let us consider the relative two-body problem with quasihomogeneous interaction defined by system (2.1) with given constants $A > 0$, $B > 0$ and $0 < \alpha < \beta$ and negative total energy $h < 0$. Also, let us define the equation

$$(2-\beta)B + (2-\alpha)Ar + 2hr^{\frac{\beta}{\beta-\alpha}} = 0. \tag{2.37}$$

Then the only possible scenarios of motion are:

(1) if $0 < \alpha < \beta < 2$ all orbits are quasiperiodic except a set of zero Lebesque measure given by ejection-collision zero angular velocity orbits. For each $h < 0$ fixed,

in the set of quasiperiodic orbits there are two stable circulatory orbits at $r = r_{cr}$, where r_{cr} is the positive solution of (2.37);

(2) if $0 < \alpha < \beta = 2$ the orbits are either quasiperiodic, or bounded ejections followed by collisions. The set of initial conditions leading to ejection-collision orbits has positive Lebesgue measure. For each $h < 0$ fixed, in the set of quasiperiodic orbits there are two stable circulatory orbits at $r = r_{cr}$, where r_{cr} is the positive solution of (2.37);

(3) if $0 < \alpha < 2 < \beta$ all orbits are either quasiperiodic, or bounded ejections followed by collisions. The set of initial conditions leading to ejection-collision orbits has positive Lebesgue measure. For each $h < 0$ fixed, if the equation (2.37) admits two positive solutions $r_{cr(1)} < r_{cr(2)}$, then the set of ejection-collision orbits is glued to the set of quasiperiodic orbits by the unstable circulatory orbit $r = r_{cr(1)}$ and in the set of quasiperiodic orbits there are two stable circulatory orbits at $r = r_{cr(2)}$; if the equation (2.37) admits one positive solution $r = r_{cr}$ then except two unstable circulatory orbits at $r = r_{cr}$ all orbits are bounded ejections-collisions; finally, if the equation (2.37) doesn't have any solutions then all orbits are bounded ejections-collisions;

(4) if $2 \leq \alpha < \beta$ all orbits are ejection-collision and the Lebesgue measure of the initial data leading to collision is infinity.

2.2.4 Zero Energy Flow in RSC

For $h = 0$, the analysis of the RSC is simplified since the term $2hr^{\beta/(\beta-\alpha)}$ in the energy integral is zero. Therefore the energy invariant manifold $\tilde{M}_{h0}$ is generated by the relation:

$$v^2 + u^2 = 2B + 2Ar = f(r). \tag{2.38}$$

Again we will discuss the phase portraits in function of the parameters α and β.

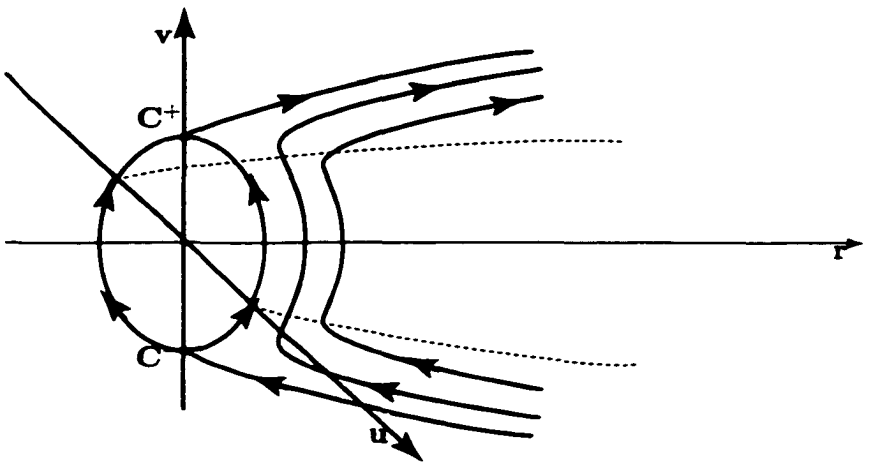

Figure 2.10: The flow in RSC for $h = 0$ and $0 < \alpha < \beta$

Case $0 < \alpha < \beta < 2$

The phase space is represented in Figure 2.10. The collision rest points $C^{\pm}$ are the only equilibria. Except on the plane $u = 0$, all orbits are coming from infinity and return asymptotically to infinity. On $u = 0$ (i.e. for radial motion) there are two orbits, one colliding in C^-, the other one ejecting from C^+. Since the collision is possible only for $u = 0$, i.e. only for zero angular momentum (see (2.10)), we conclude that the Lebesgue measure of the initial conditions leading to collision is zero.

Case $0 < \alpha < \beta = 2$

Since $\beta = 2$ the reduced system receives again the particular form (2.29). The points of the collision circle $v^2 + u^2 = 2B$ are all equilibria, sources if $v > 0$, sinks if $v < 0$, and saddles if $v = 0$. Every vertical plane $u = c$ is invariant and for $|u| = |c| \leq \sqrt{2B}$ all orbits are of collisional type. For $|u| = |c| > \sqrt{2B}$ the orbits are unbounded. Such an orbit comes from infinity, attains an r-minimal point $(r_{min}, 0, u_{max})$ and returns asymptotically to infinity (see Figure 2.11).

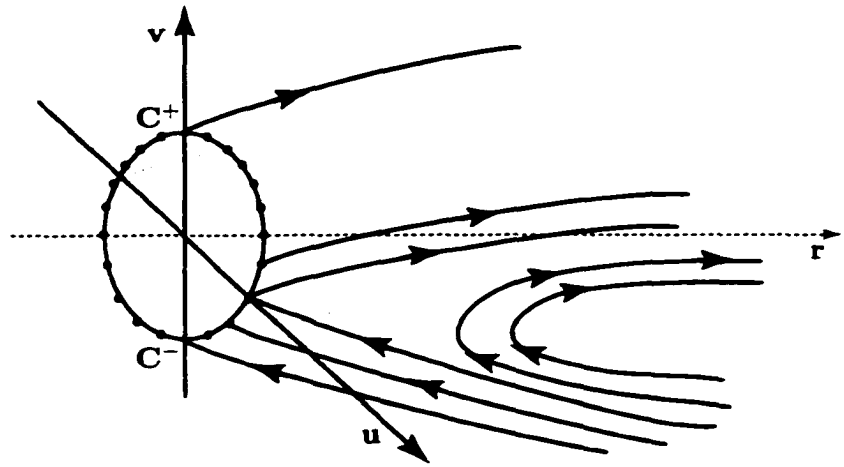

Figure 2.11: The flow in RSC for $h = 0$ and $0 < \alpha < \beta = 2$

Case $0 < \alpha < 2 < \beta$

In this subcase the rest point C^+ is a source and C^- is a sink. Using (2.27) and taking into account that $h = 0$, there are other two equilibria $R^{\pm}$ located at $(r_{cr}, 0, \pm\sqrt{2B})$ where $r_{cr} = \dfrac{B(\beta-2)}{A(2-\alpha)}$. The eigenvalues associated are given by (2.28) from where, replacing the exact value of r_{cr}, it results in $\lambda_1 = 0$ and $\lambda_{2,3} = \pm\sqrt{B(\beta-2)(\beta-\alpha)}$. It follows that $R^{\pm}$ is a degenerate saddle. The phase portrait is depicted in Figure 2.12. The orbits are either bounded of collisional type or unbounded. Also, there is a positive measure set of initial data leading to collision.

Case $2 \leq \alpha < \beta$

The phase space is depicted in Figure 2.13. All orbits with radial velocity $\sqrt{2B + \dfrac{2A(\alpha-2)}{\beta-2}r} \leq |v| \leq \sqrt{2B + 2Ar}$ are unbounded, ejecting from the source C^+, or colliding in the sink C^-. The orbits with $|v| < \sqrt{2B + \dfrac{2A(\alpha-2)}{\beta-2}r}$ are bounded of collisional type.

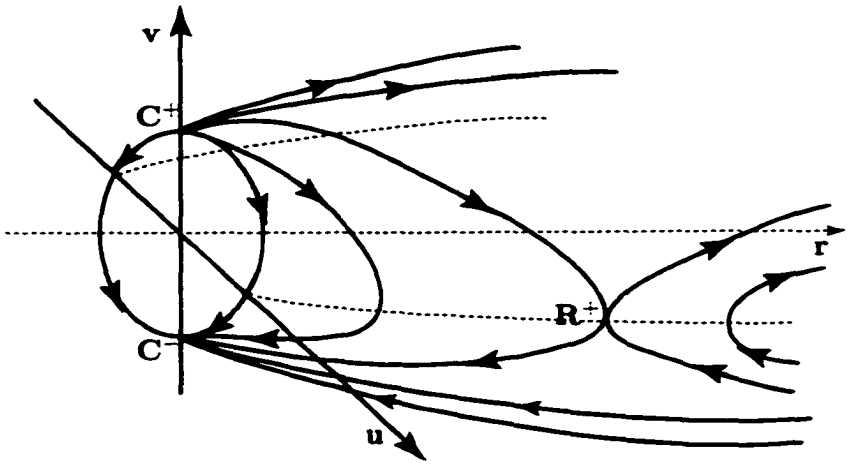

Figure 2.12: The flow in RSC for $h = 0$ and $0 < \alpha < 2 < \beta$

2.2.5 Positive Energy Flow in RSC

Case $0 < \alpha < \beta < 2$

The motion is unbounded unless it takes place on the invariant manifold $u = 0$ (see Figure 2.14). The orbits lying in $u = 0$ are the only ones attaining the collision saddle equilibria $C^{\pm}$ implying that the Lebesque measure of the set of initial conditions leading to collision is zero.

Case $0 < \alpha < \beta = 2$

Again, for $\beta = 2$, the phase space changes drastically. Sliced vertically by the invariant planes $u = c$, the energy manifold $\tilde{M}_h$ is filled in by orbits ejecting/ending from/in the equilibria circle $v^2 + u^2 = 2B$ if $|u| = |c| \leq \sqrt{2B}$ and by unbounded orbits coming from and returning asymptotically to infinity if $|u| = |c| > \sqrt{2B}$ (see Figure 2.15).

Case $0 < \alpha < 2 < \beta$

For the following remaining three subcases the phase portrait is basically the same and is depicted in Figure 2.16. The orbits are bounded of collisional type or un-

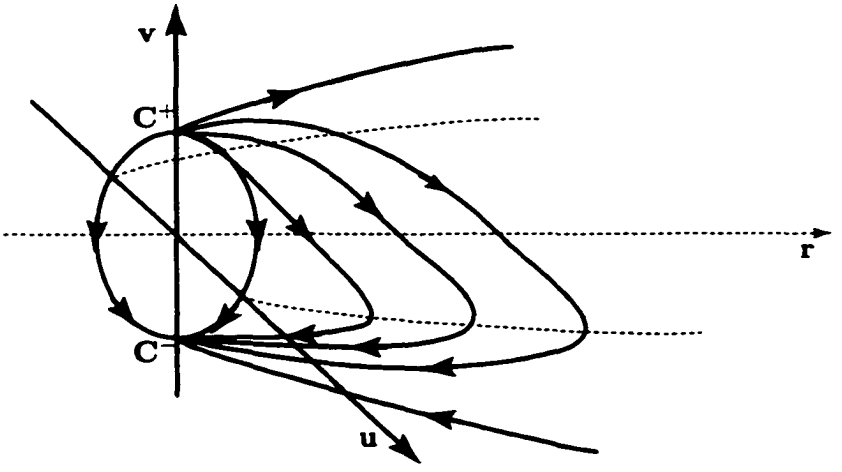

Figure 2.13: The flow in RSC for $h = 0$ and $2 \leq \alpha < \beta$

bounded and the Lebesgue measure of the set of initial conditions leading to collision is positive. Since equation (2.27) admits a real positive root $r = r_{cr}$, we conclude that besides the source C^+ and the sink C^-, there are two other rest points located at $\left(r_{cr}, 0, \pm\sqrt{f(r_{cr})}\right)$. Their eigenvalues are given by (2.27). As it will be shown, these points are degenerate saddles but in order to prove this affirmation we still have to distinguish between the three different subcases of α's location with respect to 2.

For $(0 < \alpha < 2 < \beta)$, since r_{cr} is a root of (2.27) i.e. $f(r_{cr}) - \alpha A r_{cr} - \beta B = A(2-\alpha)r_{cr} + B(2-\beta) + 2h(r_{cr})^{\beta/(\beta-\alpha)} = 0$, it results in

$$\lambda^2 = \alpha A(\alpha - 2)r_{cr} + \beta[2h(r_{cr})^{\beta/(\beta-\alpha)} + A(2-\alpha)r_{cr}]$$

or

$$\lambda^2 = A(2-\alpha)(\beta-\alpha) + 2h(r_{cr})^{\beta/(\beta-\alpha)} > 0$$

from where it follows that $R^{\pm}$ are degenerate saddles.

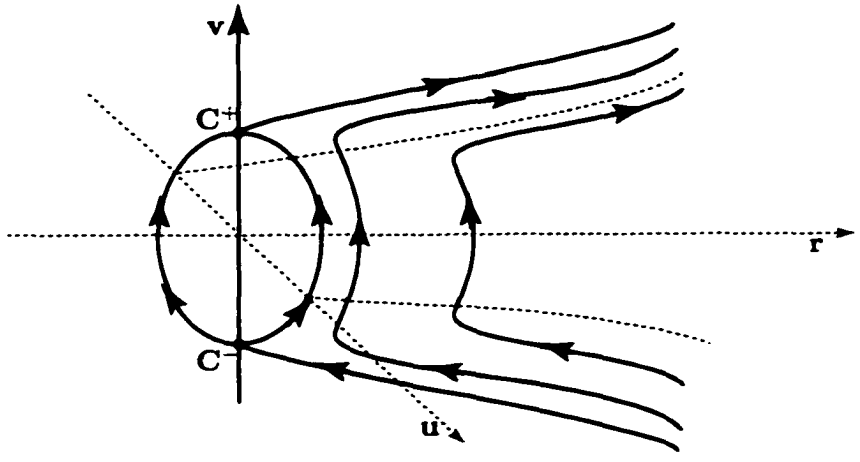

Figure 2.14: The flow in RSC for $h > 0$ and $0 < \alpha < \beta < 2$

Case $2 = \alpha < \beta$

In this situation r_{cr} can be computed exactly, namely

$$r_{cr} = \left[\frac{B(\beta-2)}{2h}\right]^{\frac{\beta-\alpha}{\beta}}. \tag{2.39}$$

The eigenvalues are given by $\lambda_1 = 0$ and $\lambda_{2,3} = \pm\sqrt{\beta B(\beta-2)}$ obtaining again that $R^{\pm}$ is a degenerate saddle (see Figure 2.16).

Case $2 < \alpha < \beta$

Here we have to return to equation (2.27). The function $g(r) = f(r) - \alpha A r - \beta B$ has a critical point for

$$r_0 = \left[\frac{A(\alpha-2)(\beta-\alpha)}{2h\beta}\right]^{\frac{(\beta-\alpha)}{\alpha}} \tag{2.40}$$

and the solution $r = r_{cr}$ of (2.27) (or $g(r) = 0$) obeys $r_{cr} > r_0$. Since r_{cr} satisfies for $g(r) = B(\beta-2) + r_{cr}[A(2-\alpha) + 2h(r_{cr})^{\frac{\alpha}{\beta-\alpha}}] = 0$, and $r_{cr} > r_0$ it follows

$$B(\beta-2) = r_{cr}[A(2-\alpha) + 2h(r_{cr})^{\frac{\alpha}{\beta-\alpha}}] > r_{cr}[A(2-\alpha) + 2hr_0{}^{\frac{\alpha}{\beta-\alpha}}], \tag{2.41}$$

and, further, after replacing r_0 with its exact value (2.40)

$$B(\beta-2) > -\frac{\alpha A(\alpha-2)}{\beta} r_{cr}. \tag{2.42}$$

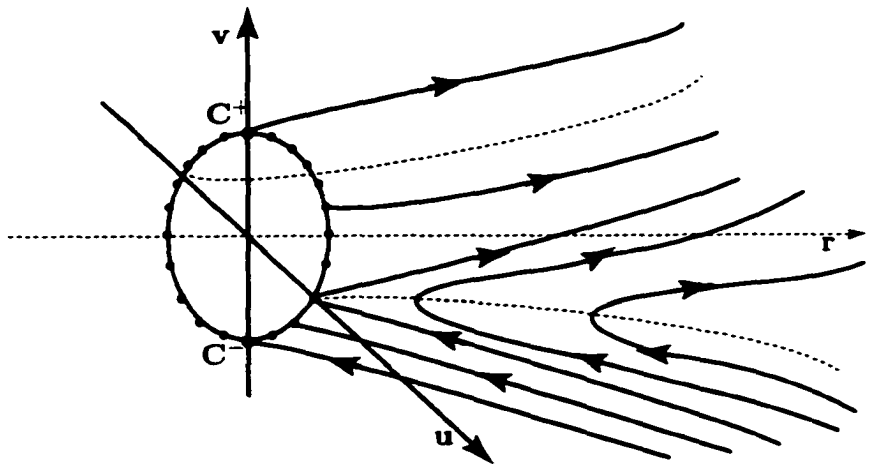

Figure 2.15: The flow in RSC for $h > 0$ and $0 < \alpha < \beta = 2$

which is equivalent to $(\lambda_{2,3})^2 > 0$. Completing the last assertion with $\lambda_1 = 0$ we deduce that $R^{\pm}$ are degenerate saddles (see Figure 2.16).

2.3 The Flow at Infinity

To provide a global picture of the flow for $h \geq 0$, we need to analyse the behaviour of the orbits attaining infinity asymptotically in time. Essentially, for each $h \geq 0$ fixed, we shall resort to an inverse transform of the radius vector r into $\rho = \frac{1}{r^{\alpha}}$, bringing the fictitious points $r = \infty$ into the so-called infinity manifolds $\rho = 0$. We fully characterize to flow on them and then, in a similar manner to the reduction performed in section 2.2.2, we retain the equations in (ρ, v, u), introduce the *Reduced System Near Infinity* (denoted RSI) and offer a complete picture of the flow on it.

We now return to system (2.1) and the transformations (2.5). Choosing $\gamma = 1$ and $\delta = 0$ (which actually means a change of variables into polar coordinates) and introducing

$$\rho = \frac{1}{r^{\alpha}}, \tag{2.43}$$

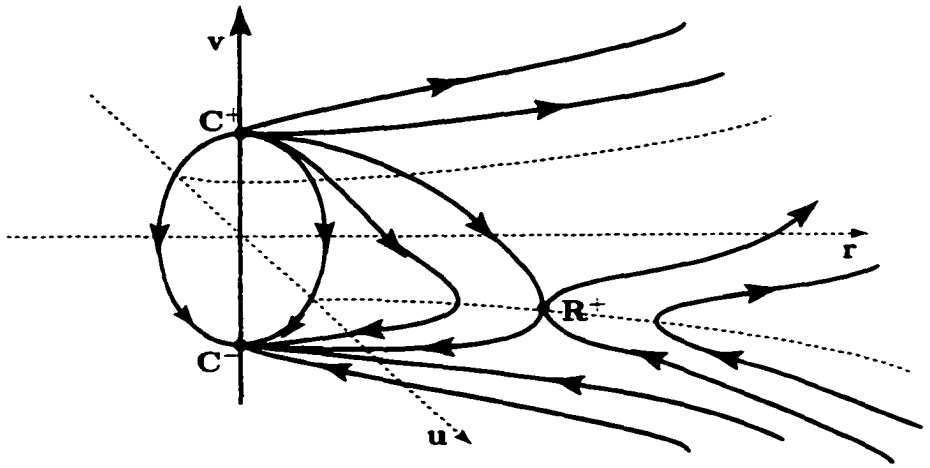

Figure 2.16: The flow in RSC for $h > 0$ and $2 < \beta$

we are led to the system:

$$\begin{cases} \rho' = -\alpha\rho v \\ \theta' = u \\ v' = u^2 - \alpha A\rho - \beta B\rho^{\frac{\beta}{\alpha}} \\ u' = -uv, \end{cases} \tag{2.44}$$

with the first integrals:

$$u^2 + v^2 = 2A\rho + 2B\rho^{\frac{\beta}{\alpha}} + 2h \tag{2.45}$$

and

$$u = c\rho^{\frac{1}{\alpha}}. \tag{2.46}$$

Replacing $\rho^{\frac{\beta}{\alpha}}$ from (2.44) with its corresponding value from (2.45) we obtain the analytical system:

$$\begin{cases} \rho' = -\alpha\rho v \\ \theta' = u \\ v' = \frac{1}{2}(2-\beta)u^2 - \frac{\beta}{2}v^2 + A(\beta-\alpha)\rho + \beta h \\ u' = -uv. \end{cases} \tag{2.47}$$

Similar to our analysis in section 4.1, we know that for any h fixed the flow is confined on the 2-dimensional invariant manifold provided by the class C^1 energy

integral, namely:

$$N_h = \{(\rho, \theta, v, u) | \, u^2 + v^2 = 2A\rho + 2B\rho^{\frac{\beta}{\alpha}} + 2h, \, \theta \in [0, 2\pi)\}. \tag{2.48}$$

2.3.1 The Infinity Manifolds

From system (2.47) it follows that for each $h \geq 0$ fixed, the manifold $\rho = 0$ is invariant under the flow. To obtain a picture of the orbits in a neighbourhood of infinity we introduce *the infinity manifolds*, denoted I_h, where $h \geq 0$, as the restriction of the energy manifold N_h to $\rho = 0$, i.e.

$$I_h = \{(\rho, \theta, v, u) | \, \rho = 0, \, \theta \in [0, 2\pi), \text{ and } v^2 + u^2 = 2h\}. \tag{2.49}$$

Unlike the collision manifold which is the uniquely defined independent of the level of energy, the fictitious infinity manifolds depend continuously on h. For each $h > 0$ fixed, the corresponding infinity manifold I_h is a 2-dimensional torus which shrinks to a circle as $h \longrightarrow 0+$.

Using the energy integral, the flow on I_h is given by:

$$\begin{cases} \theta' = u \\ v' = 2h - v^2 \\ u' = -uv. \end{cases} \tag{2.50}$$

For each $h > 0$ fixed, the infinity manifold torus possesses two circles of equilibria at $v = \pm\sqrt{2h}$ and all orbits are strictly increasing with respect to v (see Figure 2.17). If $h = 0$ the infinity manifold is a circle of degenerate equilibria.

2.3.2 The Reduced System Near Infinity (RSI)

The above description provides a local picture of the flow on the fictitious infinity manifolds. We return now to the system (2.47) and point out some of its general characteristics.

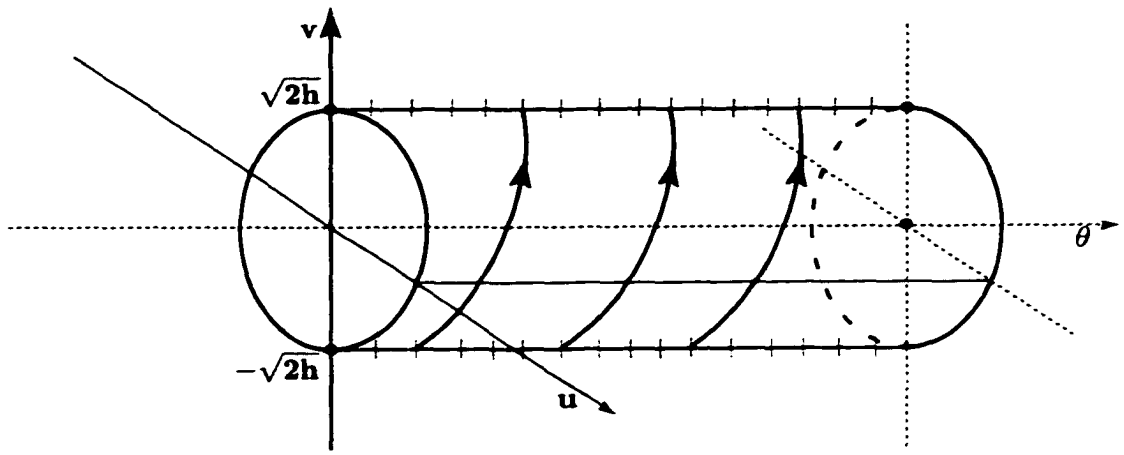

Figure 2.17: The flow on the Infinity Manifold I_h for $h > 0$

First, let us observe that the set $\{(\rho, \theta, v, u) | \, u = 0\}$ is an invariant manifold and on it the flow is always decreasing with respect to v. Second, computing the global equilibria of system (2.47), we obtain two circles of rest points located at $I_h^{\pm} := (0, \theta_0, \pm\sqrt{2h}, 0)$, $\theta_0 \in [0, 2\pi)$. Calculating the corresponding eigenvalues we deduce that I_h^- is a degenerate source with $\lambda_1 = \alpha\sqrt{2h}$, $\lambda_2 = 0$, $\lambda_3 = \beta\sqrt{2h}$, $\lambda_4 = 0$ and $I_h^+$is a degenerate sink with $\lambda_1 = -\alpha\sqrt{2h}$, $\lambda_2 = 0$, $\lambda_3 = -\beta\sqrt{2h}$, $\lambda_4 = 0$.

In section 2.2.2 we introduced the reduced system near collision RSC by taking into account that the (r, v, u) coordinates are independent of the cyclic coordinate θ. The same reasoning holds for system (2.44) as well. We isolate the θ equation and define the *Reduced System Near Infinity* (RSI):

$$\begin{cases} \rho' = -\alpha\rho v \\ v' = \frac{1}{2}(2-\beta)u^2 - \frac{\beta}{2}v^2 + A(\beta - \alpha)\rho + \beta h \\ u' = -uv, \end{cases} \tag{2.51}$$

keeping in mind that the orbits of RSI must be regarded in the full phase space $\times \mathcal{S}^1$ i.e. manifolds of solutions.

The flow of the RSI is confined to the 2-dimensional surface $\tilde{N}_h$ generated by the energy integral. The global equilibria $I_h^{\pm}$ of system (2.47) become rest points for RSI as well. Similar to the RSC system, the orbits in RSI are symmetric with respect

to the planes $\{u = 0\}$ and $\{v = 0\}$ i.e. $(r(\tau), -v(\tau), u(\tau)) = (r(-\tau), v(-\tau), u(-\tau))$ and $(r(\tau), -v(\tau), -u(\tau)) = (r(-\tau), v(-\tau), u(-\tau))$. Also, we can use the momentum integral (2.46) each time we are far enough from the singular surface $\rho = 0$ such that the lack of smoothness of (2.46) around $\rho = 0$ is not effecting our analysis.

The relative equilibria of the unreduced system are to be found as equilibria in RSI by setting $v = v' = 0$. Using calculus methods and taking into account the range of α, β and h we obtain different pictures for the flow.

2.3.3 Positive Energy Flow in RSI

Case $0 < \alpha < \beta \leq 2$

The reduced flow in this case is quite simple. There are no other equilibria except the infinity ones, namely the degenerate source ${I_h}^-$ and the degenerate sink ${I_h}^+$. The orbits are flowing out from/into the infinity manifold in the southern hemisphere, respectively, the northern hemisphere of the energy manifold. The concavity of the trajectories is changing with respect to α, being in the (ρ, u)-plane concave up if $\alpha < 1$ and concave down if $\alpha > 1$ (see Figures 2.18, respectively, 2.19).

Case $2 < \beta$

Here, besides the infinity rest points ${I_h}^{\pm}$ we obtain other two equilibria at $E^{\pm} = (\rho_{cr}, 0, \pm u_{cr})$, where ρ_{cr} solves $A(2-\alpha)\rho + B(2-\beta)\rho^{\frac{\beta}{\alpha}} + 2h = 0$ and u_{cr} verifies the energy relation for $v = 0$ and $\rho = \rho_{cr}$. The corresponding eigenvalues are given by $\lambda_{1,2} = \pm\sqrt{A\alpha(\beta-\alpha)\rho_{cr}}$ and $\lambda_3 = -|u_{cr}|$, therefore $\tilde{E}^{\pm}$ are saddles. In order to provide the picture of the reduced flow we need the following:

Lemma 2.3.1 There is an orbit, denoted $\phi(\tau)$, that starts in E^+ and ends in I_h^+. Moreover, the v component of this orbit is always positive.

Proof Since E^+ is a nondegenerate saddle, there is an orbit $\phi(\tau)$ that exits E^+ into

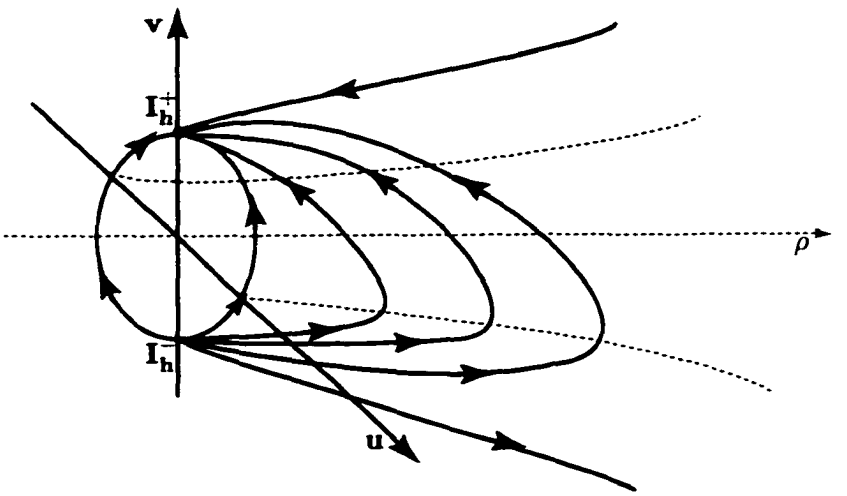

Figure 2.18: The global flow in RSI for $h > 0$ and $0 < \alpha < 1 < \beta \leq 2$

the positive halfspace $v > 0$. From system (2.51) it follows that the function $\rho(\tau)$ is decreasing with respect to time as long as v stays positive. Let us assume that there is a time τ_0 such that the v component of $\phi(\tau)$ becomes 0. Then, since the orbits are symmetric with respect to the plane $v = 0$, it follows that $\phi(\tau)$ returns to E^+. But, because the flow in confined on a 2-dimensional manifold, this would imply the existence of another fixed point inside $\phi(\tau)$ which is a contradiction.

Therefore, the v component of $\phi(\tau)$ is always strictly positive, the orbit is decreasing in ρ all the time, and the equilibrium I_h^+ is the only possible limit for $\phi(\tau)$.

Lemma 2.3.2 There is an orbit, denoted $\psi(\tau)$, that comes from "infinity" (i.e. $lim_{\tau \to (-\infty)} \rho(\tau) = \infty$ and ends in E^+. Moreover, the v component of this orbit is always positive.

Proof Since E^+ is a nondegenerate saddle, there is an orbit $\psi(\tau)$ that ends in E^+ from the positive halfspace $v > 0$. From system (2.51) it follows that the function

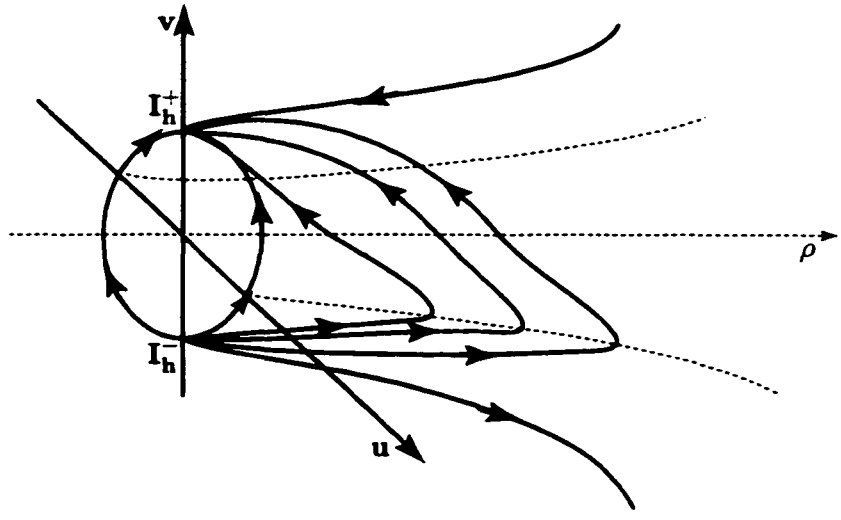

Figure 2.19: The global flow in RSI for $h > 0$ and $1 < \alpha < \beta \leq 2$

$\rho(\tau)$ is decreasing with respect to time as long as v stays positive. Going backwards in time along $\psi(\tau)$, let us assume that there was a time τ_0 subch that $v(\tau_0) = 0$. Then, since the orbits are symmetric with respect to the plane $v = 0$, it follows that $\psi(\tau)$ started at E^+. But, because the flow in confined on a 2-dimensional manifold, this would imply the existence of another fixed point inside $\phi(\tau)$ which is a contradiction.

Therefore, the v component of $\psi(\tau)$ is always strictly positive, the orbit comes from infinity, is decreasing in ρ all the time, and ends in the equilibrium E^+.

It is clear now how the orbits flow on $\tilde{N}_h$. Looking at the halfspace $u > 0$ there are 4 distinct invariant manifolds: the orbits inside $\phi(\tau)$, exiting I_h^- and ending in I_h^+; the orbits inside $\psi(\tau)$, coming from $\rho = \infty$, reaching a minimum ρ and going back to $\rho = \infty$; the orbits under $\phi(\tau)$ and $\psi(\tau)$, all exiting I_h^- and escaping to $\rho = \infty$ and, finally, the orbits above $\phi(\tau)$ and $\psi(\tau)$, all coming from $\rho = \infty$ and ending into I_h^+. Again, the concavity of the trajectories is changing with respect to α, being in the (ρ, u)-plane concave up if $\alpha < 1$ and concave down if $\alpha > 1$ (see Figures 2.20,

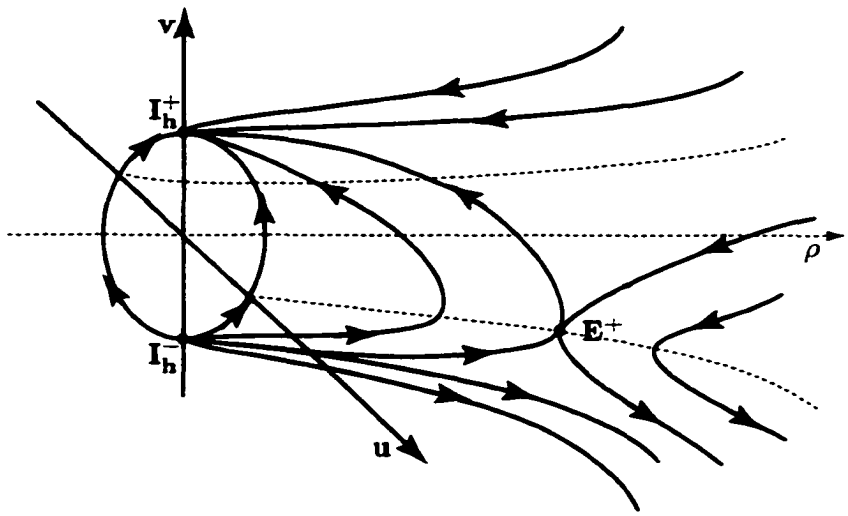

Figure 2.20: The global flow in RSI for $h > 0$ and $0 < \alpha < 1$ and $\beta > 2$

respectively 2.21).

2.3.4 Zero Energy Flow in RSI

One approach in skeching the flow in this case would be to return to the system(2.51), ignore the terms having factor h, and start all over again with a detailed analysis. But, since the system(2.51) is analytic and the infinity manifolds are differentiable for any $h \geq 0$, we are able to take full advantage of the continuity of solutions with respect to initial data.

We think about the flow that is confined on the surface $\tilde{N}_h$ which, as $h \to 0$, shrinks at its left end. At the limit $h = 0$, the projection circle of the infinity manifolds I_h of radius $\sqrt{2h}$ shrinks to the origin. Under this process of passing to the limit, the flow pictures from the case $h > 0$ preserve themselves in a neighborhood of $\rho = 0$. On the cut $\rho = 0$, the two infinity equilibria I_h^- and I_h^+ approach the origin as h tends to 0. At the limit $h = 0$, the two rest points become one degenerate equilibrium in the origin ($I^- = I^+ = origin$). The flow pictures are skeched in Figures 2.22, 2.23, 2.24, 2.25, and 2.26.

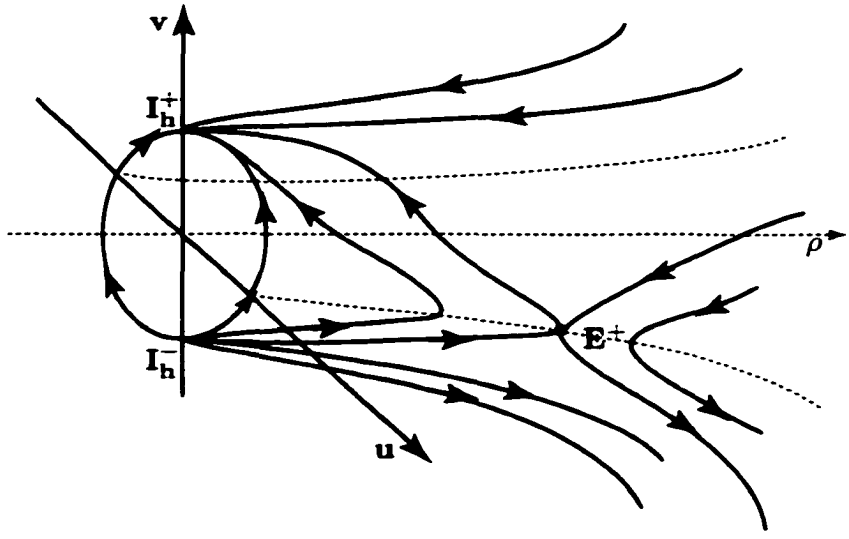

Figure 2.21: The global flow in RSI for $h > 0$ and $1 \leq \alpha$ and $\beta > 2$

2.4 The Global Flow for Non-Negative Energy

We are able now to offer a complete picture of the global flow for the quosihomogeneous two-body problem with zero or strictly positive energy.

The underlying idea is that the orbits of both system (2.8) and system (2.47) are the same as the orbits of system (2.1), only the parametrization is different. First, we approached the flow near collision looking at the fictitious collision manifold, obtaining results about the behaviour near the collision, introducing RSC and sketching the flow on it, without any information about the behaviour at infinity. Then, we moved at the other end of the flow, and, in an analogous manner, we defined the fictitious infinity manifolds, described them, introduced RSI and offered a picture of the flow in this new chart that allowed us to see the infinity points. In both systems, the flow is confined to the same 2-dimensional energy manifold that looks different with respect to the chart used in seeing it. Keeping in mind that both parametrizations are representing the phase space of the same problem, we put the two pictures head-to-head and, consequently, we obtain the portrait of the global

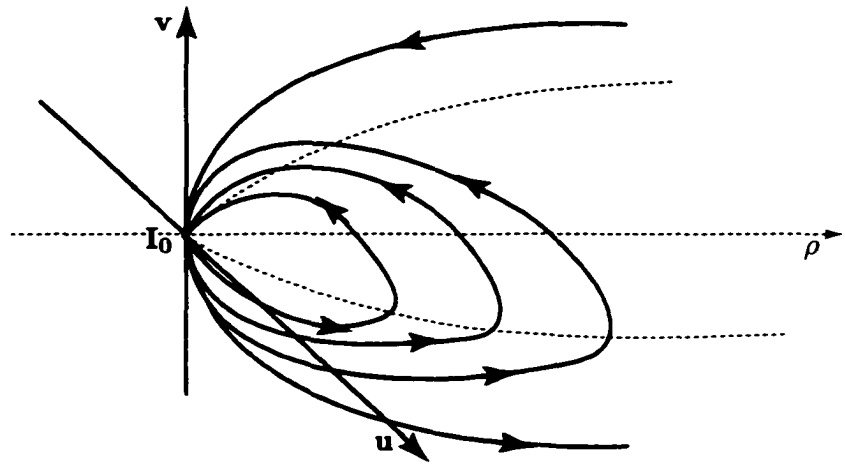

Figure 2.22: The flow in RSI for $h = 0$ and $0 < \alpha < 1$ and $\beta \leq 2$

flow.

2.4.1 The Global Flow for Positive Energy

Theorem 2.4.1 (*The global flow for strictly positive energy*)

Let us consider the relative two-body problem with quasihomogeneous interaction defined by system (2.1) with given constants $A > 0$, $B > 0$ and $0 < \alpha < \beta$ and strictly positive total energy $h > 0$.

Then the only possible scenarios of motion are:

(1) for $\beta < 2$, all orbits are capture-escape type, coming from infinity, attaining a minimum point and returning to infinity with asymptotic velocity $\sqrt{2h}$. There are two hereroclinic orbits connecting the collision equilibria with the infinity equilibria; for these orbits the angular velocity is zero (see Figures 2.27 and 2.28);

(2) for $\beta = 2$, there is a positive Lebesgue measure set of initial conditions leading to heteroclinic ejection-escape and capture-collision orbits. The rest of initial conditions, of positive measure too, lead to capture-escape orbits (see Figures 2.29 and 2.30);

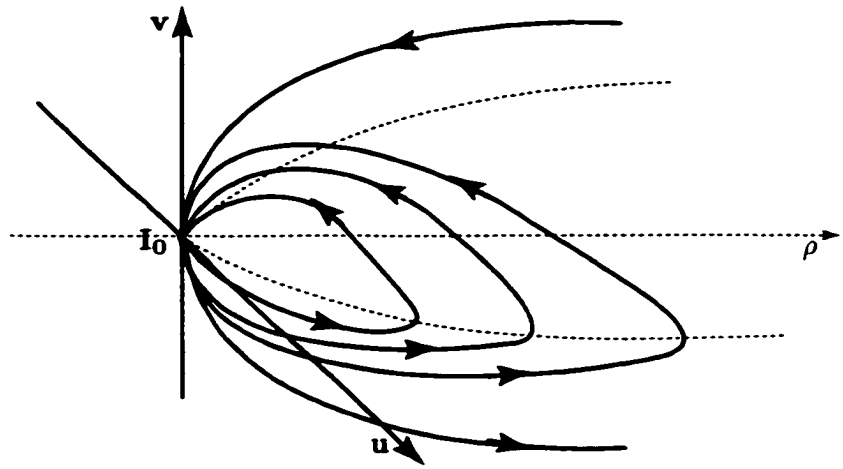

Figure 2.23: The flow in RSI for $h = 0$ and $1 \leq \alpha < \beta \leq 2$

(3) for $2 < \beta$, there is a positive Lebesque measure set of initial conditions leading to ejection-collision and capture-escape orbits. This invariant sets of orbits are connected by two unstable circulatory orbits. Also, there is only one ejection-escape, respectively, and only one capture-collision (both of them of heteroclinic type) and, moreover, for these two orbits the angular velocity is zero and the asymptotic radial velocity at $r \longrightarrow \infty$ is $\pm\sqrt{2h}$ (see Figures 2.31 and 2.32).

Corollary 2.4.2 For $\beta = 2$ and $h > 0$, all ejections are escapes.

Corollary 2.4.3 For $h > 0$, the asymptotic radial velocity at infinity is $\pm\sqrt{2h}$.

2.4.2 The Global Flow for Zero Energy

Theorem 2.4.4 (*The global flow for zero energy*)

Let us consider the relative two-body problem with quasihomogeneous interaction defined by system (2.1) with given constants $A > 0$, $B > 0$ and $0 < \alpha < \beta$ and zero total energy $h = 0$.

Then the only possible scenarios of motion are:

(1) for $\beta < 2$, all orbits are capture-escape type, coming from infinity, attaining

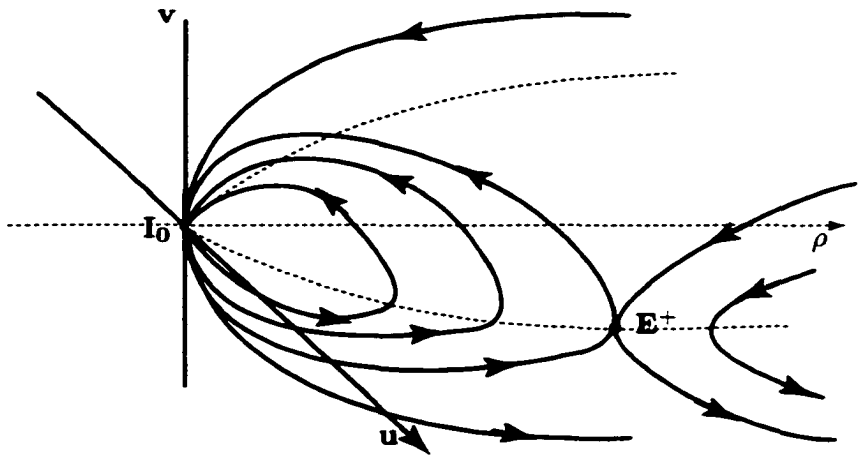

Figure 2.24: The flow in RSI for $h = 0$ and $0 < \alpha < 1$ and $2 < \beta$

a minimum point and returning to infinity with zero asymptotic velocity. There are two hereroclinic orbits connecting the collision equilibria with the infinity equilibria; for these orbits the angular velocity is zero (see Figures 2.33 and 2.34);

(2) for $\beta = 2$, there is a positive Lebesque measure set of initial conditions leading to heteroclinic ejection-escape and capture-collision orbits. The rest of initial conditions, of positive measure too, lead to capture-escape orbits (see Figures 2.35 and 2.36);

(3) for $2 < \beta$, there are the following subcases:

i) for $0 < \alpha < 2$, then there is a positive Lebesque measure set of initial conditions leading to ejection-collision and capture-escape orbits forming two invariant sets of orbits connected by two unstable circulatory orbits. Also, there is only one an ejection-escape, respectively, and only one capture-collision (both of them of heteroclinic type) and, moreover, for these two orbits, the angular velocity is zero and the asymptotic radial velocity at infinity is zero (see Figures 2.37, 2.38);

ii) for $2 \leq \alpha$, all orbits are ejection-collision except one having zero angular velocity and zero asymptotic radial velocity (see Figure 2.39).

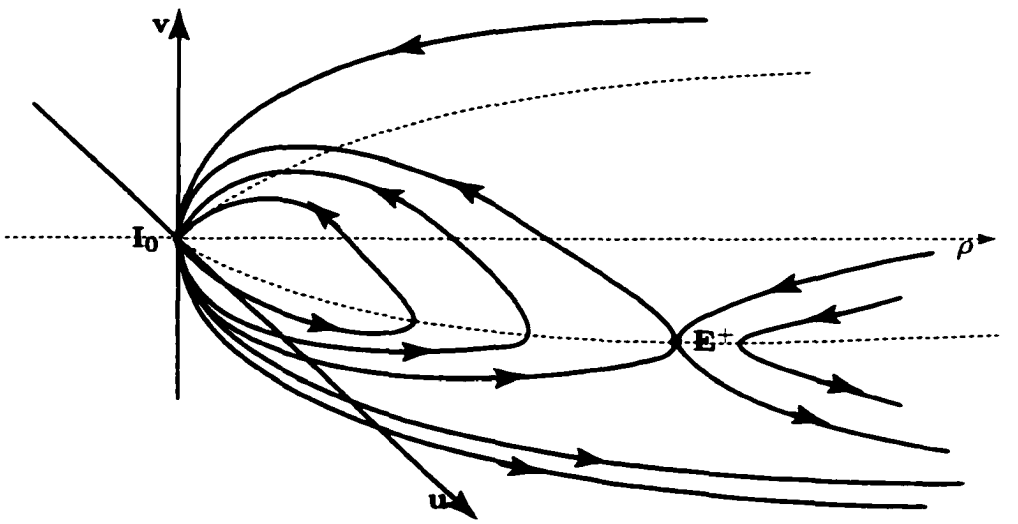

Figure 2.25: The flow in RSI for $h = 0$ and $1 \leq \alpha < 2$ and $2 < \beta$

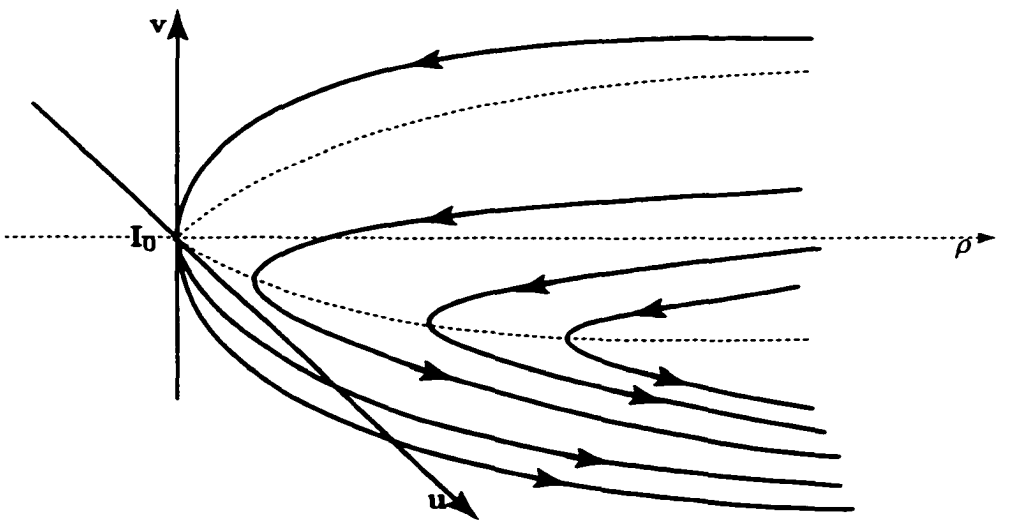

Figure 2.26: The flow in RSI for $h = 0$ and $2 \leq \alpha < \beta$

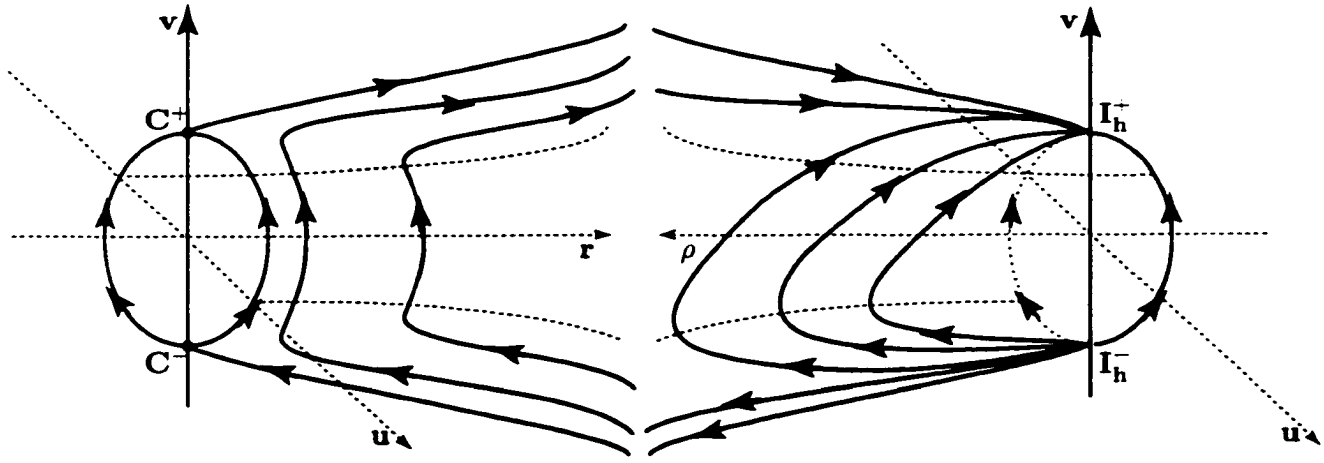

Figure 2.27: The global flow for $h > 0$ and $0 < \alpha < 1$ and $\beta < 2$

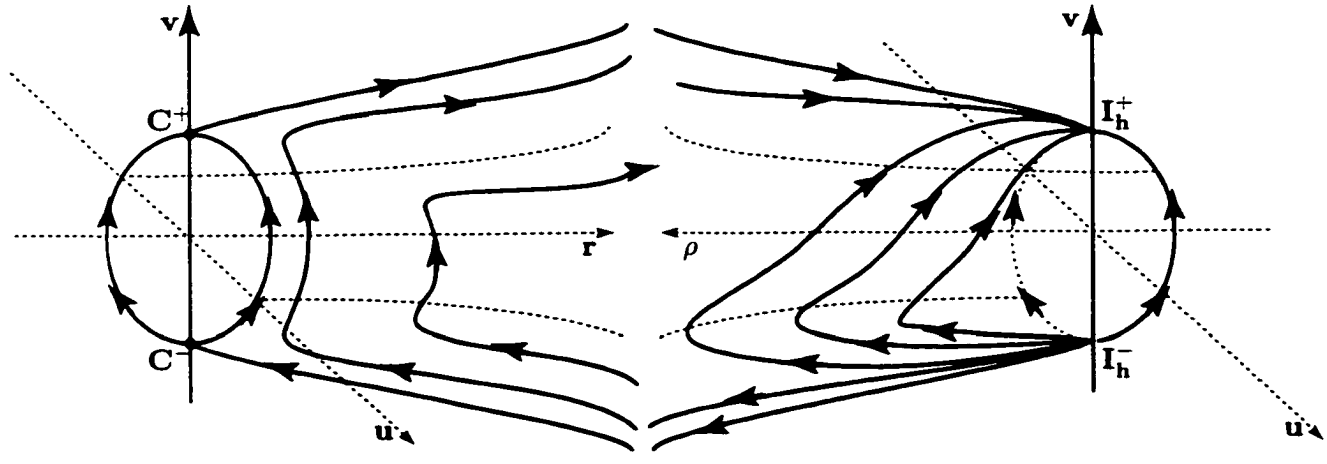

Figure 2.28: The global flow for $h > 0$ and $1 \leq \alpha < \beta < 2$

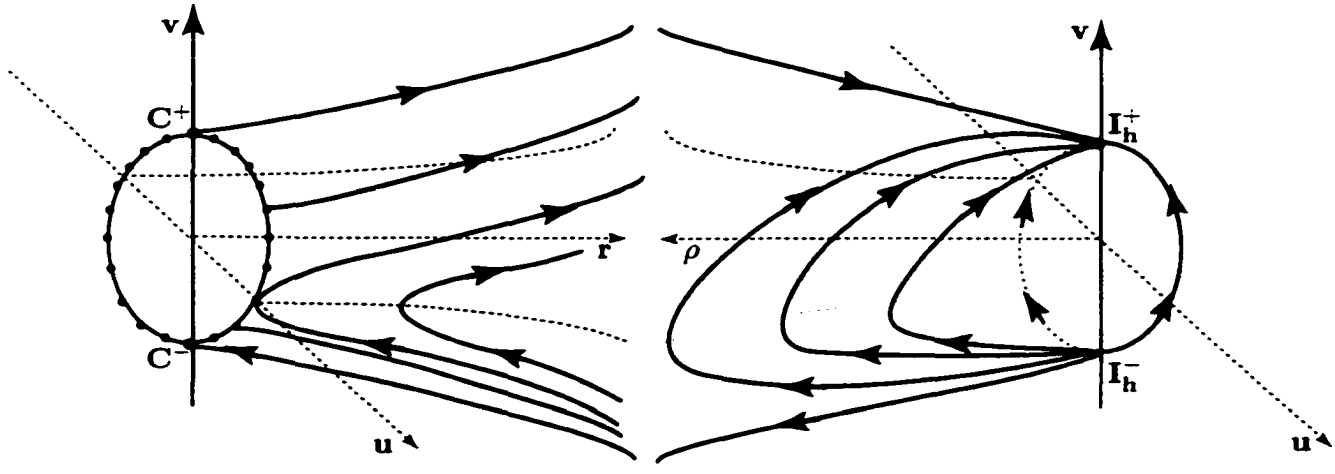

Figure 2.29: The global flow for $h > 0$ and $0 < \alpha < 1$, $\beta = 2$

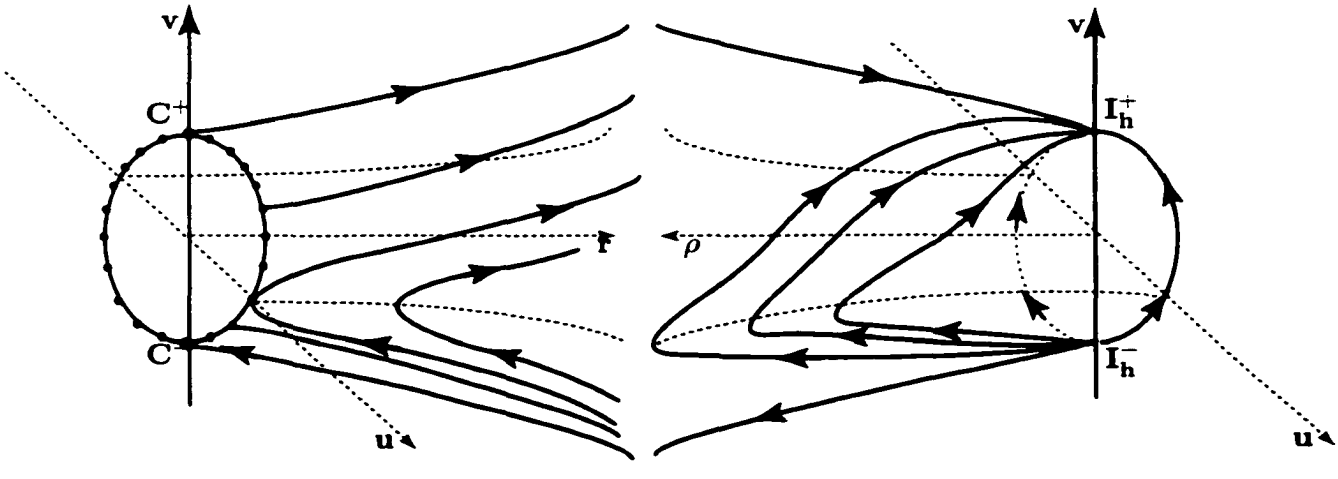

Figure 2.30: The global flow for $h > 0$ and $1 \leq \alpha < \beta = 2$

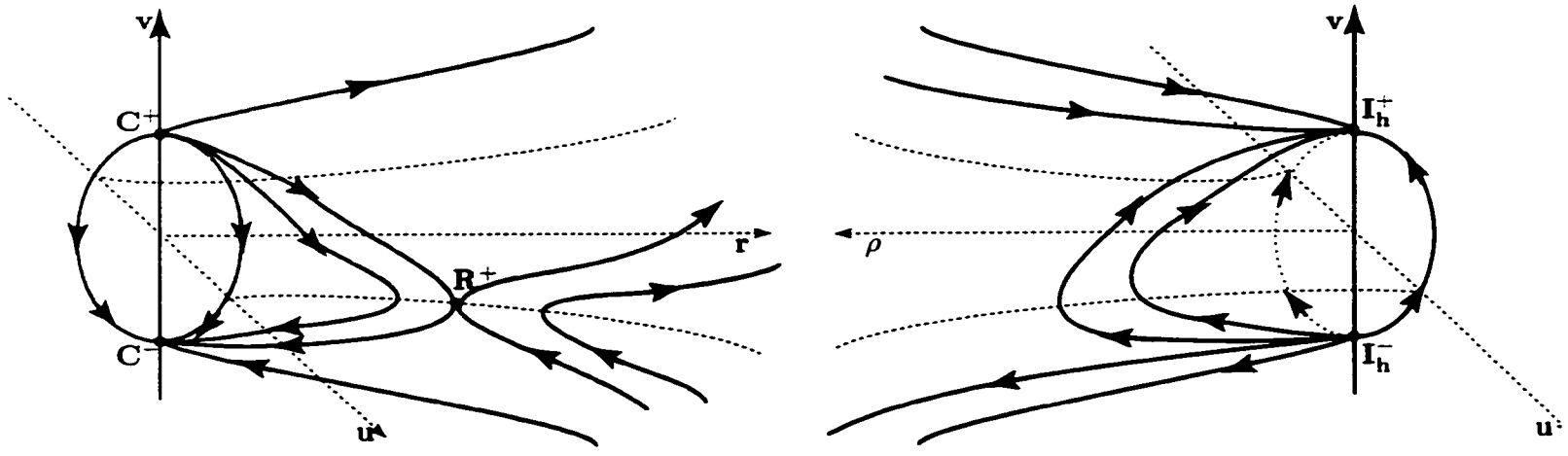

Figure 2.31: The global flow for $h > 0$ and $0 < \alpha < 1$, $\beta > 2$

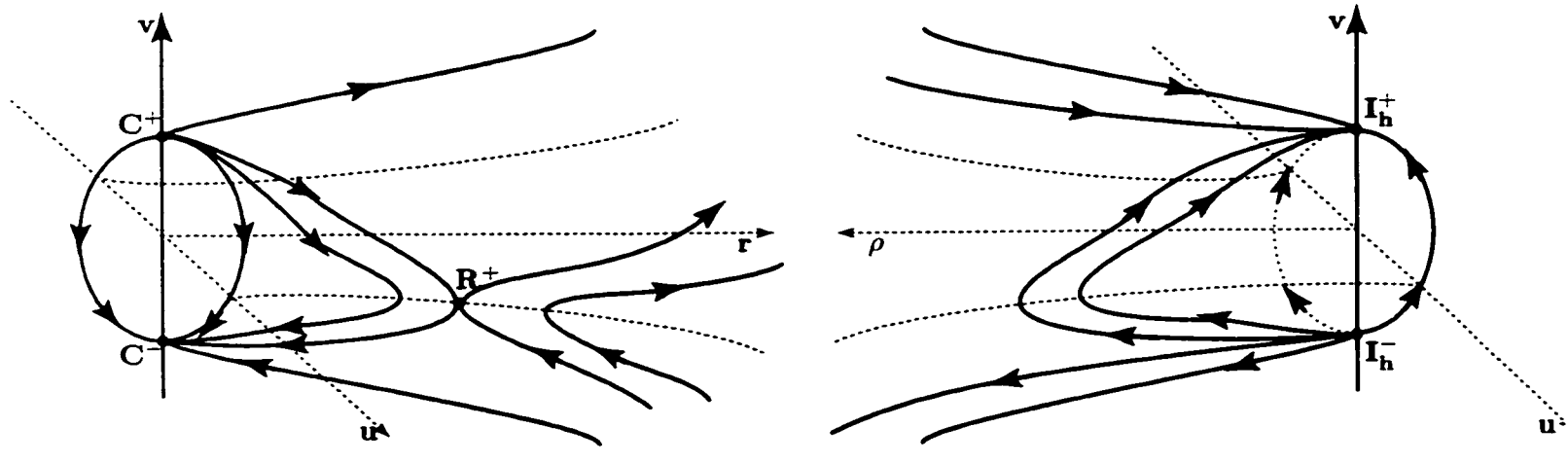

Figure 2.32: The global flow for $h > 0$ and $1 \leq \alpha$, $\beta > 2$

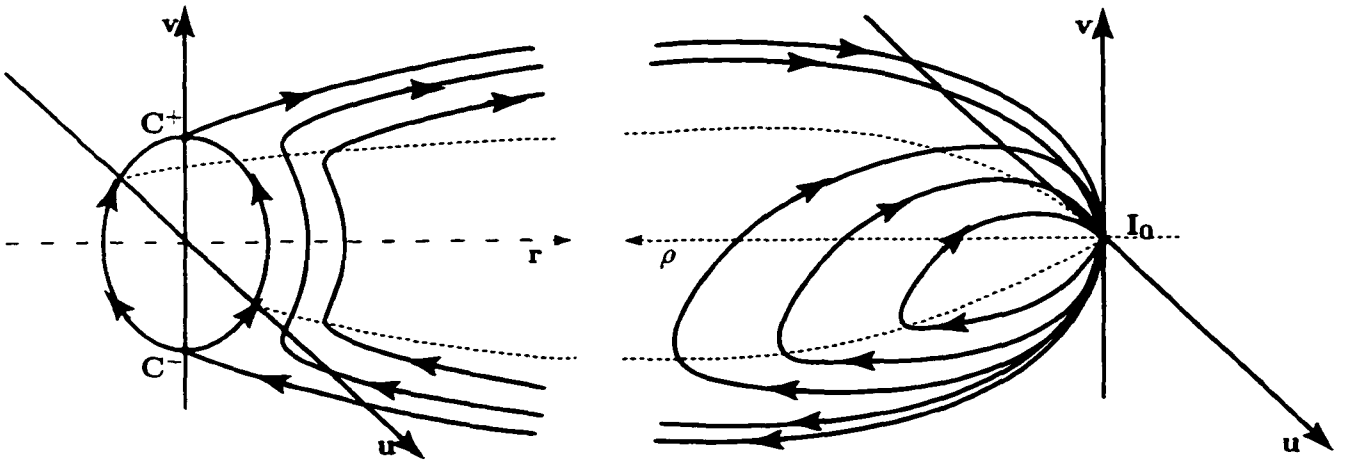

Figure 2.33: The global flow for $h = 0$ and $0 < \alpha < 1$ and $\beta < 2$

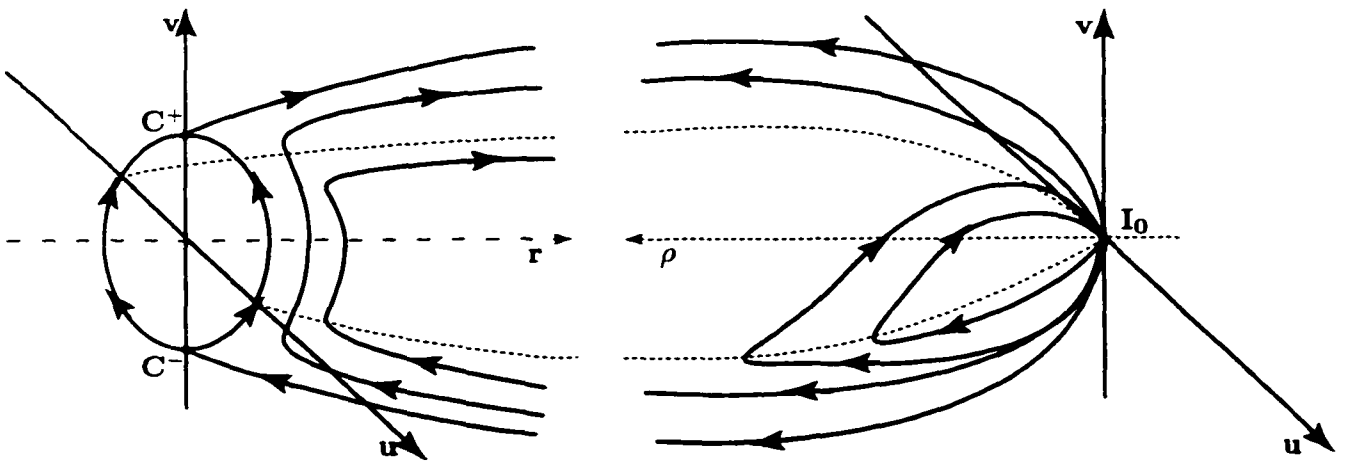

Figure 2.34: The global flow for $h = 0$ and $1 \leq \alpha < \beta < 2$

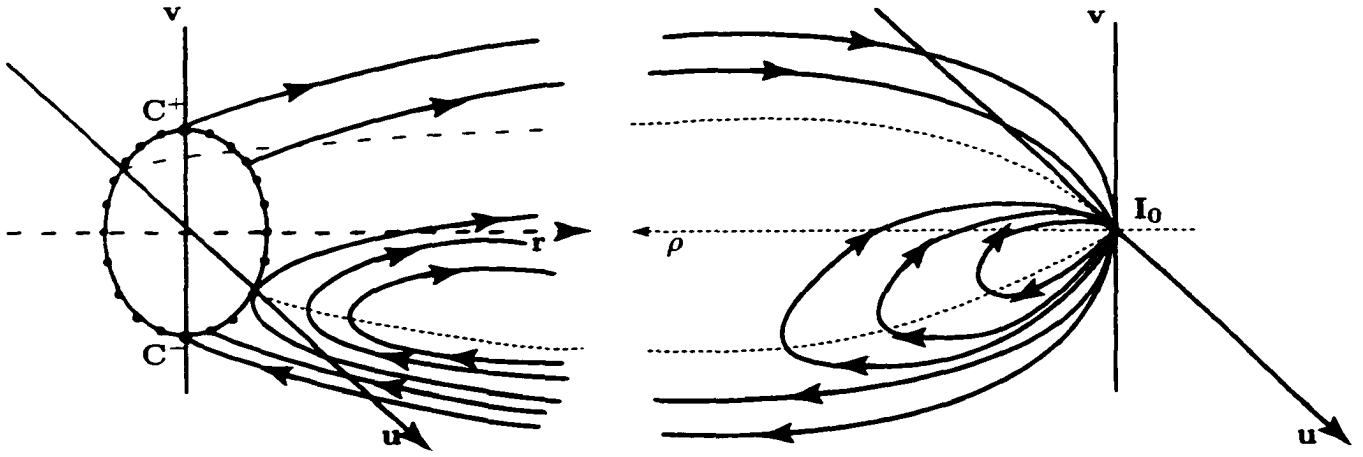

Figure 2.35: The global flow for $h = 0$ and $0 < \alpha < 1$, $\beta = 2$

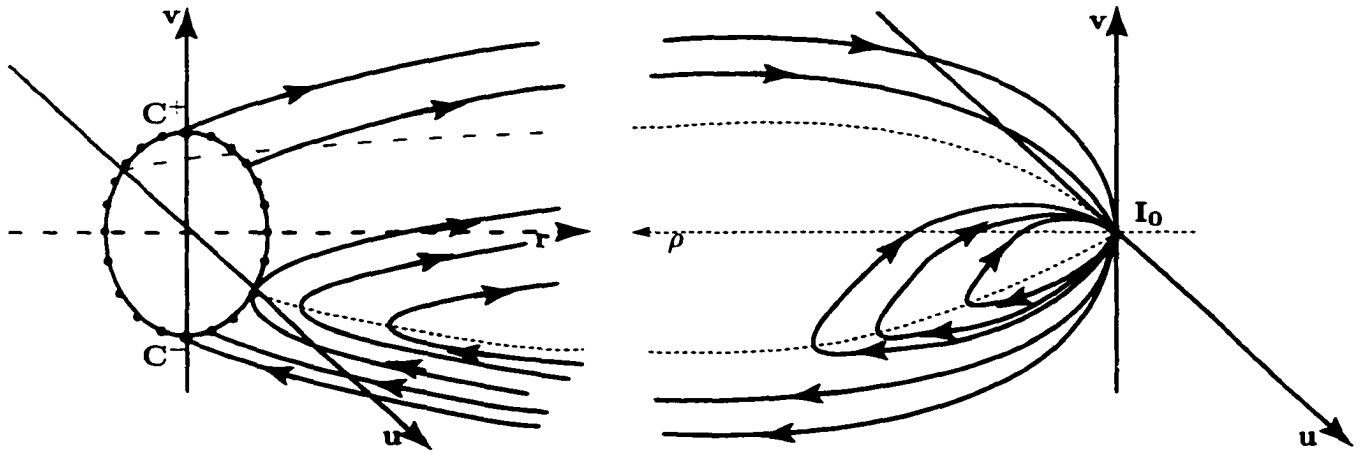

Figure 2.36: The global flow for $h = 0$ and $1 \leq \alpha < \beta = 2$

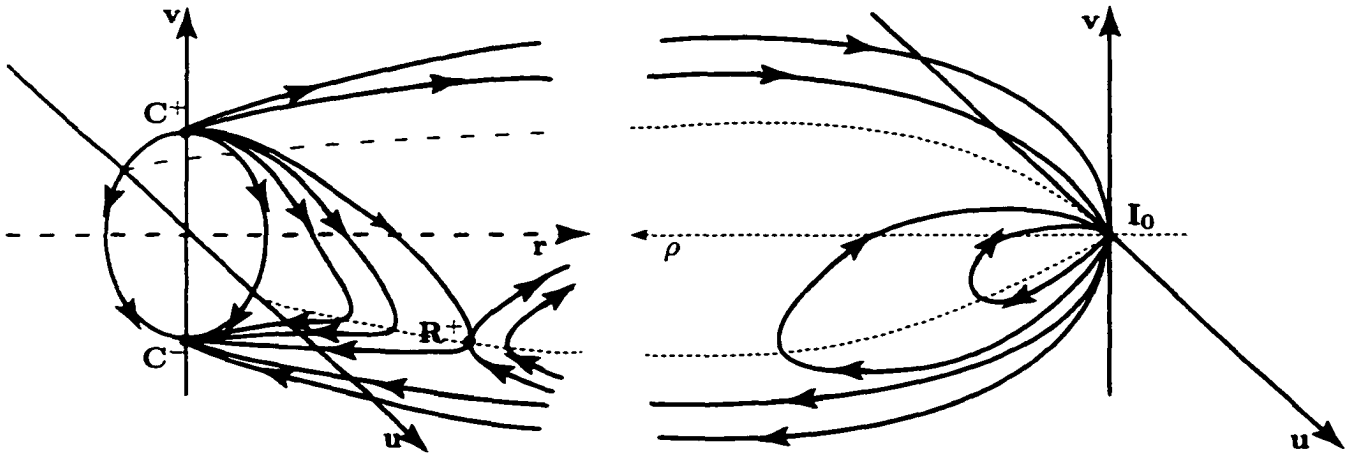

Figure 2.37: The global flow for $h = 0$ and $0 < \alpha < 1$, $\beta > 2$

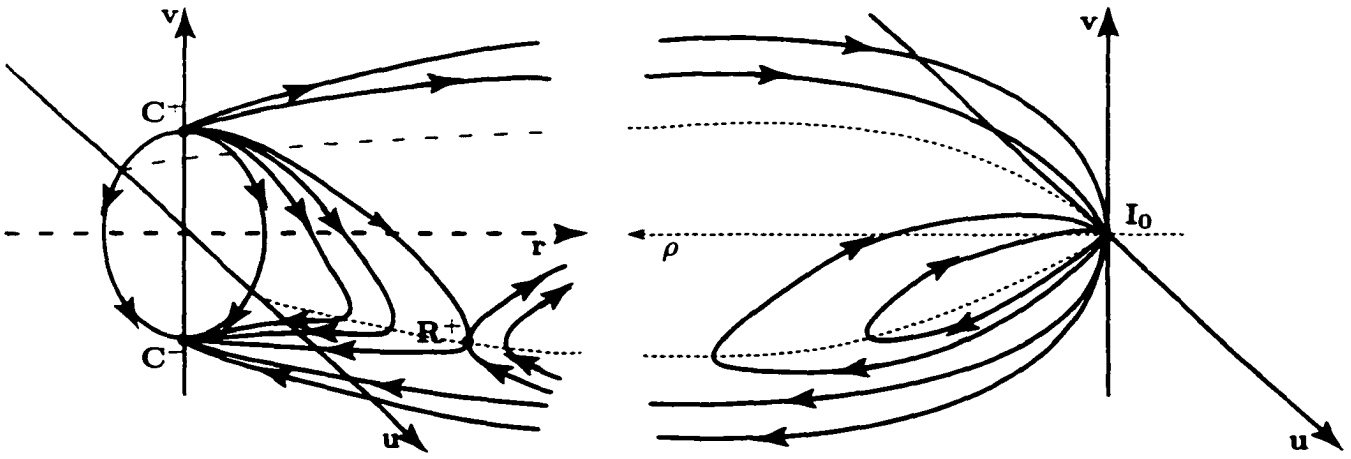

Figure 2.38: The global flow for $h = 0$ and $1 \leq \alpha < 2$, $\beta > 2$

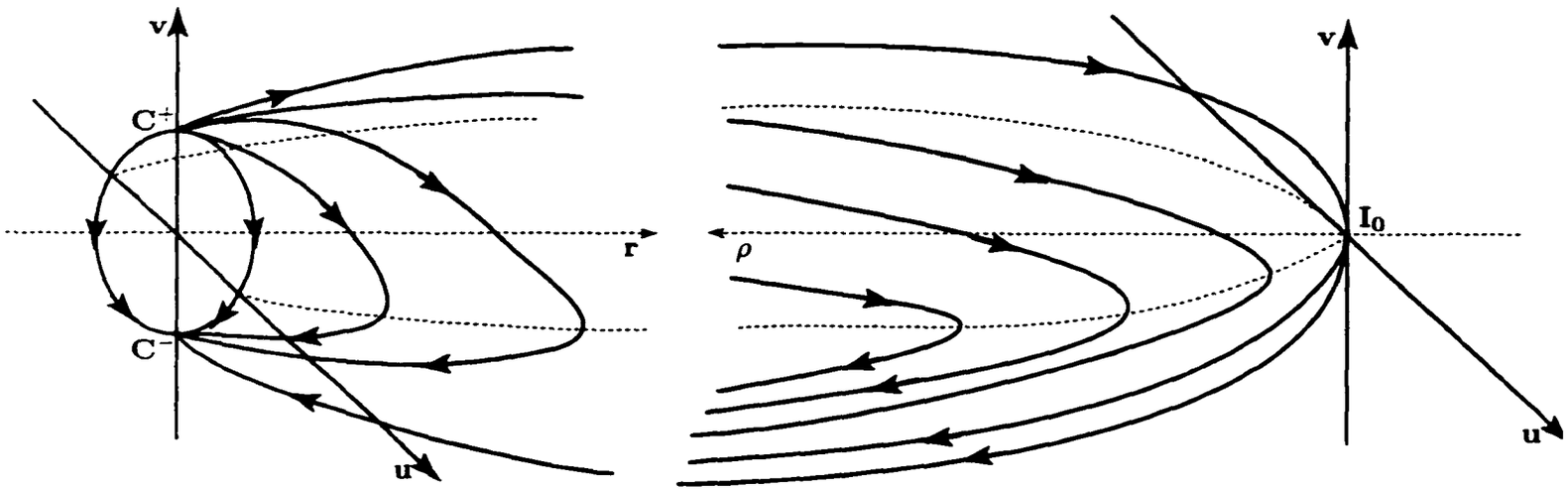

Figure 2.39: The global flow for $h = 0$ and $2 \leq \alpha < \beta$

Chapter 3

Regularization and the Scattering Problem

3.1 Isolating Blocks about an Invariant Set

Let M be a smooth manifold and let $\phi : M \times \mathbf{R} \longrightarrow M$ be a flow on M. A subset $\Lambda \subset M$ is called *invariant* if $\phi(\Lambda, \mathbf{R}) = \Lambda$. Also, if $p \in M$, we denote $\phi(p, \mathbf{R}) := \phi_p$.

Definition 3.1.1 An *isolating neighborhood* for the flow ϕ on M is an open $U \subset M$ such that $p \in \partial U$ implies $\phi_p \not\subset Cl(U)$, where $Cl(U)$ denotes the closure of U.

Observe that since points of ∂U leave $Cl(U)$, the maximal invariant set in U must be closed and is also the maximal invariant set in $Cl(U)$.

Definition 3.1.2 An invariant set Λ is called *isolated* if Λ is the maximal invariant set in some isolating neighborhood U. In this case we say U is an isolating neighborhood of Λ.

Observe that isolated invariant sets are closed, and that if U is an isolated neighborhood of Λ, then any set V between U and Λ (i.e. $U \subset V \subset \Lambda$) is also closed. The word isolated refers to the fact that there are no invariant sets between Λ and $Cl(U)$ (see Figure 3.1).

Now let B be a compact subset of M with non-empty interior and suppose that

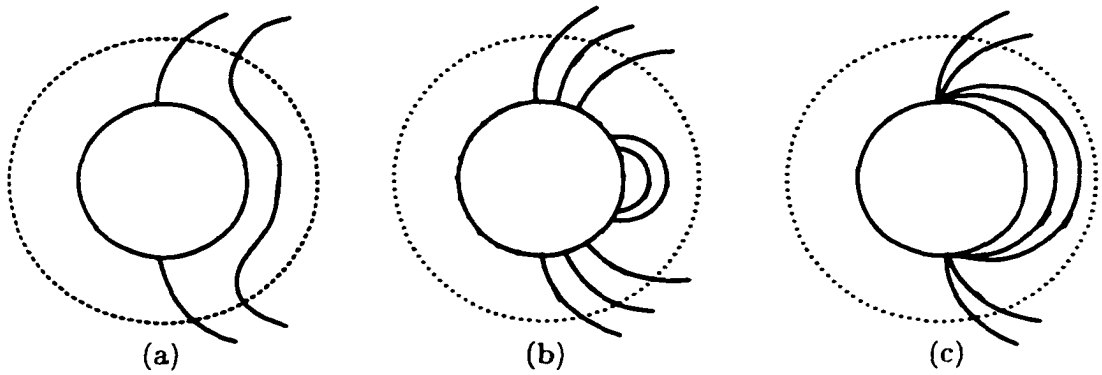

Figure 3.1: (a) Isolated and (b) and (c) non-isolated invariant sets Λ

$b = \partial B$ is a smooth submanifold of M. Define

$$b^+ := \{p \in b \mid \phi(p, (-\epsilon, 0)) \cap B = \Phi \text{ for some } \epsilon > 0\}, \tag{3.1}$$

$$b^- := \{p \in b \mid \phi(p, (0, \epsilon)) \cap B = \Phi \text{ for some } \epsilon > 0\}, \tag{3.2}$$

$$t := \{p \in b \mid \phi(p, 0) \text{ is tangent to } b\}, \tag{3.3}$$

where Φ denotes the empty set.

Definition 3.1.3 B is called an *isolating block* if $t = b^+ \cap b^-$.

Definition 3.1.4 Let Λ be an isolated invariant set, and let B be an isolating block. Then B is said to *isolate* Λ if $int(B)$ is an isolating neighborhood for Λ.

The following theorem was proved by Conley and Easton ([Con-E]).

Theorem 3.1.1 If Λ is an isolated invariant set, then there exists an isolating block which isolates Λ. If B is an isolating block, then there exists an isolated invariant set (possibly empty) which is isolated by B.

Following the procedure proposed by McGehee ([McG1]), given an application $I : M \longrightarrow \mathbf{R}$, we write

$$I^*(p,t) := I(\phi(p,t))$$

and define

$$I'(p) := (I^*)'(p,0) \text{ and } I''(p) := (I^*)''(p,0),$$

where $(I^*)'$ and $(I^*)''$ denote the time derivatives. The following lemma was proved by Wilson and Yorke ([Wi]) (the symbol D denotes the total derivative).

Lemma 3.1.1 Let $I : M \longrightarrow [0,\infty)$ and let $\delta_0 > 0$. Suppose that $DI(p) \not\equiv 0$ whenever $0 < I(p) \leq \delta_0$. Suppose also that $I''(p) > 0$ whenever $0 < I(p) \leq \delta_0$ and $I'(p) = 0$. Then $\Lambda := I^{-1}(0)$ is an isolated invariant set and $I^{-1}([0,\delta])$ is an isolating block for Λ for each $\delta \in (0,\delta_0]$.

We define the subsets of b which are asymptotic to Λ:

$$a^+ := \{p \in b^+ \mid \phi(p,[0,\infty)) \subset B\},$$

$$a^- := \{p \in b^- \mid \phi(p,(-\infty,0]) \subset B\}.$$

By definition, if $p \in b^+ - a^+$, then there exists a $t > 0$ such that $\phi(p,t) \notin B$. Thus one can define the time spent in the block for a point $p \in b^+ - a^+$ by

$$T(p) := inf\{t > 0 \mid \phi(p,t) \notin B\}.$$

Note that $\phi(p,[0,T(p))) \in B$ and that $\phi(p,T(p)) \in b^-$. Now we define the map across the block

$$\tilde{\phi} : b^+ - a^+ \longrightarrow b^- \text{ by } p \longrightarrow \phi(p,T(p)).$$

Theorem 3.1.2 (Conley and Easton [Con-E]) If B is an isolating block, then

$$\tilde{\phi} : b^+ - a^+ \longrightarrow b^- - a^-$$

is a diffeomorphism.

Definition 3.1.5 An isolating block B is said to be *trivializable* if $\tilde{\phi}$ extends uniquely to a diffeomorphism $b^+ \longrightarrow b^-$.

Lemma 3.1.2 (Conley [Con]) Suppose that Λ is an isolated invariant set and that B_1 and B_2 isolate Λ. Then B_1 is trivializable if and only if B_2 is trivializable.

Definition 3.1.6 Let B isolate Λ. Then Λ is said to be *trivializable* if B is trivializable.

We now return to the quasihomogeneous two-body problem. We take ϕ to be the flow on the manifold M_h (2.11) defined by equations (2.8). The invariant set Λ is given by relation (2.12). Define

$$I : M_h \longrightarrow \mathbf{R} \text{ by } (r, \theta, v, u) \longrightarrow r,$$

and

$$B_h(\delta) := \{p \in M_h \mid I(p) \leq \delta\}.$$

Lemma 3.1.3 Let $\beta < 2$. Given any h, there exists a $\delta_0 > 0$ such that $B_h(\delta)$ is an isolating block for Λ whenever $0 < \delta \leq \delta_0$.

Proof We apply Lemma 3.1.1 taking as $I(p)$ the previously defined function I on M_h. Then $DI(p)_{(r',\theta',v',u')} = r'$.

On the other hand the tangent space to M_h at a point $p = (r, \theta, v, u)$ is given by

$$\{(r', \theta', v', u') \mid \left(1 + h\frac{\beta}{(\beta - \alpha)} r^{\frac{\alpha}{(\beta-\alpha)}}\right) r' - vv' - uu' = 0\}$$

so it follows that $DI(p) = r'$ is zero if $(v, u) = (0, 0)$. But (r, θ, v, u) is a point on M_h and for $I(p) = r = \delta$ we get

$$|v^2 + u^2 - 2B| = 2(1 + \delta^{\frac{\alpha}{(\beta-\alpha)}})\delta$$

therefore for a $I(r_0) := \delta_0$ small enough it follows that $(v, u) \neq (0, 0)$ whenever $\delta \leq \delta_0$. Hence, $DI(p) \neq 0$ when $0 < \delta \leq \delta_0$. Now, using equations (2.8) we see that

along the flow

$$I' = r' = (\beta - \alpha)rv$$

from where, if $I(p) = r\delta$, $I' = 0$ if $v = 0$. Along the flow on M_h and for $v = 0$,

$$I'' = ((\beta - \alpha)rv)' = (\beta - \alpha)r[B(2 - \beta) + A(2 - \alpha)r + 2hr^{\frac{\beta}{(\beta-\alpha)}}]).$$

Since $B(2 - \beta) > 0$ and $r = \delta$ it follows that $I'' > 0$ whenever $0 < \delta \leq \delta_0$ for δ_0 small enough. Finally, note that $\Lambda = I^{-1}(0)$. Hence, by Lemma 3.1.1, $B_h(\delta)$ is an isolating block for Λ and the proof is complete.

By examining the figures for $\beta \geq 2$, one can observe that in all these cases the set Λ is not isolated.

We define now for the block $B_h(\delta)$:

$$b := \{p \in M_h \mid r = \delta\}$$

$$b^+ := \{p \in b \mid v \leq 0\}$$

$$b^- := \{p \in b \mid v \geq 0\}$$

$$t := \{p \in b \mid v = 0\}$$

$$a^+ := \{p \in b^+ \mid u = 0\}$$

$$a^- := \{p \in b^- \mid u = 0\}$$

Lemma 3.1.4 If Λ is a trivializable isolated invariant set for equations (2.8), then $\beta = 2(1 - 1/n)$ where n is a positive integer, $n \geq 2$.

Proof First we notice that since Λ is not an isolated invariant set when $\beta \geq 2$, we must have $\beta < 2$. Second, we write b as

$$b = \{(r, \theta, v, u) \in \mathbf{R}^4 \mid r = \delta, \text{ and } v^2 + u^2 = 2B + 2A\delta + 2h\delta^{\frac{\beta}{(\beta-\alpha)}}\}.$$

Also, we write the map across the block as

$$\tilde{\Phi} : b^+ - a^+ \longrightarrow b^- - a^-, \ \ (r, \theta, v, u) \longrightarrow (r, \tilde{\Phi}_\theta(\theta, u), -v, u),$$

where $\tilde{\Phi}_\theta$ is the second component of $\tilde{\Phi}$. On b^+, $r = \delta$ and $v = -\sqrt{2B + 2A\delta + 2h\delta^{\frac{3}{(\beta-\alpha)}} - u^2}$, therefore one can use (θ, u) as coordinates. System (2.8) being independent of θ,

$$\tilde{\Phi}_\theta(\theta, u) = \theta + \Gamma(u)$$

where Γ is a function of u defined for all $0 < u < 2B + 2A\delta + 2h\delta^{\frac{3}{(\beta-\alpha)}}$. By symmetry, $\Gamma(-u) = \Gamma(u)$. By hypothesis, $B_h(\delta)$ is trivializable, therefore $\tilde{\Phi}$ extends uniquely to a continuous map $b^+ \longrightarrow b^-$. Thus $\theta + \Gamma(0-) = \theta + \Gamma(0+) + 2\pi n$, where n is an integer and, since Γ is an odd function, it follows that $\Gamma(0+) = \pi n$.

Following McGehee's (see [McG1]) technique, we will compute the number $\Gamma(0+)$ using a geometric method. Let $p \in a^+$. Recall the definition (2.18) of $S^{\pm}$. By Lemma 2.3.1, $\omega(p_0)$ is a point s^- in S^- therefore the orbit through p_0 is actually the stable manifold of s^-. Now let $p \in b^+$ be close to p_0. The orbit through p follows closely the stable manifold of s^-, passes close to S^- and then follows closely the unstable manifold of s^-. Now we need to determine the unstable manifold of s^-.

Since the unstable manifold of s^- is a subset of Λ, we recall the angular variables (θ, χ) (2.16) on the collision manifold Λ and the equations (2.15). It follows that in the (θ, χ) variables, the unstable manifolds of points on S^- are just straight lines with slope $(1 - \beta/2)$. As we are looking for $\Gamma(0+)$, we must take $-\pi/2 \leq \chi \leq \pi/2$. If $s^- = (\delta, \theta_0, -\sqrt{2B}, 0)$, then the unstable manifold of s^- is exactly the stable manifold of $s^+ = (\delta, \theta_0 + \pi(1 - \beta/2)^{-1}, \sqrt{2B}, 0)$. So the orbit through p first follows the stable manifold of s^-, then follows the unstable manifold of s^- which coincides with the stable manifold of s^+, and finally follows the unstable manifold of s^+. So as $p \longrightarrow p_0$, the change in θ along the orbit approaches the difference in θ between

s^- and s^+ which is $\pi(1-\beta/2)^{-1}$. Therefore

$$\Gamma(0+) = \pi n = \pi(1-\beta/2)^{-1}$$

from where it follows that $\beta = 2(1-1/n)$ where n is a positive integer.

3.2 Block Regularization

In the preceding section we applied the theory of isolated invariant sets to the transformed system (2.8) for which Λ in an isolated invariant set. We turn now to our original problem, the question whether if equations (2.1) can be regularized. Here, the set Λ is the set where the vector field of (2.1) fails to be defined. One has to keep in mind that, after all, the two systems have identical orbits on $M_h - \Lambda$, only the parametrization is different.

We turn now, following Easton ([Eas]) and McGehee ([McG1]), to the definition of block regularization for system (2.1). Let M be a smooth manifold, let Λ be a compact subset of M, and let F be a vector field on $M - \Lambda$, Λ being the set where F fails to be defined. Let ψ be the flow on $M - \Lambda$ given by F (we do not require that $\psi(p,t)$ to be defined for all t).

Let B be a compact subset of M with non-empty interior and suppose thet $b = \partial B$ is a smooth manifold which does not intersect Λ. Let b^+, b^- and t be defined as in the previous section, and the definition of an isolating block be also the same. Let $\mathcal{O}(p)$ denote the orbit through p, namely

$$\mathcal{O}(p) = \{\psi(p,t) \mid \psi(p,t) \text{ is defined}\}$$

.

Definition 3.2.1 An isolating block B isolates the singularity set Λ if $\Lambda \subset int(B)$ and if $\mathcal{O}(p) \not\subset B$ for all $p \in B - \Lambda$.

The subsets a^+ and a^- are the same as before, except that now we must allow for solutions which are not defined for all t, i.e.

$$a^+ = \{p \in b^+ \mid \psi(p,t) \in B \text{ for all } t \geq 0 \text{ for which } \psi(p,t) \text{ is defined.}\}$$

$$a^- = \{p \in b^- \mid \psi(p,t) \in B \text{ for all } t \leq 0 \text{ for which } \psi(p,t) \text{ is defined.}\}$$

The map $\tilde{\psi} : b^+ - a^+ \longrightarrow b^-$ is defined in exactly the same way as the map $\tilde{\phi}$.

Definition 3.2.2 The singularity set Λ is said to be *block regularizable* if there exists a trivializable block B which isolates Λ.

As already mentioned, we follow closely McGehee's procedure for regularization. Suppose that one can isolate the singularities of a given system with an isolating block, and suppose that the map across the block can be extended. Solutions passing close to singularities then will determine uniquely an extension for a solution ending in a singularity. Thus one can construct an extended flow with the property with the property of differentiability with respect to initial data. If, on the other hand, the map across the block does not extend, then such an extended flow does not exist.

In order to apply the aforementioned procedure for regularization, one has to make extensive use of the fact that an isolated block for an ordinary differential system is *independent* of parametrization. If one cannot say anything about the orbits that are not defined on the set of singularities of the system, the same orbits are fully *visible* (i.e. are defined for all t) on the transformed system. Explicitely, in our case, the singularity at $\mathbf{x} = \mathbf{0}$ became after applying (2.6), the invariant collision manifold Λ and, consequently, *lost* orbits in $\{\mathbf{x} = \mathbf{0}\}$ became orbits defined for all t on Λ. Returning to our problem, the block $B_h(\delta)$ is an isolating block for both systems (2.1) and (2.8) and the maps $\tilde{\phi}$ and $\tilde{\psi}$ describe the same orbits. Hence $B_h(\delta)$ is trivializable for (2.1) if and only if is trivializable for (2.8).

By Lemma 3.1.4 we already know that if Λ is a trivializable isolated invariant set for (2.1) and hence for (2.8) then $\beta = 2(1 - 1/n)$. The next section will prove

the converse of this afirmation, namely that if $\beta = 2(1-1/n)$ then Λ is trivializable. Therefore, we are able to state the main result of this chapter:

Theorem 3.2.1 (*block regularization for the quasihomogeneous two body problem*)

The quasihomogeneous two body problem generated by a potential of the form $U(\mathbf{x}) = -\frac{A}{x^\alpha} - \frac{B}{x^\beta}$, $A > 0$, $B > 0$ and $0 < \alpha < \beta$ is block regularizable if and only if $\beta = 2(1 - \frac{1}{n})$, where n is a positive integer, $n \geq 2$.

3.3 Levi-Civita Regularization

The goal of this section is to prove that if $\beta = 2(1 - 1/n)$ where n is a positive integer, $n \geq 2$, then the invariant set Λ is trivializable. We start by returning to the original Hamiltonian system (2.1) and introduce a change of variables analogous to the Levi-Civita transformation of the Kepler problem ([Lev]).

Assume $\beta = 2(1 - 1/n)$, n an integer with $n \geq 2$ and consider the initial system (2.1) with the Hamiltonian functional given by (2.3) and total energy $H(\mathbf{x}, \mathbf{y}) = h = constant$. We define the new complex variables z and w by:

$$\begin{cases} \mathbf{x} = z^n, \\ \mathbf{y} = w\bar{z}^{1-n} \end{cases} \tag{3.4}$$

and consider the new Hamiltonian function by the isoenergetic transformation:

$$K(z,w) = |z|^{2(n-1)} = (H(z^n, w\bar{z}^{1-n}) - h) = \frac{1}{2}w^2 - h|z|^{2(n-1)} - 1.$$

By (3.4) the manifold $\{H = h\}$ maps into the manifold $\{K = 0\}$. Rescaling the time by

$$dt = n|z|^{2n}d\sigma$$

the vector field (2.1) transforms to:

$$\begin{cases} \frac{dz}{d\sigma} = |z^2|w, \\ \frac{dw}{d\sigma} = A(2n - n\alpha - 2)|z|^{2n-n\alpha-2}z + 2(n-1)h|z|^{2(n-1)}z \end{cases} \tag{3.5}$$

on the manifold $\{K(z,w) = 0\}$.

Equations (3.5) extend to $z = 0$ and hence the singularity at collision has been *regularized* in the sense of Levi-Civita. As an observation, one can see that $z = 0$ implies $|w|^2 = 2B$ and, therefore, solutions of (3.5) pass right through $z = 0$.

Lemma 3.2.1 Let $\beta = 2(1 - 1/n)$ where n is a positive integer, $n \geq 2$. Then Λ is a trivializable isolated invariant set for equations (2.8).

Proof By the transformations (3.4) the block $B_h(\delta)$ becomes in the (z,w) coordinates

$$\tilde{B} = \{(z,w) \in \mathbf{C}^2 \mid K(z,w) = 0, \ |z|^n \leq \delta\}.$$

We recall that the orbits of systems (3.5) are the same as the orbits of system (2.1) on $M_h - \Lambda$ and therefore as the orbits of system (2.8), only the parametrizations are different. Therefore, using the global flow analysis performed in chapter 2 and, in particular, figures 2.5, 2.10 and 2.14, one can deduce that the vector field has no invariant set inside $\tilde{B}$. Hence the asymptotic sets a^+ and a^- for $\tilde{B}$ are empty and by theorem 3.1.2, the map across the block is a diffeomorphism from the entire incoming set to the entire outgoing set. Also, using the analysis of the flow on the collision manifold one can see that the map across the block extends to a diffeomorphism between $b^+ := \{p \in b \mid v \leq 0\}$ and $b^- := \{p \in b \mid v \geq 0\}$.

3.4 Physical Interpretation: The Scattering Problem

The following section offers an alternative view over the block regularization. We will show that block regularization can be regarded as a constraint over the scattering angle of a particle undergoing a fictional collision.

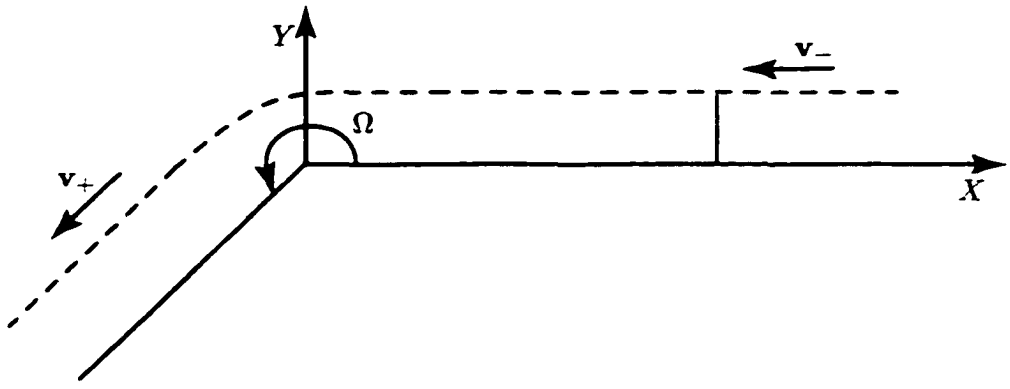

Figure 3.2: The scattering angle

We begin by recalling some well-known facts from classical mechanics ([Lan]). The two-body problem in quasihomogeneous fields is equivalent with the one-body problem (i.e. the motion of a particle - here of unit mass) in a gravitational central field with a potential source of the form $U(x) = -\frac{A}{x^\alpha} + -\frac{B}{x^\beta}$, where $A > 0$, $B > 0$ and $0 < \alpha < \beta$ ($\mathbf{x}$ being the radius vector between the mass point and the central source and $x := \|\mathbf{x}\|$). Since $U'(x)$ is positive the potential is attractive.

Let us denote by h the total energy, by c the angular momentum and by $\mathbf{v}_\pm$ the velocities of the particle at $t = \pm\infty$. If ρ is such that $c = \rho v$, it is always possible to construct a plane P with Cartezian coordinates (XOY) such that $\mathbf{v}_- = \{-v, 0\}$, $\mathbf{v}_+ = \{\tilde{v}_X, \tilde{v}_Y\}$, where $\tilde{v}_X^2 + \tilde{v}_Y^2 = v^2$. In (X, Y) plane the central source becomes the origin O and ρ is the distance between the direction at $t = -\infty$ of the particle and the OX axis. (see Figure 3.2).

As the particle is approaching the source its trajectory is deviated by the so-called *scattering angle* Ω. Following classical results ([Lan]) we know that if the equation

$$U(x) + \frac{c^2}{2x^2} = h \tag{3.6}$$

has exactly one positive solution $x = x_0 = x_0(c)$ for a $h > 0$ fixed, then the scattering angle is well defined and equals $\Omega = |\pi - \Theta|$ where $\Theta = \Theta(c)$ is given by

$$\Theta(c) = 2\int_{x_0}^{\infty} \frac{\frac{c}{x^2}dx}{\sqrt{2(h - U(x)) - \frac{c^2}{x^2}}}, \tag{3.7}$$

or, in terms of ρ, $\Theta = \Theta(\rho)$, with

$$\Theta(\rho) = 2\int_{x_0}^{\infty} \frac{\frac{\rho}{x^2}dx}{\sqrt{1 - \frac{\rho^2}{x^2} - \frac{2U(x)}{v_\infty^2}}}. \tag{3.8}$$

Proposition 3.4.1 Assume $0 < \beta < 2$. Then $\lim_{\rho \to 0+} \Theta(\rho) = \frac{2\pi}{2-\beta}$ and $\lim_{\rho \to 0-} \Theta(\rho) = -\frac{2\pi}{2-\beta}$

Proof Since $\beta < 2$, using elementary calculus it can be shown that the equation (3.6) admits an unique solution for $h > 0$ (actually the left hand side of (3.6) defines the effective (or amended) potential for the motion in a quasihomogeneous field). Therefore, the Θ angle is well defined. We point out that for $c = 0$ i.e. for $\rho = 0$ the scattering angle is not defined since equation (3.6) has not root in the quasihomogeneous case. Still we can compute the limit of $\Theta(\rho)$ as $\rho \longrightarrow \pm 0$. Mathematical speaking the function $\Theta = \Theta(\rho) : \mathbf{R} - \{0\} \longrightarrow \mathbf{R}$ is continuous everywhere on its domain which excludes the point 0. We are interested in the behaviour of this function in a neighborhood of 0.

After the change of variable $u = \rho/x$, the integral (3.8) can be expressed as

$$\Theta(\rho) = 2\int_0^{u_0} \frac{du}{\sqrt{1 + au^\alpha + bu^\beta - u^2}}, \tag{3.9}$$

where

$$a := \frac{2A}{v_\infty^2 \rho^\alpha} \text{ and } b := \frac{2B}{v_\infty^2 \rho^\beta}$$

and u_0 is the root of $1 + au_0^\alpha + bu_0^\beta - u_0^2 = 0$. Using the substitution $u = (by)^{\frac{1}{2-\beta}}$, we obtain:

$$\Theta(\rho) = \frac{2}{2-\beta}\int_0^{y_0} \frac{dy}{\sqrt{b^{-\frac{2}{2-\beta}} y^{\frac{2-2\beta}{2-\beta}} + ab^{-\frac{2-\alpha}{2-\beta}} y^{\frac{2-2\beta+\alpha}{2-\beta}} + y - y^2}}. \tag{3.10}$$

Now, if $\rho \longrightarrow 0+$, then $b^{-\frac{2}{2-\beta}} \longrightarrow 0$ and $\left(ab^{-\frac{2-\alpha}{2-\beta}}\right) \longrightarrow 0$, therefore, by Lebesgue's dominated convergence theorem:

$$\lim_{\rho\to 0+} \Theta(\rho) = \frac{2}{2-\beta}\int_0^{y_0} \frac{dy}{\sqrt{y-y^2}} = \frac{2\pi}{2-\beta} \tag{3.11}$$

By (3.8), $\Theta(-\rho) = -\Theta(\rho)$, hence $\lim_{\rho\to 0-} \Theta(\rho) = -\frac{2\pi}{2-\beta}$.

In other words, imposing the function $\Theta(\rho)$ to have equal limit as $\rho \longrightarrow -0$ and $\rho \longrightarrow +0$, respectively, we obtain that this is possible only for those values of β for with the quasihomogeneous two-body problem is block regularizable. For these values of β, in the classical framework of the scattering problem, a test particle close to a collision trajectory (i.e. with small angular momentum) has almost the same trajectory line at $t = \pm\infty$. Simple computations reveal that in the case $\beta = 2 - 2/n$, where n is an even number, $n \geq 2$, the particle approaching the source will spin around it $n-1$ times (i.e. a multiple of $n\pi$, n even) and will exit on the initial trajectory line, but in opposite sens. Similarly, if $\beta = 2 - 2/n$, where n is an odd number, $n \geq 2$, a particle with small angular momentum approaching the source will spin around it $n-1$ and a half times (i.e. a multiple of $n\pi$, n odd) and will exit on the initial trajectory line, following almost its initial path.

In the block regularization context we studied the flow and its behaviour on the fictitious collision manifold. We asked for the continuity of the solutions with respect to initial data in a neighbourhood of the collision manifold and obtained that this is possible if and only if $\beta = 2(1 - \frac{1}{n})$, where n is an integer, $n \geq 2$. A fictional particle colliding into the source (seen here as being the collision manifold) "exits" it in a *reflection* if n is even or a *transmission* if n is odd. In physical reality,

the collision manifold has no meaning, for it represents a set where motion fail to exist. A physical particle colliding into a point size source will stop there. Still, its neighbours will continue their motion as they would flow close to the fictitious particle.

At the other end, the same physical picture is obtained if one applies non-divergence conditions upon a ray of particles scattered by a quasihomogeneous source. The scattering angle of a particle is a function of the angular momentum c, function not defined at $c = 0$. Still, imposing to the particles with small c's to have almost the same trajectory line before and after scattering (i.e. the scattering angle must be the same modulo multiples of 2π as $c \longrightarrow \pm 0$), one obtaines the same result as applying block regularization. After being in the proximity of the source, particles with small c's continue their motion flowing closely to a fictitious particle that elastically bounced ($\beta = 2 - 2/n$, where n is an even number, $n \geq 2$) or just passed through the source ($\beta = 2 - 2/n$, where n is an odd number, $n \geq 2$).

Therefore one can say that the block regularization is the mathematical expression of a constraint on the classical scattering angle.

Chapter 4

A Helium Atom Model

We study the dynamics for a system of differential equations that provides a classical model for the helium atom. This model consists of a planar isosceles 3-body problem with one nucleus and two electrons, whose law of motion is given by a Maneff-type potential with charges. We first describe the qualitative features of the flow near triple collision and then find several global properties. For negative energy, we put into the evidence an open, connected manifold of uniformly bounded, collisionless solutions.

4.1 Equations of Motion

We consider 3 particles moving in a plane. Two of them, called *electrons*, have mass μ, whereas the third, called *nucleus*, has mass 1. We attach to the electrons negative charges and to the nucleus a positive one. The position of the equal-mass particles are given by the vectors $\mathbf{q}_1$ and $\mathbf{q}_2$. The position of the unit-mass particle is given by the vector $\mathbf{q}_3$. We assume that the dynamics of this system is described by a *quasihomogeneous potential* (i.e. a sum of two homogeneous functions) of the form $\mathcal{W} = \mathcal{U} + \mathcal{V}$, where

$$\mathcal{U}(\mathbf{q}) = -\sum_{i<j} \frac{e_i e_j}{|\mathbf{q}_i - \mathbf{q}_j|}, \quad \mathcal{V}(\mathbf{q}) = -\gamma \sum_{i<j} \frac{e_i e_j}{|\mathbf{q}_i - \mathbf{q}_j|^2},$$

$e_1 = e_2 = -\mu, e_3 = 1$, γ and μ are small positive constants, and $\mathbf{q} = (\mathbf{q}_1, \mathbf{q}_2, \mathbf{q}_3)$ is the *configuration* of the particle system. This means that the equations of motion are

$$\ddot{\mathbf{q}} = M^{-1}\nabla\mathcal{W}(\mathbf{q}),$$

where ∇ denotes the *gradient* and M^{-1} is the inverse of the 6-dimensional matrix M whose elements are 0 except for the diagonal ones, which are $\mu, \mu, \mu, \mu, 1, 1$. This system can be written in Hamiltonian form as

$$\begin{cases} \dot{\mathbf{q}} = \frac{\partial\mathcal{H}}{\partial\mathbf{p}} \\ \dot{\mathbf{p}} = -\frac{\partial\mathcal{H}}{\partial\mathbf{q}}, \end{cases} \tag{4.1}$$

where $\mathbf{p} = M\dot{\mathbf{q}}$ is the *momentum* and $\mathcal{H}(\mathbf{q}, \mathbf{p}) = \frac{1}{2}\mathbf{p}^t M^{-1}\mathbf{p} - \mathcal{W}(\mathbf{q})$ (with ^{t} denoting the transposed vector) is a conserved quantity called *total energy*; this is the sum of the *kinetic energy*, $\frac{1}{2}\mathbf{p}^t M^{-1}\mathbf{p}$, and the *potential energy*, $-\mathcal{W}(\mathbf{q})$. In other words, if $(\mathbf{q}, \mathbf{p})$ is a solution of (4.1), then

$$\mathcal{H}(\mathbf{q}(t), \mathbf{p}(t)) = h \text{ (constant)}. \tag{4.2}$$

We can now prove the following result, which is intuitively obvious due to the fact that the electrons have the same charge.

Collision Theorem. *The electrons cannot collide with each other, unless they also collide with the nucleus.*

Proof. If written explicitly, the integral of energy (4.2) takes the form

$$\frac{1}{2}\mathbf{p}^t M^{-1}\mathbf{p} + \frac{\mu^2}{q_{12}(t)} + \frac{\gamma\mu^2}{q_{12}^2(t)} - \frac{\mu}{q_{13}(t)} - \frac{\gamma\mu}{q_{13}^2(t)} - \frac{\mu}{q_{23}(t)} - \frac{\gamma\mu}{q_{23}^2(t)} = h,$$

where $q_{ij} = |\mathbf{q}_i(t) - \mathbf{q}_j(t)|$ is the distance between the particles i and j. As in celestial mechanics, collisions take place at finite instants of time (see [Dia]). If the electrons collide (but do not collide with the nucleus), then $q_{12}(t) \to 0$; since the collision instant is finite, q_{13} and q_{23} remain bounded. Therefore the left hand side

of the above relation tends to infinity, while the right hand side remains finite. This contradiction proves the result.

The goal of this chapter is to study a subset of solutions of system (4.1), namely that of isosceles configurations. It is easy to see that for properly chosen initial conditions, the system maintains a configuration whose shape and size can vary in time but which remains isosceles. According to the Collision Theorem and to the symmetry maintained by the configuration, the only possible collisions of the isosceles problem are triple. To exploit this symmetry, the subset of isosceles solutions is more conveniently expressed in the (Jacobi) coordinates $(\mathbf{x}, \mathbf{y})$ defined below. To obtain the new expression of the equations of motion, consider first the transformation

$$\begin{cases} \mathbf{x}_1 = \mathbf{q}_1 - \mathbf{q}_2 \\ \mathbf{x}_2 = \mathbf{q}_3 - \frac{1}{2}(\mathbf{q}_1 + \mathbf{q}_2). \end{cases}$$

Notice that the position vectors are horizontal and vertical, respectively, i.e. $\mathbf{x}_1 = (x_1, 0)$, $\mathbf{x}_2 = (0, x_2)$, which means that the motion of the three particles is expressed with respect to the base and hight of the isosceles triangle. These are the *Jacobi coordinates* used in a more general context in celestial mechanics (see e.g. [Win]). Let us further denote

$$\begin{cases} \mathbf{x} = (x_1, x_2) \\ \mathbf{y} = (y_1, y_2), \end{cases}$$

where $\mathbf{y} = A\dot{\mathbf{x}}$,

$$A = \begin{pmatrix} \frac{\mu}{2} & 0 \\ 0 & \frac{2\mu}{2\mu+1} \end{pmatrix}.$$

In $(\mathbf{x}, \mathbf{y})$-coordinates, the equations describing the motion of all isosceles solutions is given by the Hamiltonian system

$$\begin{cases} \dot{\mathbf{x}} = \frac{\partial \tilde{H}}{\partial \mathbf{y}} \\ \dot{\mathbf{y}} = -\frac{\partial \tilde{H}}{\partial \mathbf{x}}, \end{cases} \tag{4.3}$$

where

$$\tilde{H}(\mathbf{x}, \mathbf{y}) = \frac{1}{2}\mathbf{y}^t A^{-1}\mathbf{y} - \tilde{W}(\mathbf{x}),$$

$$\tilde{W}(\mathbf{x}) = \tilde{U}(\mathbf{x}) + \tilde{V}(\mathbf{x}),$$

$$\tilde{U}(\mathbf{x}) = -\frac{\mu^2}{x_1} + \frac{4\mu}{\sqrt{x_1^2 + 4x_2^2}}, \quad \tilde{V}(\mathbf{x}) = -\frac{\gamma\mu^2}{x_1^2} + \frac{8\gamma\mu}{x_1^2 + 4x_2^2}.$$

In what follows we will describe the qualitative behaviour of the flow given by equations (4.3). We will fully understand the features of the flow for $h \geq 0$. From both the physical and the mathematical points of view, the interesting case is that of negative energy, $h < 0$, as we will see in Section 10.

4.2 Transformations

In order to reach this goal we first want to understand the motion near triple collision. For this we will use a technique introduced by McGehee in 1974 (see [McG2]). The idea is to blow up the triple-collision singularity into a so-called *collision manifold*, paste the manifold to the phase space, and then understand the motion near triple collision by describing the flow on the collision manifold. From the analytical point of view this means to extend the equations of motion such that to include the triple-collision singularity. To perform the blow up we need to go through a sequence of transformations, which are all analytic diffeomorphisms. The first one is given by

$$\begin{cases} r = (\mathbf{x}^t A \mathbf{x})^{1/2} \\ \mathbf{s} = r^{-1}\mathbf{x} \\ w = \mathbf{y}^t \mathbf{s} \\ \mathbf{z} = A^{-1}\mathbf{y} - w\mathbf{s}. \end{cases}$$

Notice that the new variables are connected by the relations

$$\mathbf{s}^t A \mathbf{s} = 1 \quad \text{and} \quad \mathbf{z}^t A \mathbf{s} = 0.$$

Similar coordinates have been previously used in [Dev] and [Dia] for the study of the isosceles problem with Newtonian and Manev potentials, respectively. The coordinate r is the *moment of inertia*, which is a measure of the particles' distribution

in the plane of motion. Notice that the triple collision takes place when $r = 0$. The coordinate $\mathbf{s}$ is a rescaled configuration, whereas w and $\mathbf{z}$ are the some kind of rescaled radial and tangential momenta of the particle system. We further consider the rescaling coordinate transformation

$$\begin{cases} v = rw \\ \mathbf{u} = r\mathbf{z} \end{cases}$$

and the time-rescaling analytic diffeomorphism

$$d\tau = r^{-2}dt.$$

These lead to the system

$$\begin{cases} r' = rv \\ \mathbf{s}' = \mathbf{u} \\ v' = v^2 + \mathbf{u}^t A^{-1}\mathbf{u} - r\tilde{U}(\mathbf{s}) - 2\tilde{V}(\mathbf{s}) \\ \mathbf{u}' = -(\mathbf{u}^t A^{-1}\mathbf{u})\mathbf{s} + r(\tilde{U}(\mathbf{s})\mathbf{s} + \nabla\tilde{U}(\mathbf{s})) + 2\tilde{V}(\mathbf{s})\mathbf{s} + \nabla\tilde{V}(\mathbf{s}). \end{cases}$$

which is equivalent to equations (4.3) for $r > 0$. The prime now denotes differentiation with respect to the new fictitious time variable τ. The above gradients, $\nabla\tilde{U}$ and $\nabla\tilde{V}$ are meant in the metric induced by the matrix A. The new energy relation is

$$\frac{1}{2}(\mathbf{u}^t A^{-1}\mathbf{u} + v^2) - r\tilde{U}(\mathbf{s}) - \tilde{V}(\mathbf{s}) = r^2 h.$$

Notice that both the new system and the energy relation are now defined for $r = 0$, which means that the triple collision is not a singularity anymore. The transformation

$$\mathbf{s} = \begin{pmatrix} \sqrt{\frac{2}{\mu}} & 0 \\ 0 & \sqrt{\frac{2\mu+1}{2\mu}} \end{pmatrix} \begin{pmatrix} \cos\theta \\ \sin\theta \end{pmatrix}, \quad \mathbf{u} = u \begin{pmatrix} \sqrt{\frac{2}{\mu}} & 0 \\ 0 & \sqrt{\frac{2\mu+1}{2\mu}} \end{pmatrix} \begin{pmatrix} -\sin\theta \\ \cos\theta \end{pmatrix},$$

leads to a new system, equivalent to equations (4.3) for $r > 0$,

$$\begin{cases} r' = rv \\ \theta' = u \\ v' = u^2 + v^2 - rU(\theta) - 2V(\theta) \\ u' = 2r\dot{U}(\theta) + 2\dot{V}(\theta). \end{cases} \tag{4.4}$$

The upper dot represents differentiation with respect to θ. System (4.4) has the energy relation

$$u^2 + v^2 - 2rU(\theta) - 2V(\theta) = 2r^2h, \tag{4.5}$$

where

$$U(\theta) = -\frac{\mu^{\frac{5}{2}}}{\sqrt{2}\cos\theta} + \frac{4\mu^{\frac{3}{2}}}{\sqrt{2 + 4\mu\sin^2\theta}},$$

and

$$V(\theta) = -\frac{\gamma\mu^3}{2\cos^2\theta} + \frac{4\gamma\mu^2}{1 + 2\mu\sin^2\theta}.$$

This energy relation foliates the phase space into so-called *integral manifolds*, whose topology may change with h. If restricted to $r = 0$, the energy relation becomes $u^2 + v^2 = 2V(\theta)$. We will therefore define the collision manifold as

$$C = \{(r, \theta, v, u) | r = 0 \text{ and } u^2 + v^2 = 2V(\theta)\}.$$

This invariant set is homeomorphic to a sphere. The equations that describe the flow on C are

$$\begin{cases} r' = 0 \\ \theta' = u \\ v' = u^2 + v^2 - 2V(\theta) \\ u' = 2\dot{V}(\theta). \end{cases}$$

Our goal is to study the flow of system (4.4) for every level h of the integral manifolds, both for $r = 0$ and for $r > 0$. Notice that C is the same for every h. The flow that has physical significance is the one on the invariant set $r > 0$. Still, the study of the flow on C will give us information on the behaviour of solutions in the neighbourhood of triple collisions.

4.3 Relative Behaviour of U and V

In order to perform our analysis, we will need to understand the relative behaviour of the functions U and V for different values of the parameters μ and γ. Let θ_+^U and

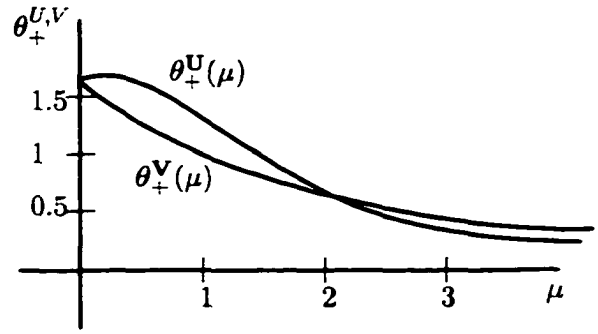

Figure 4.1: The graphs of θ_+^V and θ_+^U as functions of μ.

θ_+^V be the positive roots of the functions U and V respectively. It is easy to compute that

$$\theta_+^U \simeq \frac{\pi}{2} - \frac{1}{4}\mu \text{ and } \theta_+^V \simeq \frac{\pi}{2} - \frac{1}{2\sqrt{2}}\sqrt{\mu}.$$

For $0 < \mu < 2$ we always have $\theta_+^V < \theta_+^U$, for $\mu = 2$, $\theta_+^V = \theta_+^U$ and for $\mu > 2$, $\theta_+^V > \theta_+^U$ (see Figure 4.1).

Also, the relative behaviour of U and V is different in the intervals $(-\infty, \gamma_0)$ and $(\gamma_0, +\infty)$, where $\gamma_0 = \sqrt{\frac{2}{\mu}}(1 - \frac{4}{8-\mu})$. If $\gamma < \gamma_0$, the maximum values of U and V are

$$U_{max} = \frac{(4-\mu)\mu^{\frac{3}{2}}}{\sqrt{2}} > V_{max} = 4(8-\mu)\mu^2.$$

The corresponding graphs of U and V are given in Figure 4.2.

Notice that the negative roots of U and V, θ_-^U and θ_-^V, are symmetric for θ_+^U and θ_+^V, respectively, relative to the vertical axis. In other words, $\theta_-^U = -\theta_+^U$ and $\theta_-^V = -\theta_+^V$.

If $\gamma > \gamma_0$, then

$$U_{max} = \frac{(4-\mu)\mu^{\frac{3}{2}}}{\sqrt{2}} < V_{max} = 4(8-\mu)\mu^2.$$

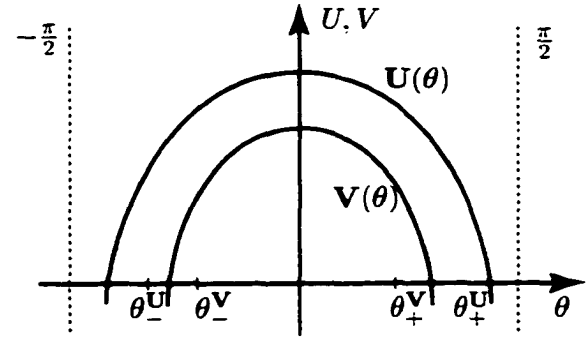

Figure 4.2: The relative behaviour of U and V for $\gamma < \gamma_0$.

Also, calculations lead to

$$\frac{dU}{d\theta} = -\mu^{3/2}\sin\theta\left[\frac{\mu}{\sqrt{2}\cos^2\theta} + \frac{32\cos\theta}{\sqrt{(2+4\mu\sin^2\theta)^3}}\right]$$

and

$$\frac{dV}{d\theta} = -2\gamma\mu^3\sin\theta\left[\frac{1}{2\cos^2\theta} + \frac{4\cos\theta}{(1+2\mu\sin^2\theta)^2}\right].$$

Since $\theta \in (\pi/2, \pi/2)$, U and V are strictly increasing on $(\pi/2, 0]$ and strictly decreasing on $[0, \pi/2)$. The corresponding graphs of U and V are depicted in Figure 4.3.

In what follows we will restrict our analysis to the case of μ and γ small, i.e. $\mu << 1$ and $\gamma < \gamma_0$, which are of physical interest for the helium and for other two-electron atoms.

4.4 The Flow on the Collision Manifold

Let us start by noticing that system (4.4) has exactly two equilibrium solutions,

$$N = \left(0, 0, \mu\sqrt{\frac{\gamma(8-\mu)}{2}}, 0\right) \quad \text{and} \quad S = \left(0, 0, -\mu\sqrt{\frac{\gamma(8-\mu)}{2}}, 0\right),$$

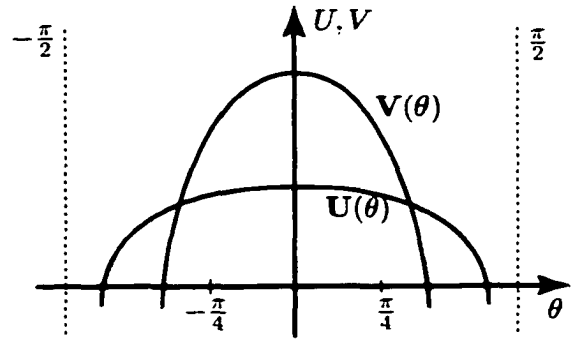

Figure 4.3: The relative behaviour of U and V for $\gamma > \gamma_0$.

and that both lie on the collision manifold C. Due to their positions on the sphere, we will call N and S the *north pole* and the *south pole*, respectively (see Figure 4.4).

Linearizing system (4.4) at the equilibrium N, we obtain the eigenvalues

$$\lambda_1 = \mu\sqrt{\frac{\gamma(8-\mu)}{2}}, \quad \lambda_2 = 2\mu\sqrt{\frac{\gamma(8-\mu)}{2}}, \quad \lambda_{3,4} = \pm 17\mu^3\gamma i.$$

If linearizing system (4.4) at the equilibrium S, the eigenvalues are

$$\psi_1 = -\mu\sqrt{\frac{\gamma(8-\mu)}{2}}, \quad \psi_2 = -2\mu\sqrt{\frac{\gamma(8-\mu)}{2}}, \quad \psi_{3,4} = \pm 17\mu^3\gamma i.$$

This shows that both N and S are nonhyperbolic equilibria that have a 2-dimensional centre manifold.

The equations (4.4) restricted to the collision manifold C take the form

$$\begin{cases} r' = 0 \\ \theta' = u \\ v' = u^2 + v^2 - 2V(\theta) \\ u' = 2\dot{V}(\theta). \end{cases} \tag{4.6}$$

Using the energy relation

$$u^2 + v^2 = 2V(\theta),$$

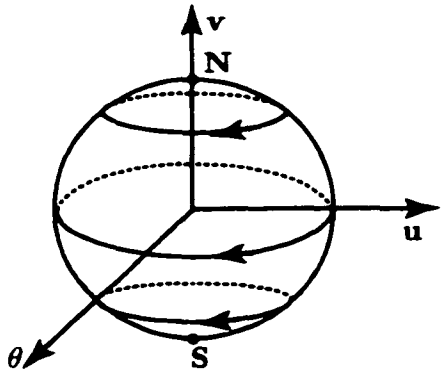

Figure 4.4: The flow on the collision manifold C.

system (4.6) becomes

$$\begin{cases} r' = 0 \\ \theta' = u \\ v' = 0 \\ u' = 2\dot{V}(\theta). \end{cases} \tag{4.7}$$

Since $v' = 0$ it follows that the flow on C is simple; it consists of periodic orbits and the two equilibria N and S (see Figure 4.4). Indeed, for every fixed value of v, the θ-component of the solution is periodic in the independent variable and alternates between two extreme values, $\theta_+(v)$ and $\theta_-(v)$, which can be computed as complicated arccosine functions. But since we don't need them further on, we will not compute them here.

4.5 The Poincaré Map

Now that the flow on C (i.e. for $r = 0$) is completely understood, we would like to clarify how the flow behaves near C. For this we will first estimate the Poincaré map for each periodic orbit $v = \textit{constant}$ belonging to the collision manifold. The goal of this section is to prove the following result.

Lemma 1. *The periodic orbits on the collision manifold have an associated Poincaré*

map with eigenvalues 1 and λ. For the orbits of the northern hemisphere (with $v > 0$), it follows that $|\lambda| > 1$, whereas for those of the southern hemisphere (with $v < 0$), it follows $|\lambda| < 1$. Along the equator ($v = 0$), the linear part of the Poincaré map has the form

$$\begin{pmatrix} 1 & 0 \\ c & 1 \end{pmatrix},$$

where $c > 0$ for small μ.

Proof. The key to the proof is to estimate the derivative DP of the Poincaré map. For this we need to follow several steps.

1. Assume that a given nonautonomous system $\mathbf{x}' = f(\mathbf{x}, \theta)$, periodic in the independent variable θ, has a periodic solution η. The first step is to compute the linear part of the system about this periodic orbit η, i.e. to obtain the matrix

   $$A(\theta) = Df(\eta(\theta), \theta),$$

   which is also periodic in θ.

2. The second step is to find the solution of the initial value problem

   $$\begin{cases} X'(\theta) = A(\theta)X(\theta) \\ X(\theta) = I, \end{cases}$$

   where I is the unit matrix. In general this cannot be done, but we will extract the desired information from the implicit form of the solution.

3. According to Floquet theory (see e.g. [Har]), we can write the solution of the above initial value problem as $X(\theta) = Q(\theta)e^{B\theta}$, where Q is a periodic function in θ. The third step is to accomplish this goal.

4. The fourth step is to compute the period T of the orbit $\eta(\theta)$.

Then the linear part of the Poincaré map for the periodic orbit η is given by the formula

$$\mathrm{DP} = e^{BT}.$$

So in order to complete the proof, we need to estimate B and determine T. Let us now proceed with this plan.

Step 1. Consider system (4.4). Since DP is independent of the choice of the local cross section, we choose this section to be the half plane

$$\{(\theta, u, v) | \theta = 0, u > 0\}.$$

which is transverse to the flow.

For a fixed value of v, we have a periodic solution η on the collision manifold C. Along one period, this periodic orbit can be divided into three parts. In part 1, θ increases from zero to the maximum value of the variable θ, namely $\theta_+(v)$, with $u > 0$. In part 2, θ decreases to the minimum value of the variable θ, namely $\theta_-(v)$, with $u < 0$. In part 3, θ increases back to zero with $u > 0$.

We will now transform system (4.4) to a nonautonomous one in which θ is the new independent variable. This will allow us to compute the period of the orbit without solving the differential equation. Using the fact that $\frac{dr}{d\theta} = \frac{dr}{d\tau} \cdot \frac{d\tau}{d\theta}$ and $\frac{dv}{d\theta} = \frac{dv}{d\tau} \cdot \frac{d\tau}{d\theta}$, it is easy to see that the autonomous system (4.4) is equivalent to the nonautonomous system

$$\begin{cases} \dfrac{dr}{d\theta} = \dfrac{rv}{u} \\ \dfrac{dv}{d\theta} = \dfrac{2r^2h + rU(\theta)}{u}, \end{cases} \tag{4.8}$$

where, from the energy relation, u is given (up to its sign) in terms of r, v, and θ. But since r and v now depend on θ we can write

$$u(\theta) = \pm\sqrt{2(r^2h + rU(\theta) + V(\theta)) - v^2}.$$

In our next computation we will need the partial derivatives of u with respect to r and v, so we write them here both explicitly and in terms of u as

$$\frac{\partial u}{\partial r} = \pm\frac{2rh+U(\theta)}{\sqrt{2(r^2h+rU(\theta)+V(\theta))-v^2}} = \frac{2rh+U(\theta)}{u}, \tag{4.9}$$

$$\frac{\partial u}{\partial v} = \pm\frac{-v}{\sqrt{2(r^2h+rU(\theta)+V(\theta))-v^2}} = -\frac{v}{u}. \tag{4.10}$$

Along an arbitrary orbit, the linear part of the vector field f that defines system (4.8) is given by

$$\begin{aligned} Df &= \begin{pmatrix} \frac{\partial}{\partial r}\frac{dr}{d\theta} & \frac{\partial}{\partial v}\frac{dr}{d\theta} \\ \frac{\partial}{\partial r}\frac{dv}{d\theta} & \frac{\partial}{\partial v}\frac{dv}{d\theta} \end{pmatrix} \\ &= \begin{pmatrix} \frac{v}{u}-\frac{rv}{u^2}\frac{\partial u}{\partial r} & \frac{v}{u}-\frac{rv}{u^2}\frac{\partial u}{\partial v} \\ \frac{4rh+U(\theta)}{u}-\frac{2r^2h+rU(\theta)}{u^2}\frac{\partial u}{\partial r} & -\frac{2r^2h+rU(\theta)}{u^2}\frac{\partial u}{\partial v} \end{pmatrix} \\ &= \begin{pmatrix} \frac{v}{u}-\frac{rv(2rh+U(\theta))}{u^3} & \frac{v}{u}+\frac{rv^2}{u^3} \\ \frac{4rh+U(\theta)}{u}-\frac{r(2rh+U(\theta))^2}{u^3} & \frac{rv(2rh+U(\theta))}{u^3} \end{pmatrix}. \end{aligned}$$

We can now see that the linear part of the flow on the periodic orbit η is given by

$$A(\theta) = Df(\eta(\theta),\theta) = \begin{pmatrix} \frac{v}{u} & 0 \\ \frac{U(\theta)}{u} & 0 \end{pmatrix},$$

which is periodic in θ. This completes Step 1.

Step 2. Next we would like to solve the initial value problem

$$\begin{cases} X'(\theta) = A(\theta)X(\theta) \\ X(\theta) = I. \end{cases}$$

The solution to this linear equation is $X(\theta) = e^{\int_0^\theta A(s)\,ds}$, but in general we cannot solve the integral $\int_0^\theta A(s)\,ds$ without explicitly knowing the periodic orbit. However,

we can write the solution in terms of this integral. Let $F(\theta) = \int_0^\theta \frac{v}{u(s)}\,ds$ and $G(\theta) = \int_0^\theta \frac{U(s)}{u(s)}\,ds$. Then

$$X(\theta) = e^{\int_0^\theta A(s)\,ds} = e^{\begin{pmatrix} F(\theta) & 0 \\ G(\theta) & 0 \end{pmatrix}} = \begin{pmatrix} e^{F(\theta)} & 0 \\ \frac{G(\theta)(e^{F(\theta)}-1)}{F(\theta)} & 1 \end{pmatrix}.$$

This completes Step 2.

Step 3. Now we would like to write $X(\theta)$ as $Q(\theta)e^{B\theta}$, where $Q(0) = I$ and Q is periodic in θ. Because $X(\theta)$ is a lower triangular matrix, $Q(\theta)$ and $e^{B\theta}$ are also lower triangular. Moreover, we can see that the eigenvalues of $X(\theta)$ are $e^{F(\theta)}$ and 1. Since $e^{B\theta}$ must contain the linear part of the logarithm of one eigenvalue, we know that $X(\theta)$ can be written as

$$X(\theta) = \begin{pmatrix} e^{\phi(\theta)} & 0 \\ \star_1 & 1 \end{pmatrix} \begin{pmatrix} e^{\alpha\theta} & 0 \\ \star_2 & 1 \end{pmatrix},$$

where $F(\theta) = \alpha\theta + \phi(\theta)$ and $\phi(\theta) = O(\theta^2)$. We have denoted by α the zero-order part of $\frac{v}{u}$, i.e.

$$\alpha = v(\gamma\mu^2(8-\mu) - v^2)^{-1/2}.$$

Note that $\star_1$ and $\star_2$ must be chosen such that $\star_1$ is zero at $\theta = 0$, $\star_1$ is periodic in θ, and $e^{\alpha\theta}\star_1 + \star_2 = \frac{G(\theta)(e^{F(\theta)}-1)}{F(\theta)}$. It is easy to see that such choices always exist. We can now write B explicitly as

$$B = \begin{pmatrix} \alpha & 0 \\ \beta & 0 \end{pmatrix},$$

where $\beta = \frac{\alpha\star_2}{e^\alpha - 1}$. This completes Step 3.

Step 4. Recall from Step 1 that we divided the trajectory of our periodic orbit η into three parts. In part 1, θ increases from zero to $\theta_+(v)$ with $u > 0$, in part 2, θ decreases to $\theta_-(v)$ with $u < 0$, and in part 3, θ increases back to zero with $u > 0$.

So the period of η is $T = 4\theta_+(v)$. We can now also claim that the derivative of the Poincaré map is

$$DP = e^{BT} = \begin{pmatrix} e^{\alpha T} & 0 \\ \star & 1 \end{pmatrix}$$

and that it leads to the eigenvalues of 1 and $e^{\alpha T}$. Since α and v always have the same sign, $v > 0$ implies that $e^{\alpha T} > 1$, whereas $v < 0$ yields $0 < e^{\alpha T} < 1$. This completes the first part of Lemma 1.

For the case when $v = 0$ and μ is small, we review the same steps as above for $v \neq 0$. The linear part of the vector field on the equator reduces to

$$A(\theta) = \begin{pmatrix} 0 & 0 \\ \frac{U(\theta)}{u} & 0 \end{pmatrix}.$$

The entry $\frac{U(\theta)}{u}$ of this matrix cannot be expressed in terms of standard functions. However, if we assume that μ is small and write the series of $\frac{U(\theta)}{u}$ with respect to μ, then, to the first order in μ,

$$A(\theta) = \begin{pmatrix} 0 & 0 \\ \sqrt{\frac{2\mu}{\gamma}} & 0 \end{pmatrix}.$$

Since $\sqrt{\frac{2\mu}{\gamma}}$ is constant, we can compute DP as

$$DP = \begin{pmatrix} 1 & 0 \\ T\sqrt{\frac{2\mu}{\gamma}} & 1 \end{pmatrix}.$$

Since $T\sqrt{\frac{2\mu}{\gamma}} > 0$, using the continuity with respect to the parameter μ, we can draw the conclusion that

$$DP = \begin{pmatrix} 1 & 0 \\ c & 1 \end{pmatrix},$$

where $c > 0$ for μ sufficiently small. Note that the eigenvalues of DP are both 1 for any μ since the eigenvalues of $A(\theta)$ are both 0 for $v = 0$ and for any μ. This completes the proof.

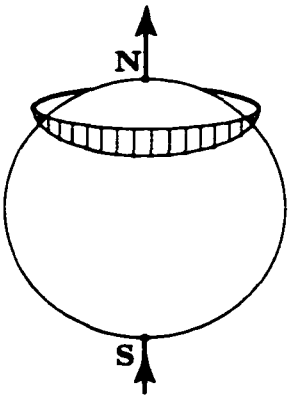

Figure 4.5: The flow in the neighbourhood of the collision manifold C.

4.6 Collision and Near-Collision Orbits

Lemma 1 of the previous section allows us now to understand the behaviour of all collision orbits. The conclusions are summarized below (see also Figure 4.5).

Theorem 2. *The south pole S of the collision manifold has a 1-dimensional local stable manifold, every periodic orbit of the southern hemisphere has a 2-dimensional local stable manifold, every periodic orbit of the northern hemisphere has a 2-dimensional local unstable manifold, the equator has both a 2-dimensional local stable and a 2-dimensional local unstable manifold, and the north pole N has a 1-dimensional local unstable manifold.*

Physical interpretation. The orbits tending to C are triple collisions between the electrons and the nucleus, whereas those tending away are triple ejections. The 1-dimensional local stable manifold of the south pole C consists of all rectilinear orbits that end in a triple collision (see Figure 4.6a). Analogously, the 1-dimensional local unstable manifold of the north pole N consists of all rectilinear orbits that start from a triple ejection. The 2-dimensional local stable manifold of the periodic orbits in

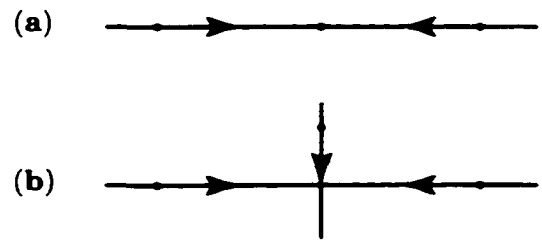

Figure 4.6: (a) Rectilinear and (b) oscillatory triple-collision orbits.

the southern hemisphere ($v = constant \leq 0$) of C consists of solutions that oscillate before colliding (see Figure 4.6 b). Another way of interpreting these solutions is to think that the electrons move on a straight line towards each other, while the nucleus oscillates up and down, the amplitude of each oscillation decreases in time until it becomes infinitesimally small and the triple collision takes place. Analogously, the 2-dimensional local unstable manifold of the periodic orbits in the northern hemisphere ($v = constant \geq 0$) of C consists of solutions that eject from a triple approach in the same oscillatory way.

Proof of Theorem 2. The statements regarding the poles S and N follow from the linearization results of Section 5, whereas the ones involving the periodic orbits for $v = constant \neq 0$ are a direct consequence of Lemma 1 in Section 6. Therefore the only assertion that is not obvious concerns the equator ($v = 0$). Due to the degeneracy of the linear part DP of the Poincaré map computed in Lemma 1, we cannot draw an immediate conclusion. To overcome this difficulty we will use the following result obtained in [Cas].

Let $F = (F_1, F_2)$ be a 2-dimensional analytic function defined in a neighbour-

hood of $(0,0)$ in $\Re^2$ with values in $\Re^2$ such that

1. $F(0,v) = \begin{pmatrix} 0 \\ v \end{pmatrix}$,
2. $DF(0,0) = \begin{pmatrix} 1 & 0 \\ c & 1 \end{pmatrix}$ with $c > 0$,
3. $\beta = D_r D_v F_1(0,0) > 0$.

Then there exist stable and unstable manifolds of $(0,0)$ which are, locally, graphs of analytic functions, that is, $W^s_{loc}(\delta) = \{(\varphi^s(v), v) | v \in (-\delta, 0)\}$ and $W^u_{loc}(\delta) = \{(\varphi^u(v), v) | v \in (0, \delta)\}$, where $\varphi^{s,u} \sim \zeta v^2$, with $\zeta > 0$ constant. (By W^s_{loc} and W^u_{loc} we have denoted the local stable manifold and the local unstable manifold, respectively). At $v = 0$ the functions $\varphi^{s,u}$ are only Lipschitz in general.

Let us now show that the conditions of the above theorem are satisfied by our Poincaré map. According to the computations presented in Lemma 1, this map is of the form

$$P(r,v) = \begin{pmatrix} P_1(r,v) \\ P_2(r,v) \end{pmatrix} = \begin{pmatrix} e^{\alpha} & 0 \\ \star & 1 \end{pmatrix} \begin{pmatrix} r \\ v \end{pmatrix} + \begin{pmatrix} O_1(r,v) \\ O_2(r,v) \end{pmatrix},$$

where O_1 and O_2 are functions containing terms of order r^2 and v^2 or higher, $\alpha = v(\gamma\mu^2(8-\mu) - v^2)^{-1/2}$, and $T > 0$ is the period. Some straightforward computations allow us to draw the following conclusions.

1. $P(0,v) = \begin{pmatrix} 0 \\ v \end{pmatrix}$.
2. From Lemma 1 it follows that $DP(0,0) = \begin{pmatrix} 1 & 0 \\ c & 1 \end{pmatrix}$, with $c > 0$.
3. $D_r D_v P_1(0,0) = \frac{T}{\mu\sqrt{\gamma(8-\mu)}} > 0$.

Since all hypotheses of the above theorem are satisfied, the existence of the 2-dimensional local stable and unstable manifolds of the equator follows. This completes the proof.

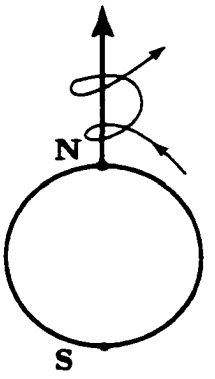

Figure 4.7: An orbit that barely misses the triple collision.

Remark 1. Though binary collisions cannot occur, the set of initial conditions leading to triple collisions has positive measure.

Remark 2. We might be tempted to think that if the electrons come close enough to the nucleus, a triple collision takes place. But there are orbits that can come very close to collision and miss it. Such an orbit is sketched in Figure 4.7. Its existence follows from the continuity of solutions with respect to initial data near the collision manifold C. In physical space this orbit behaves very much like the triple-collision oscillatory solution in Figure 4.6 b), just that when the electrons come close enough, the nucleus is not in their proximity, so the mutually repelling force of the electrons becomes stronger than the attraction force exercised by the nucleus. Therefore the electrons stop first and then change direction moving away from each other. The set of initial conditions leading to solutions of this kind has positive measure.

4.7 The Zero-Energy Case

Now that we understand the qualitative behaviour of solutions at and near triple collisions, let us find out more about the global picture. For this purpose we will

divide our analysis in 3 parts, according to the possible choices of the energy constant h. In this section we will discuss the zero-energy case and will treat the positive- and negative-energy manifolds in Sections 9 and 10, respectively. So let us assume for now that $h = 0$.

To determine the asymptotic behaviour of the solutions at infinity, we transform equations (4.4) with the help of the following change of variables,

$$\begin{cases} \rho = r^{-1} \\ \bar{u} = \rho^{\frac{1}{2}} u \\ \bar{v} = \rho^{\frac{1}{2}} v, \end{cases}$$

which is an analytic diffeomorphism. Further applying the time rescaling transformation

$$d\tau = \rho^{\frac{1}{2}} ds,$$

which is also an analytic diffeomorphism, we obtain a system equivalent to (4.4) for $r, \rho > 0$,

$$\begin{cases} \rho' = -\rho\bar{v} \\ \theta' = \bar{u} \\ \bar{v}' = \bar{u}^2 + \frac{1}{2}\bar{v}^2 - U(\theta) - 2\rho V(\theta) \\ \bar{u}' = -\frac{1}{2}\bar{u}\bar{v} + 2\dot{U}(\theta) + 2\rho\dot{V}(\theta), \end{cases} \tag{4.11}$$

where the prime now denotes differentiation with respect to the new fictitious time variable s and the dot means differentiation relative to θ. In these new coordinates, the energy relation (4.5) with $h = 0$ takes the form

$$\bar{u}^2 + \bar{v}^2 - 2U(\theta) - 2\rho V(\theta) = 0. \tag{4.12}$$

Let us define the *infinity manifold* with the help of relation (4.12) as

$$I = \{(\rho, \theta, \bar{v}, \bar{u}) | \rho = 0, \bar{u}^2 + \bar{u}^2 = 2U(\theta)\}.$$

This definition is justified by the fact that the flow on I represents the virtual motion at infinity. Indeed, if $r \to \infty$ (i.e. when the distance between at least two particles becomes infinite), then $\rho \to 0$. The infinity manifold is also homeomorphic to a

sphere (see Figure 4.8). The flow on I is described by system (4.11) restricted to the infinity manifold I and is expressed through the equations

$$\begin{cases} \rho' = 0 \\ \theta' = \bar{u} \\ \bar{v}' = \bar{u}^2 + \frac{1}{2}\bar{v}^2 - U(\theta) \\ \bar{u}' = -\frac{1}{2}\bar{u}\bar{v} + 2\dot{U}(\theta). \end{cases} \tag{4.13}$$

The energy relation (4.12) on the infinity manifold is given by

$$\bar{u}^2 + \bar{v}^2 = 2U(\theta). \tag{4.14}$$

Let us now determine the flow on I. For this notice first that system (4.11) (as well as (4.13)) has two equilibria:

$$\bar{N} = \left(0, 0, \sqrt{\frac{2U(0)}{3}}, 0\right) \text{ and } \bar{S} = \left(0, 0, -\sqrt{\frac{2U(0)}{3}}, 0\right),$$

which lie on I and we will therefore call *infinite north pole* and *infinite south pole*, respectively. The eigenvalues of $\bar{N}$ are

$$\bar{\lambda}_{1,3} = \mp\sqrt{\frac{2U(0)}{3}}, \quad \bar{\lambda}_{2,4} = \frac{1}{4}\left(-\sqrt{\frac{2U(0)}{3}} \pm \sqrt{\frac{2U(0)}{3} - 66\sqrt{2}\mu^{\frac{5}{2}}}\right).$$

whereas those of $\bar{S}$ are

$$\bar{\psi}_{1,3} = \pm\sqrt{\frac{2U(0)}{3}}, \quad \bar{\psi}_{2,4} = \frac{1}{4}\left(\sqrt{\frac{2U(0)}{3}} \pm \sqrt{\frac{2U(0)}{3} - 66\sqrt{2}\mu^{\frac{5}{2}}}\right).$$

Thus for $\mu < \frac{4}{169}$ all eigenvalues of $\bar{N}$ and $\bar{S}$ are real, $\bar{\lambda}_1, \bar{\lambda}_2, \bar{\lambda}_4 < 0$, $\bar{\lambda}_3 > 0$, $\bar{\psi}_1, \bar{\psi}_2, \bar{\psi}_4 > 0$, and $\bar{\psi}_3 < 0$.

Using (4.14) and the third equation of system (4.13), we obtain that

$$\bar{v}' = \frac{1}{2}\bar{u}^2,$$

which means that the flow on I is increasing with respect to the variable $\bar{v}$, so there are no periodic orbits. Thus the flow on the infinity manifold looks as in Figure 4.8:

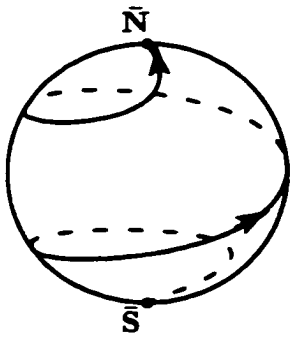

Figure 4.8: The flow on the infinity manifold I.

all non-equilibrium solutions connect the infinity south pole with the infinity north pole. This will help us understand the global flow on the zero-energy manifold. Let us first prove the following result.

Lemma 3. *Every solution (r, θ, v, u) of system (4.4) for which $h = 0$ is such that $v' \geq 0$ with $v' = 0$ only at triple collisions.*

Proof. ¿From the energy relation (4.5) we have that

$$2[U(\theta)r + V(\theta)] = u^2 + v^2 \geq 0, \tag{4.15}$$

which implies that $U(\theta)r + V(\theta) \geq 0$. Recalling the definitions of U and V in Section 4, notice that $U(\theta) > V(\theta)$ for μ and γ small (see Figure reffig302). From this and (4.15) it now follows that

$$(r + 1)U(\theta) > 0,$$

so $U(\theta) > 0$. This also implies that θ belongs to the interval (θ_-^U, θ_+^U) (see Figure 4.2). Using further the energy relation (4.5) with $h = 0$ and the third equation in (4.4), we obtain that

$$v' = rU(\theta),$$

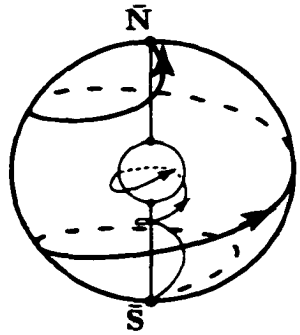

Figure 4.9: The flow on the zero-energy manifold, $h = 0$.

so $v' \geq 0$. Notice that $v' = 0$ only if $r = 0$, i.e. at triple collision. This completes the proof.

We can now fully understand the qualitative behaviour of the flow for $h = 0$, a manifold that can be represented as the region between the two nested spheres C and I. Notice, however, that this representation is given in two different charts. One chart is that of equations (4.4), which is convenient to use for describing the motion in the neighbourhood of C; the other chart is that of equations (4.13) and it suits the description of the flow near I. Since systems (4.4) and (4.13) are equivalent in the open region between the nested spheres I and C and since this representation allows us to visualize the global flow on the zero-energy manifold, we will further use it. The manifold $h = 0$ contains 5 classes of orbits. Their description and physical interpretation are given below.

1. The solution connecting the infinity south pole $\bar{S}$ of I with the south pole S of C represents a rectilinear orbit in which the electrons are captured from infinity and end up in a collision with the nucleus.

2. The solution connecting the north pole N of C with the infinity north pole

$\bar{N}$ of I represents a rectilinear orbit in which the electrons eject from a triple approach with the nucleus and escape to infinity.

3. The solutions connecting the infinity south pole $\bar{S}$ with the infinity north pole $\bar{N}$ that avoid the collision manifold C represent oscillatory orbits in which the electrons are captured from infinity and end up evading to infinity. without to encounter collisions. The solution drawn in Figure 4.7 also belongs to this class.

4. The solutions connecting the infinity south pole $\bar{S}$ of I with any of the periodic orbits of the southern hemisphere of C (including the equator) represent orbits in which the electrons are captured from infinity and then lead to an oscillatory triple collision with the nucleus.

5. The solutions connecting any of the periodic orbits of the northern hemisphere of C (including the equator) with the infinity north pole $\bar{N}$ of I, represent orbits in which the electrons eject from a triple approach with the nucleus and escape to infinity through oscillatory motion.

From the above we can draw the following conclusion, which shows that the dynamics on the zero-energy manifold is uninteresting from the point of view of the helium atom.

Theorem 4. *Every solution* (r, θ, v, u) *of system (4.4) for which* $h = 0$ *is such that* $\lim_{\tau \to -\infty} r(\tau) = \infty$ *or* $\lim_{\tau \to \infty} r(\tau) = \infty$, *therefore it is unbounded.*

4.8 The Positive-Energy Case

In this section we will show that the qualitative behaviour of the flow for $h > 0$ is similar to the one in the zero-energy case. Unfortunately we cannot use the

infinity-manifold technique of Section 8 and therefore do not have the previous nice representation of the phase space. But we can rely on the analogy with the orbits drawn in Figure 4.9. Let us first prove the following result.

Lemma 5. *Every solution (r, θ, v, u) of system (4.4) for which $h > 0$ has the property that $v' \geq 0$, with $v' = 0$ only at triple collisions.*

Proof. From the energy relation (4.5) we can write that

$$\frac{1}{2}(u^2 + v^2) = hr^2 + U(\theta)r + V(\theta).$$

Since $u^2 + v^2 \geq 0$ it follows that $hr^2 + U(\theta)r + V(\theta) \geq 0$. Using the properties of quadratic polynomials, we see that this inequality is satisfied for all r when $h > 0$ and $U^2(\theta) \leq 4hV(\theta)$. This happens only if $V(\theta) \geq 0$, i.e. if θ belongs to the interval (θ_-^V, θ_+^V). But in this interval $U(\theta) > 0$. From the third equation of system (4.4) and the energy relation (4.5) it follows that

$$v' = r(2rh + U(\theta)),$$

which means that $v' \geq 0$. Obviously $v' = 0$ only if $r = 0$, i.e. at triple collisions. This completes the proof.

Using the continuity of the solutions with respect to initial data, it becomes clear that the qualitative features of the flow for $h > 0$ are very similar to the ones of the zero-energy manifold. Since every solution is increasing with respect to v, no periodic solutions occur and since there are no equilibria other than N and S, an orbit can belong only to one of the following classes: capture-collision, capture-escape, or ejection-escape. Therefore we can draw a conclusion similar to the one in Theorem 4.

Theorem 6. *Every solution (r, θ, v, u) of system (4.4) for which $h > 0$ is such that $\lim_{\tau \to -\infty} r(\tau) = \infty$ or $\lim_{\tau \to \infty} r(\tau) = \infty$, therefore it is unbounded.*

This implies that the dynamics on the positive-energy manifold is also simple but uninteresting from the point of view of the helium atom.

4.9 The Negative-Energy Case

This is the case in which we can put into the evidence a large class of solutions that may be interesting for the helium and other two-electron atoms. For this let us start by noticing that if we use the energy relation (4.5), the first and third equations of system (4.4) can be written as

$$\begin{cases} r' = rv \\ v' = r(2hr + U(\theta)). \end{cases} \tag{4.16}$$

We will further regard (4.16) as an independent system in which the only information we retain about U is that it is a bounded function of θ in the interval (θ_-^U, θ_+^U). The time-rescaling transformation

$$d\sigma = rd\tau$$

changes (4.16) into the equivalent system

$$\begin{cases} r' = v \\ v' = 2hr + U(\theta), \end{cases} \tag{4.17}$$

where the prime now denotes differentiation with respect to the new time variable σ and, by abusing the notation, r, v, and $U(\theta)$ are now functions of σ. Notice however that this transformation may introduce solution singularities. In other words there may exists solutions defined on an open interval (σ_1, σ_2) for which at least one end, σ_1 or σ_2, is finite.

Denotiong $\omega^2 := 2(-h)$, system (4.17) can be written as the second-order equation

$$r'' + \omega^2 r = U(\theta), \tag{4.18}$$

which represents a forced harmonic oscillator. The corresponding homogeneous equation $r'' + \omega^2 r = 0$ leads to bounded solutions that oscillate up and down with

positive and negative values for r. Of course, in our original equation $r'' - 2hr = U(\theta)$, r cannot take negative values. Moreover, if $r = 0$ at some point in time, the solution encounters a triple collision.

Since we are using only the fact that U is bounded for θ in the interval (θ_-^U, θ_+^U), it will be impossible to obtain the exact solution of (4.18). But we can show that, within the open and connected set of solutions Γ (which will be defined in the proof Theorem 14), r can be estimated as

$$0 < r(\sigma) < R_{max}.$$

In other words, every solution in Γ will be proved to be bounded and collisionless.

In preparation for our main result, let us prove the following lemmas.

Lemma 7. *For every solution (r, θ, v, u) of system (4.4) for which $h < 0$, the range of the component θ is included in the interval (θ_-^U, θ_+^U).*

Proof. Since $h < 0$, it follows from the energy relation (4.5) that

$$rU(\theta) + V(\theta) > 0.$$

Since $U(\theta) > V(\theta)$ for every θ, we can draw the conclusion that $(r+1)U(\theta) > 0$, so $U(\theta) > 0$ and therefore θ belongs to the interval (θ_-^U, θ_+^U), at most. This completes the proof.

Lemma 8. *For every solution (r, θ, v, u) of system (4.4) for which $h < 0$, there is a θ^h, $0 < \theta^h < \theta_+^U$ such that $|\theta(\sigma)| \leq \theta^h$ for any σ.*

Proof. Taking into account that the energy relation 4.5 can be written as:

$$\frac{1}{2}(u^2 + v^2) = hr^2 + rU(\theta) + V(\theta), \tag{4.19}$$

and denoting by $f(r, \theta)$ the right hand side of 4.19. i.e.

$$f(r, \theta) := hr^2 + rU(\theta) + V(\theta), \tag{4.20}$$

we observe that $f(r,\theta)$ must be positive at any time. The idea of the proof is to show that for every fixed negative energy level h, the θ component is bounded by a θ_c^h with $0 < \theta_c^h < \theta_+^U$, where every c is a positive level of the functional $f(r,\theta)$. If this is the case, then the θ component is bounded by

$$\theta^h := \sup_{c\geq 0} \theta_c^h, \tag{4.21}$$

and if $0 < \theta^h < \theta_+^U$, the conclusion follows.

Therefore we will prove that for every fixed $h < 0$ and $c \geq 0$, $\theta_c^h := \sup\{|\theta| \mid f(r,\theta) = c\}$ is such that $0 < \theta_c^h < \theta_+^U$ and $\sup_{c\geq 0} \theta_c^h := \theta^h < \theta_+^U$.

Let us observe that for $\theta \geq \theta_+^U$ we have $U(\theta_+^U) = 0$, $V(\theta_+^U) < 0$ and hence,

$$f(r,\theta_+^U) = hr^2 + rU(\theta_+^U) + V(\theta_+^U) < 0. \tag{4.22}$$

Now, let us assume that $\theta_c^h \geq \theta_+^U$. Then, since $f(r,\theta)$ is continuous and well defined for any r and θ ($|\theta| < \frac{\pi}{2}$), there is a sequence $\{(r_i,\theta_i)\}_{i\geq 0}$, such that $\lim_{i\to\infty}(r_i,\theta_i) := (\tilde{r},\tilde{\theta})$ with $\tilde{\theta} \geq \theta_+^U$. It follows that for i large enough, $U(\theta_i) \leq 0$, $V(\theta_i) < 0$ (see Figure 4.2) and, consequently, $f(r_i,\theta_i) = hr_i^2 + rU(\theta_i) + V(\theta_i) \leq 0$ since at the limit, by (4.22), $f(\tilde{r},\tilde{\theta}) < 0$. But $f(r,\theta)$ must be positive at any time: contradiction. Therefore $\theta_c^h < \theta_+^U$ for any $c \geq 0$.

It remains to prove that $\sup_{c\geq 0} \theta_c^h < \theta_+^U$. Let us assume that $\sup_{c\geq 0} \theta_c^h = \theta_+^U$. Then there is a sequence $\{c_i\}_{i\geq 0}$ such that $\lim_{i\to\infty} \theta_{c_i}^h = \theta_+^U$. Then, for any r, $f(r,\theta_{c_i}^h) = c_i \geq 0$ and $\lim_{i\to\infty} f(r,\theta_{c_i}^h) = f(r,\theta_+^U) < 0$; contradiction. Therefore, $\sup_{c\geq 0} \theta_c^h < \theta_+^U$.

Lemma 9. *For every $h < 0$ fixed, the r component of system 4.4 is bounded.*

Proof. We have to show that there are initial conditions for which the r-component of system 4.4 is bounded.

We start by observing that, since $\theta \in [-\theta^h, \theta^h]$, the range of $U(\theta)$ is $[U(\theta^h), U(0)]$ with $U(\theta^h) > 0$. In other words, the right hand side of (4.18) is always a strictly

positive number in between $[U(\theta^h), U(0)]$. Also, one can explicitely solve eq (4.18) obtaining:

$$\begin{array}{l} r(\sigma) = [c_1 + \frac{1}{\omega}\int_0^\sigma U(\theta(s))\cos(\omega s)ds]\sin(\omega\sigma) + \\ \quad [c_2 - \frac{1}{\omega}\int_0^\sigma U(\theta(s))\sin(\omega s)ds]\cos(\omega\sigma), \end{array} \tag{4.23}$$

or, using some trigonometry,

$$\begin{array}{l} r(\sigma) = \sqrt{\left(\sqrt{c_1^2+c_2^2}\cos\omega_0 - \frac{U(\theta(\sigma))}{\omega^2}\right)^2 + (c_1^2+c_2^2)\sin^2\omega_0}\cos(\omega\sigma - \omega_1) + \\ \quad + \frac{U(\theta(\sigma))}{\omega^2}, \end{array} \tag{4.24}$$

and further,

$$\begin{array}{l} r(\sigma) = \sqrt{(c_1^2+c_2^2) - \frac{2\sqrt{c_1^2+c_2^2}U(\theta(\sigma))}{\omega^2}\cos\omega_0 + \frac{U^2(\theta(\sigma))}{\omega^4}}\cos(\omega\sigma - \omega_1) + \\ \quad + \frac{U(\theta(\sigma))}{\omega^2}. \end{array} \tag{4.25}$$

where $\omega = \sqrt{-2h}$, $\omega_0 = \arctan\frac{c_2}{c_1}$ and $\omega_1 = \omega_1(\sigma) = \arctan\dfrac{\frac{U(\theta(\sigma))}{\omega^2} - \sqrt{c_1^2+c_2^2}\cos\omega_0}{\sqrt{c_1^2+c_2^2}\sin\omega_0}$.

It follows

$$r(\sigma) \le \sqrt{(c_1^2+c_2^2) - \frac{2\sqrt{c_1^2+c_2^2}U(\theta(\sigma))}{\omega^2}\cos\omega_0 + \frac{U^2(\theta(\sigma))}{\omega^4}} + \frac{U(\theta(\sigma))}{\omega^2}$$

and further, since $U(\theta) \le U(0)$

$$r(\sigma) \le \sqrt{(c_1^2+c_2^2) + \frac{2\sqrt{c_1^2+c_2^2}U(0)}{\omega^2} + \frac{U^2(0)}{\omega^4}} + \frac{U(0)}{\omega^2} := r_{max}^{c_1,c_2}$$

which is the upper bound of $r(\sigma)$ as function of the initial conditions (c_1, c_2).

We will focus now on proving that there exists an open set of initial conditions for which the solutions remain strictly positive at any time. More precisely, we will show that there exists an open set V_δ^h in $\mathbf{R}^2$ such that if $(c_1, c_2) \in V_\delta^h$ then $r(\sigma) > 0$

for any σ. The proof flows as the following: first we make use of the positivity and the good properties of $U(\cdot)$ (i.e. $U(\cdot)$ strictly positive real function with compact range) and approximate $U(\cdot)$ by a sequence of positive step functions $U_n(\cdot)$. Then, we prove that if the right hand side of (4.18) is given by a strictly positive step function (i.e. by an infinite sum $\sum_{i\geq 0} \alpha_i \chi_{A_i}$ with $\alpha_i > 0$, $A_i \bigcap A_j = \phi$), then there is an open set of initial condition (c_1, c_2) such that for any $\delta > 0$ with $\min_{i\geq 0} \alpha_i - \delta > 0$, $r(\sigma) > \delta$ for all σ. Further, we estimate the distance between solutions of (4.18) and solutions of the equation with right hand side $U_n(\cdot)$. We prove that this distance is monotonic with respect to the distance between $U(\cdot)$ and $U_n(\cdot)$. The last step is almost trivial: solutions of (4.18) and solutions of the equation with right hand side $U_n(\cdot)$ stay close; the latter posseses a set of initial for which solutions are above $\delta > 0$: it follows that for the same set of initial conditions. solutions of (4.18) are above 0. Formally:

Lemma 10. *Given $U(\cdot) : \mathbf{R} \longrightarrow [U(\theta^h), U(0)]$ continuous and $U(\theta^h) > 0$. there is a sequence $U_n(\cdot)$ of strictly positive step functions such that: $(\forall)\ \epsilon > 0$, $(\exists)\ N > 0$ positive integer such that $|U(s) - U_n(s)| < \epsilon$ $(\forall)\ n > N$ and $(\forall)\ s$.*

Proof. Since $U(\cdot) : \mathbf{R} \longrightarrow [U(\theta^h), U(0)]$ is continuous with compact range, $U(\cdot)$ is $\mathcal{L}^\infty$ integrable. But any function of this type can be uniformly approximated by a sequence of step functions. Moreover, since $\min_{\sigma\in\mathbf{R}} U(\sigma) > 0$, the approximant sequence $U_n(\sigma)$ can be chosen to be strictly positive and the conclusion follows.

Observation We can always choose $U_n(\cdot)$ such that, as it will be needed later, $U_n(\theta(0)) = U(\theta(0))$ for all n. Moreover, we can always choose $U_n(\cdot)$ such that $U(s) - U_n(s) > 0$ for all s for n large enough.

Lemma 11. *Let $U_n(\cdot)$ be as in Lemma 10 where n is large enough such that for all $\delta > 0$ with $U(\theta^h) - \delta > 0$, $U(\theta^h) - \delta < U_n(\cdot) < U(0) + \delta$. Also, let us consider the*

initial value problem $r_n'' + \omega^2 r_n = U_n(\theta(\sigma))$, $r_n(0) = c_2 + U_n(\theta(0))$, $(r_n)'(0) = c_1$. *Then there is an open set* V_δ^h *such that for all values* $(c_1, c_2) \in V_\delta^h$, $r_n(\sigma) > \delta$ *for all* σ.

Proof. Let $\delta > 0$ with $U(\theta^h) - \delta > 0$, $U(\theta^h) - \delta < U_n(\cdot) < U(0) + \delta$. We will prove that for all $(c_1, c_2) \in V_\delta^h := \{(c_1, c_2) \mid \sqrt{c_1^2 + c_2^2} < U(\theta^h) - \delta\}$, the solutions of the initial value problem

$$\begin{cases} r_n'' + \omega^2 r_n = U_n(\theta(\sigma)), \\ r_n^{(i)}(0) = c_2 + U_n(\theta(0)), \quad (r_n^{(i)})'(0) = c_1 \end{cases} \tag{4.26}$$

are such that $r_n(\sigma) > \delta$ for all σ.

Since $U_n(\cdot)$ is a step function, we represent it formally as

$$U_n(\sigma) = \sum_{i \geq 0} \alpha_i \chi_{[\sigma_i, \sigma_{i+1})}(\sigma)$$

where α_i are strictly positive constants with $U(\theta^h) - \delta < \alpha_i < U(0) + \delta$, $(\forall)$ i and $U_n(\theta(0)) = U(\theta(0)) = \alpha_0$ for all n. Then the solution of (4.26) can be represented as

$$r_n(\sigma) = \sum_{i \geq 0} r_n^{(i)}(\sigma) \chi_{[\sigma_i, \sigma_{i+1})}, \tag{4.27}$$

where on each interval $[\sigma_i, \sigma_{i+1})$ we have the initial value problem

$$\begin{cases} (r_n^{(i)})'' + \omega^2 r_n^{(i)} = \alpha_i, \\ r_n^{(i)}(\sigma_i) = r_n^{(i-1)}(\sigma_i), \quad (r_n^{(i)})'(\sigma_i) = (r_n^{(i-1)})'(\sigma_i). \end{cases} \tag{4.28}$$

We will use induction with respect to i, proving that on each of the intervals $[\sigma_i, \sigma_{i+1})$

$$r_n(\sigma) = \sqrt{c_1^2 + c_2^2} \cos(\omega\sigma - \omega_i) + \alpha_i$$

. For $i = 0$, i.e. on $[\sigma_0, \sigma_1)$, we have

$$\begin{cases} (r_n^{(0)})'' + \omega^2 r_n^{(0)} = \alpha_0, \\ r_n^{(0)}(\sigma_i) = c_2 + \alpha_0, \quad (r_n^{(i)})'(\sigma_i) = c_1. \end{cases} \tag{4.29}$$

with solution

$$r_n(\sigma) = \sqrt{c_1^2 + c_2^2}\cos(\omega\sigma - \omega_0) + \alpha_0. \tag{4.30}$$

Let us assume that for i fixed, i.e. on $[\sigma_i, \sigma_{i+1})$, we have

$$r_n(\sigma) = \sqrt{c_1^2 + c_2^2}\cos(\omega\sigma - \omega_i) + \alpha_i$$

and therefore, at the limit,

$$r_n^i(\sigma_{i+1}) = \sqrt{c_1^2 + c_2^2}\cos(\omega\sigma_{i+1} - \omega_i) + \alpha_i. \tag{4.31}$$

$$(r_n^{(i)})'(\sigma_{i+1}) = -\frac{1}{\omega}\sqrt{c_1^2 + c_2^2}\sin(\omega\sigma_{i+1} - \omega_i). \tag{4.32}$$

Then on $[\sigma_{i+1}, \sigma_{i+2})$:

$$\begin{cases} (r_n^{(i+1)})'' + \omega^2 r_n^{(i+1)} = \alpha_{i+1}, \\ r_n^{(i+1)}(\sigma_{i+1}) = r_n^i(\sigma_{i+1}), \ \ (r_n^{(i+1)})'(\sigma_{i+1}) = (r_n^{(i)})'(\sigma_{i+1}), \end{cases} \tag{4.33}$$

with solution

$$r_n(\sigma) = \sqrt{\left[\frac{(r_n^{(i)})'(\sigma_{i+1})}{\omega}\right]^2 + \left(r_n^i(\sigma_{i+1}) - \alpha\right)^2}\cos(\omega\sigma - \omega_i) + \alpha_0. \tag{4.34}$$

Using (4.31) and (4.32) it follows that $r_n(\sigma) = \sqrt{c_1^2 + c_2^2}\cos(\omega\sigma - \omega_{i+1}) + \alpha_{i+1}$ where with $\omega_{i+1} = \arctan\left(r_n^i(\sigma_{i+1}) - \alpha\right)/\left[\frac{(r_n^{(i)})'(\sigma_{i+1})}{\omega}\right]$.

Hence, for all i, i.e. on each of $[\sigma_i, \sigma_{i+1})$, we have

$$r_n(\sigma) = \sqrt{c_1^2 + c_2^2}\cos(\omega\sigma - \omega_i) + \alpha_i.$$

Now, for all σ,

$$r_n(\sigma) = \sqrt{c_1^2 + c_2^2}\cos(\omega\sigma - \omega_i) + \alpha_i > -\sqrt{c_1^2 + c_2^2} + \alpha_i > U(\theta^h) - \sqrt{c_1^2 + c_2^2} > \delta$$

and the conclusion follows.

Lemma 12. *Let us consider the initial value problems* $r'' + \omega^2 r = U(\theta(\sigma))$ *and* $r_n'' + \omega^2 r_n = U_n(\theta(\sigma))$ *with* $r(0) = r_n(0) = c_2 + U(\theta(0))$, $r'(0) = (r_n)'(0) = c_1$ *for*

all n (recall that $U_n(\theta(0)) = U(\theta(0))$ for all n). Then $(\forall)\epsilon > 0$, $(\exists)N > 0$ such that $|r(\sigma) - r_n(\sigma)| < \epsilon$, $(\forall)n > N$ and $(\forall)\sigma$.

Proof. Let us consider $r'' + \omega^2 r = U(\theta(\sigma))$ with $r(0) = c_2 + U(\theta(0))$, $r'(0) = c_1$. The solution is given by (4.23). On the other hand, The solution of $r_n'' + \omega^2 r_n = U_n(\theta(\sigma))$ with the same initial values is given by

$$\begin{aligned} r_n(\sigma) = &[c_1 + \tfrac{1}{\omega}\textstyle\int_0^\sigma U_n(\theta(s))\cos(\omega s)ds]\sin(\omega\sigma) + \\ &[c_2 - \tfrac{1}{\omega}\textstyle\int_0^\sigma U_n(\theta(s))\sin(\omega s)ds]\cos(\omega\sigma). \end{aligned} \tag{4.35}$$

It follows that

$$\begin{aligned} |r(\sigma) - r_n(\sigma)| = \tfrac{1}{\omega}\Big| &\sin(\omega\sigma)\textstyle\int_0^\sigma (U(\theta(s)) - U_n(\theta(s)))\cos(\omega s)ds - \\ &-cos(\omega\sigma)\textstyle\int_0^\sigma (U(\theta(s)) - U_n(\theta(s)))\sin(\omega s)ds\Big|, \end{aligned} \tag{4.36}$$

and further, using that we have chosen $U_n(\cdot)$ such that $U(\theta(s)) - U_n(\theta(s)) > 0$ and applying an intermediate value property on $(0, \sigma)$

$$\begin{aligned} |r(\sigma) - r_n(\sigma)| = \tfrac{1}{\omega}\Big| &\sin(\omega\sigma)(U(\theta(\xi)) - U_n(\theta(\xi)))\textstyle\int_0^\sigma \cos(\omega s)ds - \\ &-cos(\omega\sigma)(U(\theta(\xi) - U_n(\theta(\xi)))\textstyle\int_0^\sigma \sin(\omega s)ds\Big|, \end{aligned} \tag{4.37}$$

where $\xi \in (0, \sigma)$. Taking into account that the difference $(U(\theta(\xi) - U_n(\theta(\xi))$ is as small as we need, i.e. $(U(\theta(\xi) - U_n(\theta(\xi)) < \tilde{\epsilon}$ for n large enough, simple calculations lead to

$$\begin{aligned} |r(\sigma) - r_n(\sigma)| &= \tfrac{\tilde{\epsilon}}{\omega}\Big|\sin(\omega\sigma)\textstyle\int_0^\sigma \cos(\omega s)ds - \cos(\omega\sigma)\int_0^\sigma \sin(\omega s)ds\Big| = \\ &= \tfrac{\tilde{\epsilon}}{\omega}\Big|\tfrac{1}{\omega}(\sin^2(\omega\sigma) + \cos^2(\omega\sigma)) - \tfrac{\cos(\omega\sigma)}{\omega}\Big| \leq \tfrac{2\tilde{\epsilon}}{\omega^2}. \end{aligned} \tag{4.38}$$

Choosing $\tilde{\epsilon} = \epsilon\omega^2/2$, the conclusion follows.

Lemma 13. *Let us consider the initial value problem $r'' + \omega^2 r = U(\theta(\sigma))$ with $r(0) = c_2 + U(\theta(0))$, $r'(0) = c_1$. Then for all $\delta > 0$ such that $U(\theta^h) - \delta > 0$ there is an open set V_δ^h such that for all values $(c_1, c_2) \in V_\delta^h$, $r_n(\sigma) > 0$ for all σ.*

Proof. Let $V_\delta^h := \{(c_1, c_2) \mid \sqrt{c_1^2 + c_2^2} < U(\theta^h) - \delta\}$ as in Lemma 11. Let $(c_1, c_2) \in V_\delta^h$. We know by Lemma 12 that for any $\epsilon > 0$, $|r(\sigma) - r_n(\sigma)| < \epsilon$ for all σ and n large enough. Also, by Lemma 11, if $\delta > 0$ is such that $U(\theta^h) - \delta > 0$, then $r_n(\sigma) > \delta$ for all σ. Let us fix $\delta > 0$ such that $U(\theta^h) - \delta > 0$. Then there is $\epsilon > 0$ such that $\delta - \epsilon > 0$. Them for n large enough

$$r(\sigma) = r(\sigma) - r_n(\sigma) + r_n(\sigma) > -\epsilon + \delta > 0$$

for all σ. This completes the proof.

Theorem 14. *There exists an open, connected invariant manifold Γ whose orbits are bounded and collisionless.*

Proof. By the previous Lemma we know that for a fixed $h < 0$ and for initial conditions $(c_1, c_2) \in \Gamma_h = \bigcup_{\delta > 0} V_\delta^h = \{(c_1, c_2) \mid \sqrt{c_1^2 + c_2^2} < U(\theta^h) - \delta\}$ the orbits are such that $0 < r(\sigma) < r_{max}^{c_1, c_2}$ for any σ. It follows that Γ_h is an open set in $\mathbf{R}^2$ and contains the set of initial conditions leading to collisionless motion along a fixed negative level of energy $h < 0$.

We define Γ as the entire set of initial conditions leading to collisionless orbits, i.e. $\Gamma := \bigcup_{h<0} \Gamma_h$. Since every Γ_h is open, Γ is open, too. On another hand, $f(r, \theta)$ (see (4.20)) varies smoothly with respect to h, θ^h varies smoothly with respect to h (see Lemma 8) and, sinces $h < 0 \neq 0$, $\frac{U(\theta^h)}{\omega^2}$ varies smoothly with respect to h (recall that $\omega = \sqrt{-2h}$). Therefore, as h varies, the manifolds Γ_h deforms continuously one into another and their reunion Γ is connected. Finally, by definition, the orbits in Γ are collisionless, therefore, an orbit in starting in Γ stays in it at any time. Therefore, Γ is invariant.

Notice that every solution in Γ is defined for all real σ. In other words no solution has singularities because r is bounded both from above and away from zero from below, so neither collisions nor pseudocollisions can occur (see [Xia]). Moreover, for

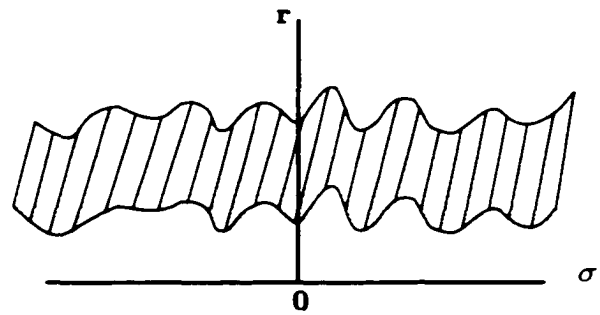

Figure 4.10: A possible range in which r can vary if c_1, c_2, and h are fixed.

c_1, c_2, and h given, r can vary in time only in the wave-like band given by the above inequalities, which qualitatively looks as in Figure 4.10. This completes the proof.

The manifolds Γ for $h < 0$ are the ones interesting for the helium atom. The physical interpretation of the orbits in Γ is that the electrons move in opposite directions back and forth on a horizontal line while the nucleus oscillates up-and-down on a vertical line that crosses the line of the electrons and is such that the electrons are symmetric with respect to it. Thus this system satisfies the minimal requirements for offering a model of the helium atom within the framework of classical mechanics.

Bibliography

[Arno] Arnol'd, V.I. Mathematical Methods of Classical Mechanics (2nd ed.). New York: Springer–Verlag (1989).

[Cas] Casasayas, J., Fontich, E., Nunes, A. Invariant manifolds for a class of parabolic points, Nonlinearity **5**, 1193-1210 (1992).

[Con] Conley, C.: Isolated Invariant Sets and the Morse Index, CBMS Regional Conference Series in Mathematics, **38**, AMS, Providence (1978).

[Con-E] Conley, C., Easton, R.: Isolated Invariant Sets and Isolating Blocks, Trans. Amer. Math. Soc. **158**, 35-61 (1971).

[Del] Delgado, J., Diacu, F.N., Lacomba, E.A., Mingarelli A., Mioc, V., Perez-Chavela, E., Stoica, C.: The global flow in the Manev problem, J. Math. Phys. **37**, 2748-2761 (1996).

[Dev] Devaney, R.: Triple collision in the planar isosceles three-body problem. Invent. math. **60** (1980). 249-267.

[Dia] Diacu, F.: Near-collision dynamics for particle systems given by quasihomogeneous potentials, Journ. Differential Equations **128**, 58-77 (1996).

[Dia-M] Diacu, F., Mioc, V., Stoica, C.: Phase-space structure and regularization of Manev-type problems, Nonlinear Analysis **41**, 1029-1055, (2000).

[Eas] Easton, R.: Regularization of vector fields by surgery, J. Diff. Eq. **10**, 92-99 (1971).

[Fen] Fenichel, N.: Persistence and smoothness of invariant manifolds for flow, Indiana Univ. Math. J. **21**, 193-226 (1971).

[Gu] Guckenheimer, J., Holmes, P.: Nonlinear Oscillations, Dynamical Systems and Bifurcation of Vector Fields, (2nd ed.). New York: Springer–Verlag (1986).

[Hag] Hagihara Y., Celestial Mechanics, MIT Press, Cambridge, MA, 1975, vol. I and II

[Har] Hartman, P.: *Ordinary Differential Equations*, Birkhüser, Boston, 1982.

[Ill] Illner, R., Bobylev, A.V.: Collision Integrals for Attractive Potentials, J. Stat. Phys. **95**, 663-650 (1999).

[Lan] Landau, L.D., Lifshits, E.M.: Mechanics, Pergamon Press, Oxford-London-Paris, 1960.

[Lev] Levi-Civita, T.,: Sur la regularization du probleme des trois corps, Acta Math. **42**, 99-144 (1920).

[McG1] McGehee, R.: Double collision for a classical particle system with nongravitational interactions, Comment. Math. Helvetici **56**, 524-557 (1981).

[McG2] McGehee, R.: Triple collision in the collinear three-body problem, Inventiones math. **27**, 191-227 (1974).

[Mi-St1] Mioc, V., Stoica, C.: Discussion et résolution complète du problème des deux dans le champ gravitationnel de Maneff (with V. Mioc) - *C. R. Acad. Sci. Paris*, **320**, ser.I, 645-648, (1995).

[Mi-St2] Mioc, V., Stoica, C.: Discussion et résolution complète du problème des deux dans le champ gravitationnel de Maneff (II) (with V. Mioc) - *C. R. Acad. Sci. Paris*, **321**, ser.I, 961-964, (1995).

[Per] Perez-Chavela, E., Vela-Arevalo, L.V.: Triple collision in the quasihomogeneous Collinear Three-Body Problem, Journ. Differential Equations **148**, 186-211 (1998).

[P] Poincaré, H.: *New Methods of Celestial Mechanics*, Amer. Inst. Phys., 1993.

[Pol] Pollard H., Mathematical Introduction to Celestial Mechanics, Prentice-Hall, 1966

[Sie] Siegel, C.L., Moser, J.,: Lectures in celestial mechanics, New York: Springer-Verlag (1971)

[St1] Stoica, C., Mioc, V.: The Schwarzschild problem in astrophysics, Astrophysics and Space Science **249**, No.1, 161-173 (1997).

[St2] Stoica, G., Stoica G.: Branch regularization of quasihomogeneous functions, Rev. Romaine de Math. Pures et Appliquees, 1998

[T-C] Tanner, G., Cvitanović, P.: Helium atom, in *Classical and Quantum Chaos* (book in preparation), Chap. 19.

[Wi] Wilson, F.W., Yorke, J.: Lyapunov functions and isolating blocks, J. Diff. Eq **13**, 106-123 (1973).

[Win] Wintner, A.: *The Analytical Foundations of Celestial Mechanics*, Princeton Univ. Press, Princeton, NJ, (1941).

[Xia] Xia, Z.: The existence of noncollision singularities in the N-body problem, Annals Math. **135**, 411-468 (1992).